National Library of Canada
Bibliothèque nationale du Canada

Canadian Theses Service
Services des thèses canadiennes

Ottawa, Canada
K1A 0N4

CANADIAN THESES
THÈSES CANADIENNES

NOTICE

The quality of this microfiche is heavily dependent upon the quality of the original thesis submitted for microfilming. Every effort has been made to ensure the highest quality of reproduction possible.

If pages are missing, contact the university which granted the degree.

Some pages may have indistinct print especially if the original pages were typed with a poor typewriter ribbon or if the university sent us an inferior photocopy.

Previously copyrighted materials (journal articles, published tests, etc.) are not filmed.

Reproduction in full or in part of this film is governed by the Canadian Copyright Act, R.S.C. 1970, c. C-30. Please read the authorization forms which accompany this thesis.

AVIS

La qualité de cette microfiche dépend grandement de la qualité de la thèse soumise au microfilmage. Nous avons tout fait pour assurer une qualité supérieure de reproduction.

S'il manque des pages, veuillez communiquer avec l'université qui a conféré le grade.

La qualité d'impression de certaines pages peut laisser à désirer, surtout si les pages originales ont été dactylographiées à l'aide d'un ruban usé ou si l'université nous a fait parvenir une photocopie de qualité inférieure.

Les documents qui font déjà l'objet d'un droit d'auteur (articles de revue, examens publiés, etc.) ne sont pas microfilmés.

La reproduction, même partielle, de ce microfilm est soumise à la Loi canadienne sur le droit d'auteur, SRC 1970, c. C-30. Veuillez prendre connaissance des formules d'autorisation qui accompagnent cette thèse.

THIS DISSERTATION
HAS BEEN MICROFILMED
EXACTLY AS RECEIVED

LA THÈSE A ÉTÉ
MICROFILMÉE TELLE QUE
NOUS L'AVONS REÇUE

NL 339 (r. 86/01)

Canada

278

National Library of Canada
Bibliothèque nationale du Canada

Canadian Theses Division
Division des thèses canadiennes

Ottawa, Canada
K1A 0N4

0-315-27009-8

PERMISSION TO MICROFILM — AUTORISATION DE MICROFILMER

• Please print or type — Écrire en lettres moulées ou dactylographier

Full Name of Author — Nom complet de l'auteur

marco Fiori

Date of Birth — Date de naissance
Nov / 01 / 58

Country of Birth — Lieu de naissance
NILE - FRANCE

Permanent Address — Résidence fixe
28 - 9109 112 Street
Edmonton ALberta
T6G 2C6

Title of Thesis — Titre de la thèse
EMULSION FLOODING OF LLOYDMINSTER HEAVY OILS

University — Université
University of ALBERTA

Degree for which thesis was presented — Grade pour lequel cette thèse fut présentée
Master of Science

Year this degree conferred — Année d'obtention de ce grade
1983

Name of Supervisor — Nom du directeur de thèse
Dr. S.M. Farouq Ali

Permission is hereby granted to the NATIONAL LIBRARY OF CANADA to microfilm this thesis and to lend or sell copies of the film.

The author reserves other publication rights, and neither the thesis nor extensive extracts from it may be printed or otherwise reproduced without the author's written permission.

L'autorisation est, par la présente, accordée à la BIBLIOTHÈQUE NATIONALE DU CANADA de microfilmer cette thèse et de prêter ou de vendre des exemplaires du film.

L'auteur se réserve les autres droits de publication; ni la thèse ni de longs extraits de celle-ci ne doivent être imprimés ou autrement reproduits sans l'autorisation écrite de l'auteur.

Date
October 14, 1983

Signature

NL-91 (4/77)

THE UNIVERSITY OF ALBERTA

EMULSION FLOODING OF LLOYDMINSTER HEAVY OILS

by

(C) MARCO FIORI

A THESIS

SUBMITTED TO THE FACULTY OF GRADUATE STUDIES AND RESEARCH

IN PARTIAL FULFILMENT OF THE REQUIREMENTS FOR THE DEGREE

OF : MASTER OF SCIENCE

IN

PETROLEUM ENGINEERING

DEPARTMENT OF MINERAL ENGINEERING

EDMONTON, ALBERTA

FALL, 1983

THE UNIVERSITY OF ALBERTA

RELEASE FORM

NAME OF AUTHOR MARCO FIORI

TITLE OF THESIS EMULSION FLOODING OF LLOYDMINSTER HEAVY OILS

DEGREE FOR WHICH THESIS WAS PRESENTED : MASTER OF SCIENCE

YEAR THIS DEGREE GRANTED FALL, 1983

Permission is hereby granted to THE UNIVERSITY OF ALBERTA LIBRARY to reproduce single copies of this thesis and to lend or sell such copies for private, scholarly or scientific research purposes only.

The author reserves other publication rights, and neither the thesis nor extensive extracts from it may be printed or otherwise reproduced without the author's written permission.

(SIGNED) .....

PERMANENT ADDRESS:

Les Guilloteaux

17100 SAINTES

FRANCE

DATED June 10 19 83

THE UNIVERSITY OF ALBERTA

FACULTY OF GRADUATE STUDIES AND RESEARCH

The undersigned certify that they have read, and recommend to the Faculty of Graduate Studies and Research, for acceptance, a thesis entitled EMULSION FLOODING OF LLOYDMINSTER HEAVY OILS submitted by MARCO FIORI in partial fulfilment of the requirements for the degree of : MASTER OF SCIENCE in PETROLEUM ENGINEERING.

.....

Supervisor

.....

.....

Date...September..22,.1983.....

This thesis is dedicated to the late

Jean Baptiste GAZZI

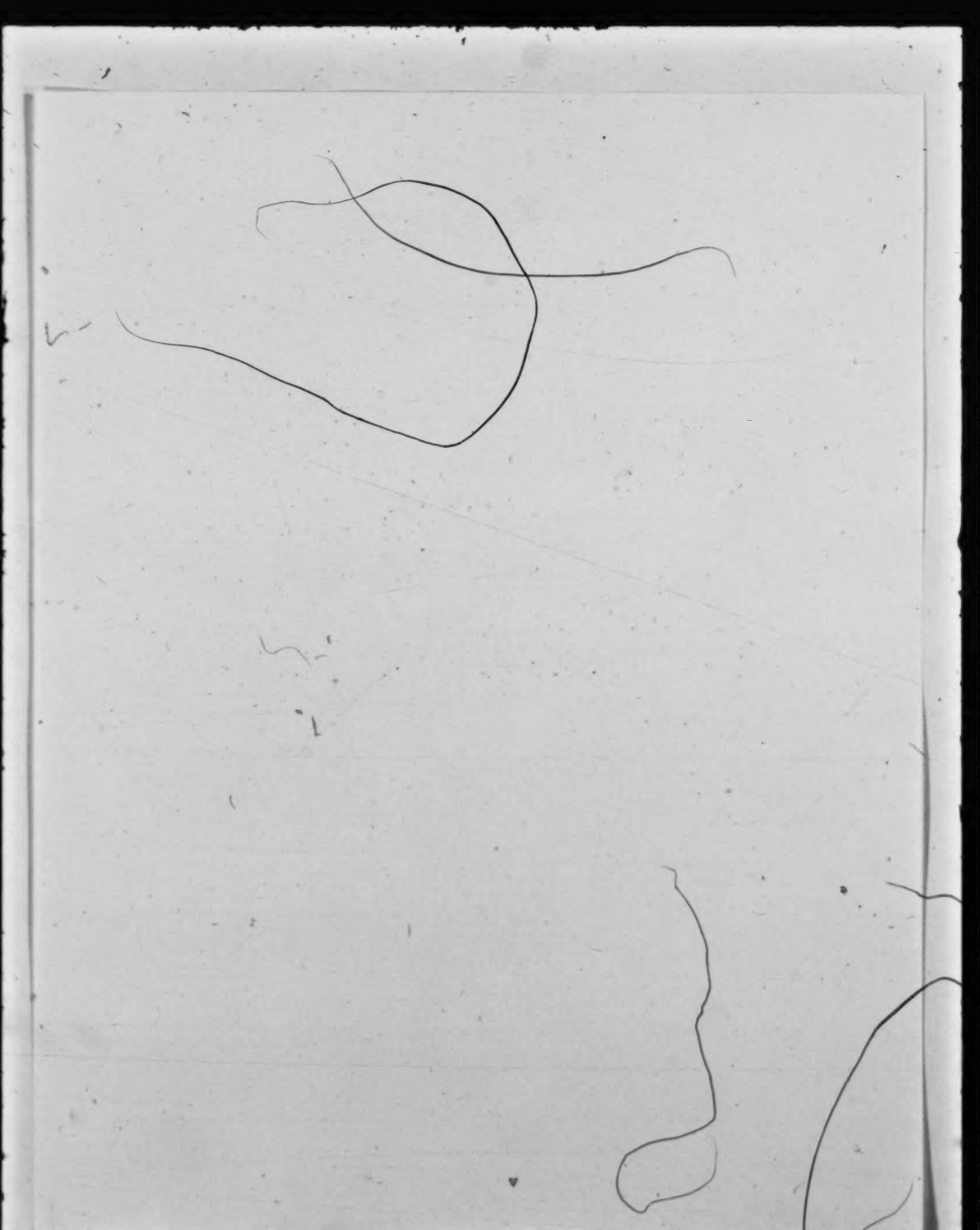

ABSTRACT

The following work reports a study of the practical aspects of emulsion flooding for heavy oils such as those produced in the Lloydminster area. A systematic study of the parameters influencing the emulsification process was conducted. It was found that by using 92 percent wellhead crude as the oil component and a 0.10 percent by weight sodium hydroxide solution, a stable, single phase, water-in-oil (W/O) emulsion could be formed. The viscosity of this emulsion which was too high for practical injection was reduced to 0.220 Pa·s (220 cp) by addition of 13 percent synthetic crude. Prior to testing the effectiveness of a slug of this emulsion in displacing heavy oil from a sand pack, its rheological behaviour was investigated; varying amounts of aqueous and oleic phases were blended with the emulsion and the resulting mixtures were analysed. It was observed that mixtures containing at least 30 percent water resulted in either a gel or very high viscosity W/O emulsion.

Six sand pack displacements were conducted for three different slug sizes under various initial conditions. It was found that an emulsion slug equal to 30 percent of the pore volume followed by distilled water displaced 80.3 percent of the oil in place after 1.5 pore volumes were injected. Waterflooding recovered 43.0 percent of the oil in place after 1.2 pore volumes were injected while partial waterflooding followed by injection of a slug (30 percent of

the pore volume) resulted in the recovery of 69.3 percent of the oil in place after 1.7 pore volumes were injected. All displacements, where emulsion slugs were present, showed increasing injection pressure with time.

ACKNOWLEDGEMENTS

The author is indebted to Dr. S. M. FAROUQ ALI for his guidance as thesis supervisor.

The author also wishes to thank Dr. J. T. RYAN for permitting access to invaluable laboratory equipment from the Chemical Engineering Department.

Diligent assistance from the Mineral Engineering technical staff as a whole is greatly appreciated.

Finally, acknowledgement is given to the Alberta Oil Sands Technology and Research Authority for funding this research.

Table of Contents

Chapter		Page
1.	INTRODUCTION	1
2.	DEFINITIONS	7
3.	LITERATURE REVIEW	9
	3.1 CLASSICAL EMULSION THEORY	9
	3.2 EMULSIONS IN PETROLEUM RESEARCH	26
4.	STATEMENT OF THE PROBLEM	31
5.	EXPERIMENTAL EQUIPMENT, MATERIALS AND PROCEDURE	33
	5.1 EMULSIFICATION	33
	5.1.1 Interfacial Tension	33
	5.1.2 Emulsion Preparation	36
	5.1.3 Microscope Observations	41
	5.1.4 Rheological Properties	43
	5.2 SAND PACK DISPLACEMENTS	44
	5.2.1 Packing the Core	45
	5.2.2 Determination of Permeability	47
	5.2.3 Determination of Porosity	47
	5.2.4 Displacement Procedure	47
6.	DISCUSSION OF RESULTS	50
	6.1 INTERFACIAL TENSION	50
	6.2 EMULSION PREPARATION	58
	6.3 MICROSCOPE OBSERVATIONS	66
	6.3.1 Crude Oil	66
	6.3.2 Crude Oil with a Drop of Sodium Hydroxide Solution	68
	6.3.3 100 Percent Crude Oil Emulsion	68
	6.3.4 90 Percent Crude Oil Emulsion	69

6.3.5 70 Percent Crude Oil Emulsion 69

6.4 Aging of Emulsions 71

6.4.1 75 percent Crude Oil Emulsion 74

6.4.2 Crude Oil 75

6.5 RHEOLOGICAL PROPERTIES 78

6.6 SOLVENT EFFECTIVENESS 98

6.7 HEAVY OIL RECOVERY EXPERIMENTS 103

6.7.1 Effect of Slug Size 107

6.7.2 Effect of a Prior Waterflood on Emulsion Slug Process 115

6.7.3 Effect of Core Length 118

7. CONCLUSIONS 123

8. RECOMMENDATIONS 125

9. References Cited 127

10. Appendix A 132

11. Appendix B 142

12. Appendix C 154

13. Appendix D 157

14. Appendix E 164

15. Appendix F 178

16. Appendix G 194

List of Tables

Table		Page
1	Optimum Composition Selection	64
2	Sand Pack Displacement Parameters	106
3	Flood Results	114
A-1	Interfacial Tension (50/50)	134
A-2	Tensiometer Correction Factors.	135
A-3	Interfacial Tension (25/75)	136
A-4	Tensiometer Correction Factors.	137
A-5	Interfacial Tension (75/25)	139
A-6	Tensiometer Correction Factors.	140
A-7	Water Analysis Report	141
B-1	Emulsion Preparation Quantities	143
B-2	Preparation Temperature Effect.	144
B-3	Emulsion Phases Water Content	145
B-4	Emulsion pH and Relative Volumes.	148
B-5	Mixture Composition	151
B-6	Conversion from Crude to Oil Content.	153
C-1	Eyehill Crude Aging	155
D-1	Water Content Estimation.	158
D-2	Optimality of 92 Percent Emulsion	159
D-3	W/O Phase Data.	160
D-4	Phase Diagram Data.	162
E-1	Rheological Data-Eyehill Crude.	165

E-2 Mixtures-Apparent Viscosity 166
E-3 Solvent Effectiveness-1% Benzene. 170
E-4 Solvent Effectiveness-Benzene 172
E-5 Solvent Effectiveness-Xylenes 174
E-6 Solvent Effectiveness-Synthetic Crude 176
E-7 Apparent Viscosities-Benzene/Xylenes. 177
F-1 Samples-Rheological Data. 183
F-2 Linear Regression Analysis. 192
F-3 Heavy Oil and Emulsion Rheology 193
G-1 Permeability Calculations 195
G-2 Pore Volume Determination 196
G-3 Initial Sand Pack Conditions. 203
G-4 Effluent Analysis-Run 1 204
G-5 Pressure History-Run 1. 205
G-6 Oil Production History-Run 1. 206
G-7 Effluent Water Salinity Analysis-Run 1. 207
G-8 Effluent Analysis-Run 2 208
G-9 Pressure history-Run 2. 209
G-10 Oil Production History-Run 2. 211
G-11 Effluent Water Salinity Analysis-Run 2. 213
G-12 Effluent Analysis-Run 3 214
G-13 Pressure History-Run 3. 215
G-14 Oil Production History-Run 3. 217
G-15 Effluent Water Salinity Analysis-Run 3. 219
G-16 Effluent Analysis-Run 4 220
G-17 Pressure History-Run 4. 221
G-18 Oil Production History-Run 4. 223

G-19 Effluent Water Salinity Analysis-Run 4. 225
G-20 Effluent Analysis-Run 5 226
G-21 Pressure History-Run 5. 228
G-22 Oil Production History-Run5 230
G-23 Effluent Water Salinity Analysis-Run 5. 232
G-24 Effluent Analysis-Run 6 233
G-25 Pressure History-Run 6. 235
G-26 Oil Production History-Run 6. 237
G-27 Effluent Water Salinity Analysis-Run 6. 239

List of Figures

Figure	Page
1 - Coalescence Patterns.	13
2 - Eyehill Crude-Dimpling Effect	14
3 - Eyehill Crude-Water Droplets Aggregations	15
4 - Eyehill Crude-Lamella Formation	16
5 - Experimental Dynamic Tensions for an Acid Crude Oil	20
6 - Effect of Phase Volume Ratio on Dynamic Tension	21
7 - Effect of α on Transient Solute Adsorption	21
8 - Effect of K_{-2} on Transient Solute Adsorption	22
9 - Effect of β on Transient Solute Adsorption	22
10 - Interfacial Tension Measurement.	34
11 - Correction Factor for Interfacial Tension	35
12 - Cross-Section of the Blending Container.	37
13 - Equipment Layout	46
14 - Pore Volume Determination.	48
15 - Eyehill/Caustic Solution Tension (25/75 ratio)	51
16 - Eyehill/Caustic Solution Tension (50/50 ratio)	52
17 - Eyehill/Caustic Solution Tension (75/25 ratio)	53
18 - Eyehill/Caustic Solution Tension (all ratios).	56
19 - W/O Emulsion Produced versus Crude Utilized.	60
20 - pH in Each Phase versus Percent Crude Utilized	62
21 - Original Eyehill Crude-no stirring.1400x	67
22 - 100% Eyehill Crude-5 min. stirring.1750x	70

23 - 90% Eyehill Crude 10% NaOH solution.1750x. 70
24 - 70% Eyehill Crude 30% NaOH solution. 700x. 72
25 - 70% Eyehill Crude 30% NaOH solution.1750x. 72
26 - Effect of Time on Drop Size Distribution 76
27 - 75% Eyehill Crude 25% NaOH solution. 175x. 77
28 - 75% Eyehill Crude 25% NaOH solution.1750x. 77
29 - Sample Composition 80
30 - Water Content of W/O Emulsions 81
31 - Rheology of Samples 11, 16, 17, and 25 83
32 - Optimal Emulsion Rheology. 84
33 - Sample 5 Rheology; Log-Log Scales. 85
34 - Samples 5, 6, and 11 Rheology; Semi-Log Scales . . . 86
35 - Sample 5 Rheology; Arithmetic Scales 88
36 - Samples 6, 11, 16, 17, and 25; Rheology. 89
37 - Optimal Emulsion; Apparent Viscosity 91
38 - Sample 5; Apparent Viscosity 92
39 - Sample 9; Apparent Viscosity 93
40 - Apparent Viscosity Chart; Shear Rate: 1.55 s^{-1} . . . 95
41 - Apparent Viscosity Chart; Shear Rate: 9.71 s^{-1} . . . 96
42 - Apparent Viscosity Chart; Shear Rate: 15.45 s^{-1}. . . 97
43 - Effect of Benzene on Emulsion Viscosity. 99
44 - Comparison of Solvents Effectiveness 101
45 - Effect of Synthetic Crude on Emulsion Viscosity. . .102
46 - Rheology of Heavy Oil and Eyehill Emulsion 104
47 - Pressure and Oil Cut Histories-Run 1 105
48 - Pressure and Oil Cut Histories-Run 2 108
49 - Pressure and Oil Cut Histories-Run 3 109

50 - Pressure and Oil Cut Histories-Run 4 110
51 - Effect of Emulsion Slug Size on Recovery 113
52 - Salinity of Effluent; Runs 2, 3, and 4 116
53 - Pressure and Oil Cut Histories-Run 5 117
54 - Salinity of Effluent; Runs 1, 5, and 6 119
55 - Pressure and Oil Cut Histories-Run 6 121
56 - Effect of Emulsion on Waterflood Recovery. 122
F-1 - Calibration Fluid Rheology. 179
F-2 - Weissenberg Transducer Calibration: AT'N=20 180
F-3 - Weissenberg Transducer Calibration: AT'N=100. . . .181
F-4 - Weissenberg Transducer Calibration: AT'N=200. . . .182
F-5 - Sample 6 Rheology; Log-Log Scales 189
F-6 - Samples 6 and 11 Rheology; Arithmetic Scales. . . .190
F-7 - Sample 9 Rheology 191
G-1 - Pore Volume Determination 202

NOMENCLATURE

A	interfacial area, sq cm
C_i	surface-active agent concentration in the bulk in phase i, fraction
C_i^s	surface-active agent concentration in a layer in phase i, fraction
D_i	surface-active agent diffusion coefficient in phase i, sq cm / s
E	total specific surface energy, dyne / cm
h	thickness of adsorbed layer, cm
H^*	reduced surface-active agent tension-lowering ability, dimensionless
k_i	adsorption rate constant in phase i, dimensionless
k_{-i}	desorption rate constant in phase i, dimensionless
K	consistency index, Pa·s
n	flow index, dimensionless
$R_{a,i}$	net solute adsorption rate, cm / s
t	time, s
t^*	dimensionless time
V_i	volume in phase i, cu cm

Greek Symbols

α	reduced area, sq cm / cu cm
β	reduced volume ratio, dimensionless
γ	interfacial tension, dyne / cm
Γ	surface-active agent adsorption, cm
Γ^*	dimensionless surface-active agent adsorption
δ_i	Nernst film thickness, cm
Δ	reduced diffusion coefficient ratio, dimensionless
K_{-i}	reduced desorption rate constant, dimensionless
λ_i	reduced film thickness, dimensionless
μ_o	oil viscosity, Pa·s
Π	disjoining pressure, dyne / sq cm
τ	shear stress, pa
σ	shear rate, s^{-1}

1. INTRODUCTION

Emulsions are divided into two categories: macroemulsions and microemulsions. In the case of a macroemulsion, the size of the dispersed phase drops varies from 1000 to 50000 nanometers (1 to 50 microns). For a microemulsion, the size of the dispersed drops varies from 100 to 1000 nanometers (0.1 to 1 micron). Most of the work to-date has been done in the area of microemulsions. Field tests of microemulsion flooding are being conducted and laboratory studies of microemulsion behaviour are numerous. By comparison, relatively little work is being done in the area of macroemulsions. Only one field test is known to have been conducted at this time. Laboratory studies are few, and most of them date back to 1973. These studies are concerned with the flow properties of macroemulsions in porous media. The emulsions used were invariably oil-in-water. No study of water-in-oil petroleum macroemulsions nor any systematic study of their flow properties is known to the author. The present study deals with water-in-oil macroemulsions prepared with the Eyehill crude produced in the Lloydminster area.

The relevance of this work can be justified on the basis of the relatively low productivity of some heavy oil reservoirs in the Lloydminster area which are unsuitable for thermal recovery. As reported by Jameson (1973), primary production yields between two and eight percent of the oil in place, there. Because of an adverse mobility ratio,

waterflooding is not effective and permits the recovery of an additional two percent of the oil in place. Consequently, the possibility of using emulsion flooding as an enhanced oil recovery method has been suggested. Emulsion flooding has several advantages over other secondary recovery methods. First, being a non-thermal method it is applicable to thick and thin pays alike. Second, the low mobility emulsion bank, driven by water, will cause reservoir oil ahead to bank effectively. However, the mobility ratio between the injection water and the emulsion at the back of the emulsion bank is highly unfavourable. Therefore there is some concern about viscous fingering of water into the emulsion bank. The deleterious effect of fingering can be delayed by using a large enough emulsion slug. Furthermore, slug injection may be difficult if the apparent viscosity of the emulsion is too high.

The objective of this study is to determine whether the idea of emulsion flooding is technically feasible given the type of oil under consideration, namely the Eyehill heavy oil. Of all the different possible emulsions, the only combination studied here is a water-in-oil macroemulsion. It is composed of distilled water containing sodium hydroxide and of Eyehill wellhead crude containing already fifty nine percent connate water as dispersed drops. Wellhead crude is thus already a water-in-oil emulsion. Removal of connate water from the wellhead crude by vacuum distillation is technically feasible but alters the chemical

properties of the oil. The ions present in the water must go as solids into the oil when the water evaporates. In addition, vacuum distillation is costly when done on a large scale. In this study, cost is always kept in perspective because Lloydminster heavy oil is a product which requires extensive refining to become saleable. It was therefore decided to use the produced crude oil-water emulsion, referred to as "crude" hereinafter, as the oleic phase in the emulsions prepared for this study. Cost is also the reason why caustic is preferred to commercial emulsifiers.

The first stage was to determine whether stable mixtures of Eyehill wellhead crude and caustic solutions could be formed. If the caustic solution and the wellhead crude could not remain as a homogeneous mixture, there was no point in investigating this combination any further. The mixture behaviour depended on the nature of both the oil and the emulsifying agent used. In the present case, the Eyehill crude is what is commonly termed an acidic crude. It contains a wide array of fatty acids which are very reactive and act as natural surfactants in the oil. These fatty acids react with the emulsifying agent in the water (sodium hydroxide in this case) to give a soap which lowers the interfacial tension and improves the chances of obtaining a homogeneous mixture. It is generally conceded that interfacial tension plays a major role during emulsification. If the interfacial tension is low, the energy required to create new interfaces between the two

liquids is relatively small. As a consequence, the chances of obtaining a homogeneous mixture are greatly improved. This was the rationale for devoting the first part of this study to the examination of the parameters that affect interfacial tension. The goal was to determine under what conditions interfacial tension could be lowered sufficiently to obtain homogeneous mixtures. The caustic concentration which provided the lowest interfacial tension was selected.

The second stage was to prepare mixtures of Eyehill wellhead crude and of the selected caustic solution. Even though the interfacial tension was the lowest possible under the given cicumstances, not all mixtures were homogeneous. Depending on the relative amounts of wellhead crude and caustic solution the mixtures either remained homogeneous or readily separated. It is important to know which mixtures are homogeneous and for how long. If an emulsion flooding project were to be successful, the emulsion slug injected should remain homogeneous. If phase separation occurs (break-down), the purpose of using an emulsion bank to provide efficient displacement would be defeated. So the principal goal of this part of the research was to find a mixture that remained homogeneous for a long period of time. Another goal was to test that mixture to see how blending it with distilled water or wellhead crude, or both, affected it. In the reservoir, an emulsion bank could encounter varying saturations of water and heavy oil. It is important to be able to predict how combinations of these three fluids

(i.e. emulsion, distilled water, and heavy oil) behave. If the emulsion broke down, efficiency of displacement would drop. If the viscosity of the emulsion increased drastically, the porous medium would become plugged. A third goal was to control emulsion viscosity. This was achieved by using solvents among other methods. If the viscosity of the emulsion were too high, injection pressures would be prohibitively high. The amount of solvent added was limited by two factors. First, solvents are costly and the emulsion flooding technique must be inexpensive to remain attractive. Second, the mobility ratio between the in-situ oil and the emulsion bank at the front, must remain acceptable for the displacement to be efficient. In summary, the second stage of this study was involved with the rheology of the selected emulsion and of numerous resulting mixtures simulating possible reservoir conditions.

The third and final stage of this study consisted of selected sand pack displacement experiments, simulating "one dimensional" flow of an emulsion bank through an unconsolidated porous medium. In these experiments, the emulsion was injected as a slug and driven by distilled water. Depending on its size, the emulsion slug may bank a significant portion of the in-place oil prior to break-down due to adverse viscosity ratio at the rear. These factors, as well as the initial oil saturation, affect the ultimate recovery of the in-place oil. Of the six runs conducted, four were conducted in oil-saturated sand packs with brine

present at a residual saturation. The possible application of emulsion flooding for Lloydminster heavy oil was appraised, based upon available results. Guidelines were suggested for future work.

2. DEFINITIONS

This section is designed to minimize any ambiguity with regard to the terms that may arise. During the course of this study it became necessary to make use of words which may convey several meanings. Each of these words is defined below.

Oil refers to the actual petroleum substance, free of any water content.

By wellhead crude, or crude, is meant a combination of oil and connate water as received from the field. In this case, the Eyehill crude is composed of oil containing fifty nine percent connate water in the form of dispersed droplets. It is already an emulsion.

During emulsification, several phases may appear. The word "phase" here refers to an actual visible, distinct liquid layer, as seen in a beaker. This layer may be an emulsion (water-in-oil or oil-in-water) or just oil, or just aqueous solution. A single phase emulsion is an emulsion where only one uniform layer is visible.

For the purpose of this study, a mixture is the result of blending a single phase emulsion with either crude or distilled water, or both. One or several phases may result, some of which may be emulsions.

Under the microscope, an emulsion will show the dispersed phase as droplets. Drops or droplets only refer to a liquid.

In the same fashion, particles only refer to solid fragments, in particular sand grains sometimes present in the emulsion.

By stability of an emulsion is meant its ability to remain in the same condition as when it was first formed. Signs of instability include separation of phases and/or change in drop size distribution.

By waterflood is meant the injection of distilled water in a sand pack initially saturated with oil and containing brine at an irreducible saturation.

By an emulsion flood is meant the injection of a slug of water-in-oil emulsion followed by the injection of distilled water in a sand pack with same initial saturation conditions as above.

3. LITERATURE REVIEW

3.1 CLASSICAL EMULSION THEORY

Emulsion theory has developed in fields such as chemistry and pharmacy where the components used are either pure or of known composition. Moreover the components are usually chosen such that viscosity does not cause any major problems during emulsification or during emulsion stability analysis. The fundamental principles, however, remain the same and shall be reviewed in the following paragraphs.

The major concern in any emulsion study lies with the interfacial phenomena. Emulsification is essentially a process by which new contact surfaces are created. For example, Martin (1969) reports that a cube of substance of volume 1 cm^3 has a surface area of 6 cm^2. When broken down into 10^{21} particles, the composite surface area is 6000 m^2, the area of a football field. Stability of the emulsion determines whether the two liquids can maintain such a large contact area or whether the surfaces collapse. During emulsification, stability is governed by the amount of energy stored in the surface area between oil and water. Any water-oil system tends to minimize this free surface energy by reducing the size of the contact area and by inducing coalescence of the dispersed droplets. To avoid this result, a surface-active agent can be added to either phase during emulsification. This agent reacts with components in the other phase to form soaps which gather at

the interface between the two liquids and lower the interfacial tension. Thus the work necessary to create new surfaces is minimized and the drops created are both smaller and of more uniform size.

Sherman and co-workers (1968) observed that smaller drops resulted in higher viscosity and greater stability. As the concentration of the dispersed phase increased, viscosity also increased but high concentration and high stability were usually incompatible. Also, lowering interfacial tension is not the only role of the emulsifier. Its real importance lies in the manner in which it affects the interface and determines whether the emulsion formed would be preferentially of the water-in-oil (W/O) or oil-in-water (O/W) type.

In classical emulsion theory, it is generally conceded that during mixing the phase added becomes the dispersed phase. There are several ways of mixing but Sherman and co-workers (1968) report that there is an optimal agitation time beyond which no further emulsification occurs. This optimal time varies between 1 and 5 minutes. Beyond that time, the rate at which new drops are created equals the rate at which colliding drops recombine. With regard to emulsification, they also add that the interfacial area generated increases with the rotational speed of the mixer, the stirrer diameter, and with a decrease in container tank diameter. Energy input increases as the rotational speed increases; this energy is stored in the emulsion through

creation of new interface. A larger stirrer diameter and/or smaller tank diameter increases the amount of turbulence generated by the blades which in turn intensifies the mixing of the two phases. The larger the difference in velocities, the larger the interfacial area created; the difference in velocities can be attributed either to a difference in densities or in viscosities. According to emulsion theory, emulsification becomes easier as temperature increases because both viscosity and interfacial tension may decrease. Viscosity may be modified either by additives or alteration of drop size. Many of the physico-chemical properties of emulsions depend upon drop size and drop size distribution.

Kitchener (1968), one of Sherman's co-workers, reviewed the concept of emulsion stability. He postulated that the addition of a third component was essential to the formation of stable emulsions. Such an additive may belong to one of four categories:

* inorganic electrolytes which create electrical double layers around the drops.
* soaps and detergent emulsifying agents with 1 or more pair of hydrophilic and hydrophobic groups.
* macromolecular emulsifying agents such as proteins, gums, and starches.
* finely divided insoluble solids collecting

at the interface between the drops and the continuous medium, such as asphaltenes.

The only way to achieve stability is by preventing drop coalescence. Two neighbouring droplets are subjected to both short and long range forces. Short range forces affect the structure of the interface while long range forces play a role in the flocculation. Coalescence may then occur following three possible mechanisms (see Figures 1 to 4):

* for large drops where forces of inertia are much larger than surface forces, a dimpling effect is observed. Coalescence may then occurs at the ring of contact.
* smaller drops remain convex and touch only at one point where coalescence begins.
* in the presence of an emulsifying agent, a flat lamella forms between two droplets and delays coalescence.

Hydrostatic forces tend to thin the film while surface forces oppose this tendency. The balance between the two determines the emulsion stability. Kitchener cites Derjaguin as the investigator of this phenomenon. Derjaguin defined disjoining pressure as the change in specific free surface energy with a change in lamella or liquid layer thickness. In the case of an emulsion, when two liquid drops are pushed toward one another, the pressure in the region between them increases rapidly. In the process, the liquid drops may deform themselves in different fashions. A

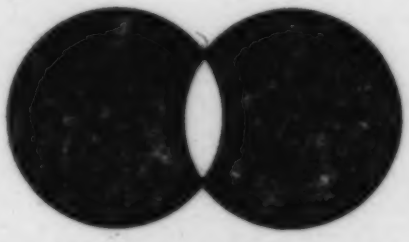

Dimpling Effect

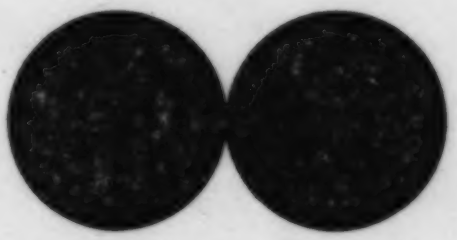

Point Contact

Lamella Effect

Figure 1. Patterns of Coalescence

Figure 2: Eyehill Crude - Dimpling Effect

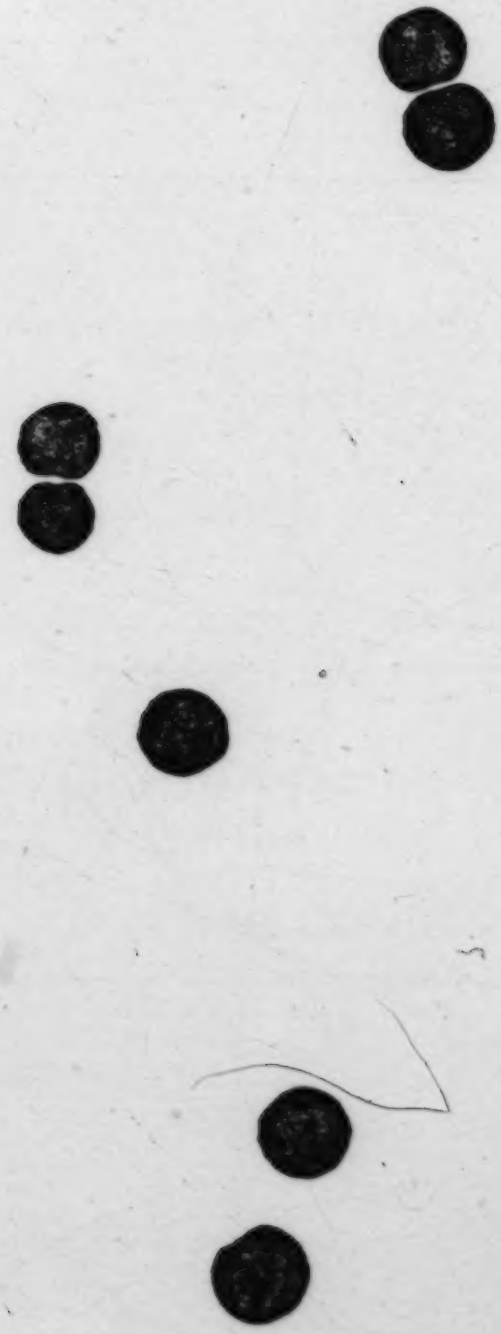

Figure 3: Eyehill Crude - Water Droplets Aggregations

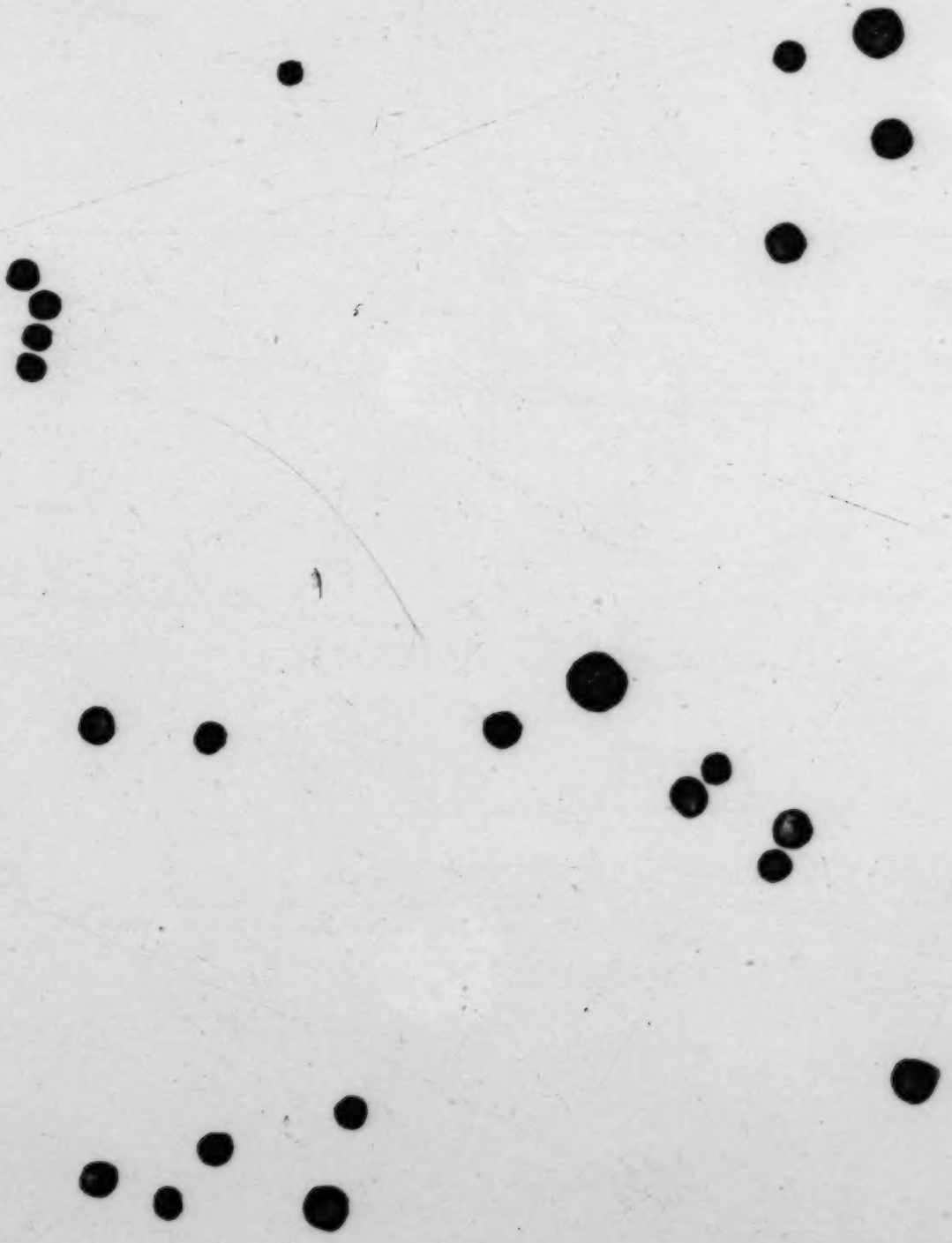

Figure 4: Eyehill Crude - Lamella Formation

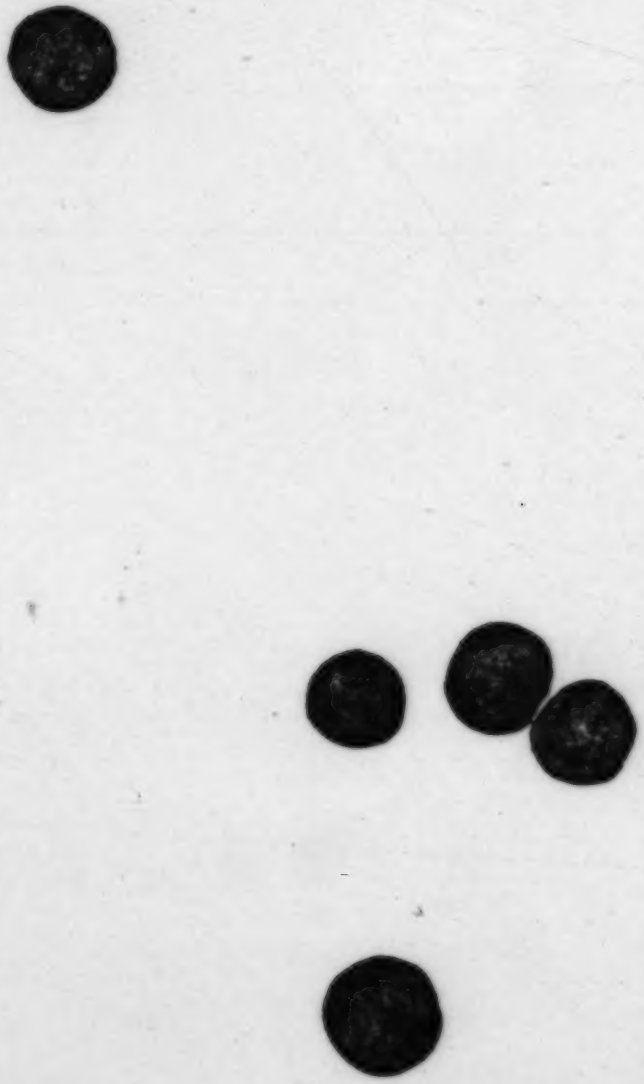

lamella may appear between them. Any deformation of a spherical shape means an increase in surface area and thus a local change in repartition of surface energy. According to Derjaguin, this change could be positive or negative depending on the thickness of the liquid layer. This means that the disjoining pressure can be positive or negative. If it is positive, it opposes hydrostatic forces; if it is negative, coalescence rapidly results. Derjaguin reached the conclusion that two types of forces were present at the lamella interface. He called surface force of the first kind the interfacial tension, γ, which acts along the plane of the interface. The surface force of the second kind is the disjoining pressure, $\Pi(h)$, which acts perpendicular to the plane of liquid film. Therefore, the total specific surface energy of a thin, plane, parallel lamella of liquid is given by

$$E = \gamma + \int \Pi(h) \cdot dh \qquad (1)$$

The integral is very small in magnitude compared to the interfacial tension but it is the only term affecting film equilibrium. Both attractive and repulsive forces should be taken into account in the evaluation of the surface forces of the second kind. Kitchener (1968) indicates that attractive forces between macroscopic bodies render thin liquid lamellae inherently unstable. The thinning would accelerate sharply as the lamella thickness reaches a critical "range of action". The actual coalescence would hence be a very rapidly occurring event.

Rubin and Radke (1980) formulated a physical model for the evolution of interfacial tension when a surface-active agent is transferred from one liquid phase to another. They decomposed the mechanism into five stages:

1. Convective-diffusion from one bulk phase to the interface
2. Adsorption into the interface
3. Reaction at the interface
4. Desorption from the interface
5. Convective-diffusion into the second bulk phase.

They also accounted for the fact that both liquid volumes are finite. Depending on the relative rates of adsorption and/or desorption at the interface, the resulting tension was observed to vary significantly. Rubin and Radke investigated the change in interfacial tension, γ, with time (Figure 5), with phase volume ratio, β, (Figure 6), and with the ratio of interfacial area to oleic phase volume, α, (Figure 7). Symbols Γ^* and t^* dehote reduced quantities. They explained their observations on the basis of a linear kinetics model which they described as the Henry sorption kinetics model. It can be represented as follows.

$$\text{Solute in phase 1} \underset{k_{-1}}{\overset{k_1}{\rightleftharpoons}} \text{Solute adsorbed} \underset{k_{-2}}{\overset{k_2}{\rightleftharpoons}} \text{Solute in phase 2}$$

Constants k_1 and k_2 represent the adsorption rates while k_{-1} and k_{-2} represent the desorption rates. In addition, they

expressed the net rate of adsorption from either phase per unit area, $R_{a,i}$ as

$$R_{a,i} = k_i \cdot C_i^s - k_{-i} \cdot \Gamma \quad , \; i=1,2 \tag{2}$$

where k_i and k_{-i} were the adsorption and desorption rate constants, C_i^s is the concentration of surface-active agent in the adjacent sublayer of phase i, and Γ is the relative surface excess concentration of surface-active agent. They found a strong dependence of Γ on the relative values of the sorption rate constants (Figure 8).

Rubin and Radke also reported three other equations which completed the mathematical description of the mechanism. Levich's equation accounted for any accumulation of surface-active agent at the liquid-liquid interface

$$\frac{d\Gamma}{dt} = R_{a,1}(C_1^s, \Gamma) + R_{a,2}(C_2^s, \Gamma) \tag{3}$$

In each liquid phase, convective-diffusion followed the Nernst film model

$$V_i \cdot \frac{dC_i}{dt} = -\frac{A \cdot D}{\delta_i}(C_i - C_i^s) \quad , \; i=1,2 \tag{4}$$

where C_i is the surface-active agent concentration in the bulk of the liquid phase i, D, the surface-active agent diffusion coefficient and δ_i, the Nernst film thickness coefficient. In addition, V is the volume of phase i and A, the interfacial area.

Rubin and Radke mentioned a third equation expressing the net rate of adsorption in terms of the convective-diffusion coefficient

$$R_{a,i} = \frac{D_i}{\delta_i} \cdot (C_i - C_i^s) \quad , \; i=1,2 \tag{5}$$

Initially the concentration of surface-active agent in phase

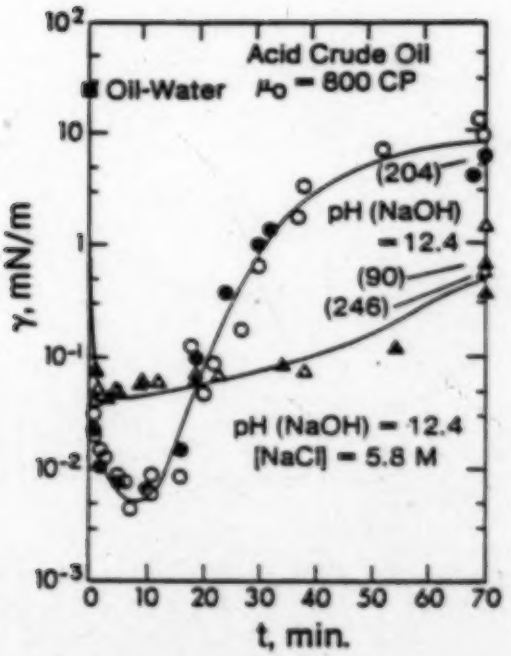

Figure 5. Experimental dynamic tensions for an acid crude oil (Long Beach California) in caustic. Differing symbols of the same shape indicate independent experiments, and the numbers in parentheses indicate time in minutes.(from E. Rubin and C.J. Radke, Chem. Eng. Science, 35, Copyright [1980], Pergamon Press, Ltd).

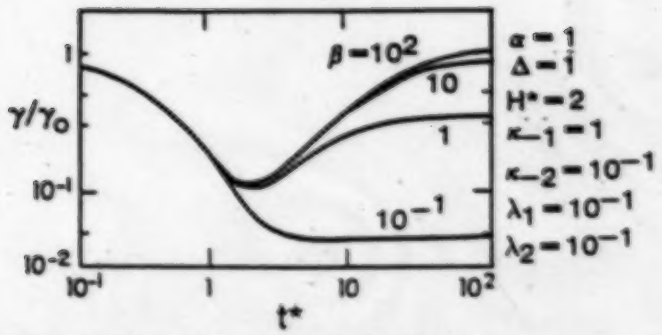

Figure 6. The effect of phase volume ratio β on dynamic tension. (from E. Rubin and C.J. Radke, Chem. Eng. Science, 35, Copyright [1980], Pergamon Press, Ltd).

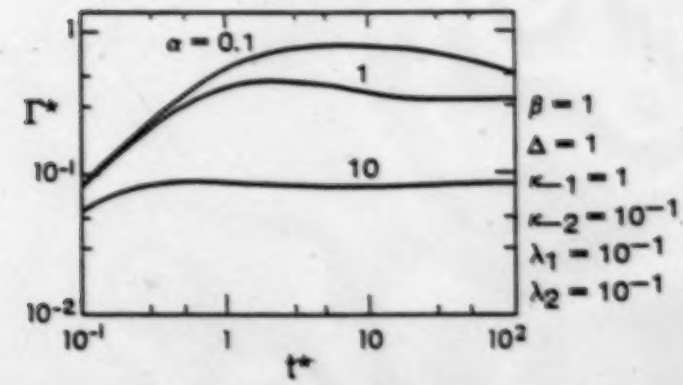

Figure 7. The effect of α on transient solute adsorption. (from E. Rubin and C.J. Radke, Chem. Eng. Science, 35, Copyright [1980], Pergamon Press, Ltd).

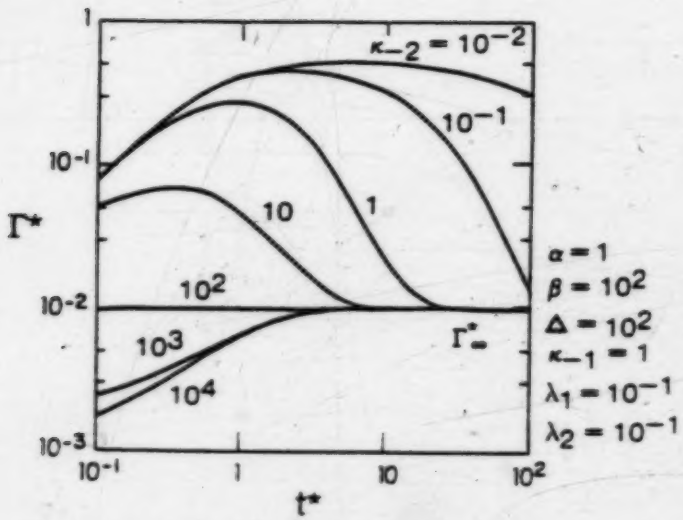

Figure 8. The effect of κ_{-2} on transient solute adsorption for a large volume ratio of phase 2 to phase 1. (from E. Rubin and C.F. Radke, Chem. Eng. Science, 35, Copyright [1980], Pergamon Press, Ltd).

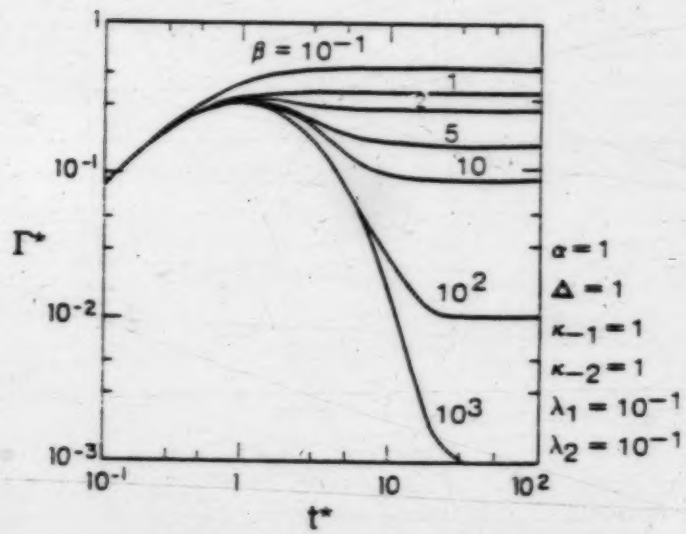

Figure 9. The effect of phase volume ratio β on transient solute adsorption (from E. Rubin and C.J. Radke, Chem. Eng. Science, 35. Copyright [1980], Pergamon Press, Ltd).

1 is a constant, concentration in phase 2, zero, and adsorption, zero.

Figure 5 shows a very strong time dependence of interfacial tension on an acid crude-caustic solution system. In Figure 8, the dimensionless surface excess concentration of surface-active agent, Γ^*, is seen to be a strong function of the difference in magnitude between the reduced desorption coefficients in the two liquid phases, everything else being constant. In Figure 9 only the phase volume ratio is varied and Γ^* varies over up to three orders of magnitude. If the surface excess concentration of surface-active agent varies, the interfacial tension, γ, also varies. Rubin and Radke reported that

$$\gamma/\gamma_o = 1 - H^* \cdot \Gamma^* \qquad (6)$$

where γ_o is the tension between the two liquid phases when there is no surface-active agent and H^* is a measure of the ability of the surface-active agent to lower interfacial tension. Therefore, interfacial tension is shown to be a strong function of volume ratio at any given time.

Figure 6 represents γ/γ_o versus time for different desorption rate constants. Again, strong dependence of γ upon β can be observed. Finally, since volumes of each phase were finite, variations in the ratio of interfacial area to phase volume, α, had an effect on interfacial tension. This effect can be seen in Figure 7; at any given reduced time t^*, α has a large effect on Γ^*, the reduced excess concentration of surface-active agent at the

interface.

In their experiments, Rubin and Radke used mineral oils containing known amounts of oleic acid and contacted with caustic-sodium chloride solutions. Use of these results for elucidating the behaviour of petroleum crude oils contacted with caustic solutions can therefore only be qualitative.

Rheology is another field where emulsions show peculiar patterns of behaviour. Rheology may be defined as the study of deformation and flow of matter. Sherman and co-workers (1968) report that concentrated emulsions tend to behave like solids in the initial stages of shear. But emulsions do not have the ability to return to their initial state like a solid . The shearing work exerted would not be totally dissipated either, as with liquids. Emulsion behaviour lies somewhere in between these two extremes and whether it approaches more the solid or the liquid behaviour depends on the nature and concentration of the dispersed phase. This was observed by Frederickson (1964) as reported by Sherman.

Most emulsions obey non-Newtonian fluid flow models. Otswald and de Waele (1925) were the first to alter Poiseuille's equation to include plastic flow. However, power law equations are not physical laws and one can only acknowledge the dependence of apparent viscosity on rate of shear. Sherman (1968) observed that no completely satisfactory theory has yet emerged to explain non-Newtonian flow. Existing flow theories are based on a

flocculation/deflocculation model and assume a long chain configuration for aggregate structures. Sherman added that W/O emulsions form complex aggregates which render the elaboration of a proper model more difficult.

Finally it has been recognized that drop size and size distribution affect emulsion behaviour in many ways. Sweeney and Geckler (1954) first indicated that drop size influences the flow properties of emulsions. In particular, they observed that the smaller the drop size is, the smaller the dispersed phase concentration needs to be for it to have a pronounced influence on the emulsion rheology. In fact, when the mean diameter is less than a few microns, the influence of drops of diameter smaller than the mean will be larger than the influence of drops of diameter greater than the mean. Consequently, a plot of apparent viscosity as a function of mean diameter would not reflect the full influence of drops with sizes below the mean diameter. Viscosity data for emulsions with the same mean diameter can only be compared if the size distribution patterns are the same. It does not follow that different emulsions would have identical mean sizes just because they are prepared according to the same procedure. This is especially true in the case of emulsions of different dispersed phase concentrations. More energy has to be applied to higher concentration emulsions in order to obtain the same mean size.

3.2 EMULSIONS IN PETROLEUM RESEARCH

By its very nature, industrial research has been more inclined to direct its efforts toward finding practical solutions to specific problems caused by emulsions in the field rather than to attempt to develop fundamental knowledge on petroleum emulsions in general. Most of the work has been done with microemulsions and micellar solutions rather than macroemulsions.

Some interesting observations were reported in the field of interfacial tension. Dupeyrat (1978) noted that for a fixed sulphonate concentration the value of interfacial tension decreases monotonically as salinity is increased. Similar results were found by Cooke et al as reported by Chan (1979). Cooke noticed that the reaction of caustic solutions with organic acids in the crude oil resulted in the formation of soaps at the oil/water interface. Not only was the interfacial tension substantially reduced but the sand wettability was reversed from water-wet to preferentially oil-wet given the right pH, temperature and salinity conditions. Subsequently, a viscous W/O emulsion was produced. Chan (1979) added that of all parameters, the presence of salt in the caustic solution was essential in achieving this wettability reversal. Salt in solution prevented solubilization of the soaps; in the absence of salt, the soaps became soluble in the caustic solution and favoured water-wetting of the sand grains.

An interesting observation was reported by Rubin and Radke (1980) citing McCaffery's work on alkaline waterflooding. His dynamic interfacial tension model showed that the manner in which interfacial tension increases beyond the local minimum value depends on the volume ratio of water to oil; the larger the volume ratio, the larger the interfacial tension. The implications are far-reaching. For example, in the spinning drop apparatus the volume ratio is between several hundred and a thousand, according to McCaffery. In the oil reservoir however, the volume ratio is between one and three. McCaffery concluded then that the spinning drop interfacial tension data is only indicative of the lowest achievable reservoir equilibrium value.

Jones et al (1978) reiterated that low interfacial tension alone is not a guarantee of emulsion stability. In this respect their work agrees with classical emulsion theory. However, they noted that significant changes in interfacial properties occurred with aging even though the emulsions were kept under a nitrogen blanket.

MacKay et al (1973) in their study of W/O emulsions formed after an oil spill found no change in interfacial tension value as the surfactant concentration was increased. They concluded that their emulsions were not typical and that the water/oil interface did not exhibit the usual electric double layer.

Strassner (1968), in his study of the effect of pH on interfacial films and emulsion stability, reported that

maximum interfacial tension coincided with minimum interfacial film formation around a pH value of 6.

Little attention has been given in petroleum research to the effect of preparation method on the resulting emulsions. Berridge et al (1968) noted the formation of an O/W emulsion which under vigorous agitation reverted to a W/O "mousse". The term mousse was coined during the Torrey-Canyon incident which sent 200000 tons of oil on the coasts of the English channel. Choice of the word "mousse" was mainly guided by the froth-like appearance of the water-in-oil emulsions obtained. This term will be used repeatedly throughout this study. Berridge et al (1968) prepared emulsions with distilled water, tap water and sea water; in all cases, mousses were obtained. They also observed that mousses made from high asphaltene content crude were stable for many months. Their conclusion was that asphaltenes play a key role in mousse formation.

The largest contribution of the petroleum research has been in the correlation of emulsion stability with the nature of the interfacial films. Strassner (1968) recognized that emulsions are stabilized primarly by films. He determined that asphaltenes and resin fractions were sensitive to pH and that this in turn affected their ability to form films, stabilize emulsions and influence wettability. From his study emerged four major observations:

* acid pH is most favourable to the formation of strong rigid interfacial films produced by asphaltenes.
* basic pH is ideal for the formation of mobile interfacial films produced by resins.
* the presence of asphaltenes will render silica preferentially oil-wet.
* asphaltenes make more stable emulsions than do resins.

Strassner (1968) also confirmed some well-known results. An acid pH results in the formation of a stable W/O emulsion with solid films at the liquid-liquid interface. Such an emulsion promotes oil-wetting. A basic pH produces a stable O/W emulsion with mobile soap interfacial films. Characteristically, water-wetting results. Note the correspondence between the nature of the external phase and preferential wetting.

Jones et al (1978) added that these interfacial films behave as mechanical barriers to coalescence; emulsion stability depends on the time required for these interfacial films to form. The longer the two liquids are in contact, the greater the stability. For North Sea crude oils, they found that incompressible non-relaxing films produced highly stable emulsions independently of the salinity as long as the calcium ion content was high. As an aside, they reported that most W/O emulsions break down when subjected to temperatures higher than 65°C.

Cratin (1969), studying the effect of pH on emulsions, concluded that stability was at a minimum at the phase inversion point.

As a final note, Jennings et al (1974) investigating the caustic waterflooding process for heavy oils observed that a stable emulsion diluted with distilled water to a caustic concentration of 0.005 weight percent (0.00125 M) retained all its stability.

One can make several observations when comparing the classical emulsion theory as it is being investigated with pure liquids and the petroleum research as it is being done in the industry. The areas of concern are not always the same. The oil industry is not so much concerned with the problem of creating emulsions as it is with the problem of demulsification. The majority of the oil produced throughout the world is produced as an emulsion and separating the oil from the water has always been, so far, the chief goal. As a result, interfacial tension, the influence of mixing, and the concept of stability have been the three most studied areas of emulsion formation.

4. STATEMENT OF THE PROBLEM

A systematic approach was followed throughout this study. The first parameter to be investigated was interfacial tension. The lower the interfacial tension between the crude and the caustic solution, the better the two would mix and the better the resulting emulsion would be. Once the lowest possible interfacial tension had been determined, the optimal caustic concentration had thus been fixed.

The second parameter to be investigated was the relative volumes of crude and caustic solution (at the optimal concentration) needed for the resulting emulsion to be a single phase. This emulsion was completely defined by the amount of crude and caustic solution involved, and by the concentration of the caustic solution. Now that a particular emulsion had been selected, the object of the study was to thoroughly test it.

In a field situation, this particular emulsion would be used to displace oil in the reservoir. In doing so it may come in contact not only with oil but also water. As a result, the emulsion may be altered by going from single phase into two phases or its viscosity may increase to the point where the emulsion would plug the porous medium.

In an attempt to predict the behaviour of the emulsion in-situ, the chosen emulsion was tested by mixing it with various amounts of crude and distilled water. This resulted in a series of ternary diagrams showing the number of phases observed in each case (Figure 29), the water content in each

phase (Figure 30), and the apparent viscosity at a set shear rate for each mixture (Figures 40 to 42). This same emulsion was also studied for stability under solvent addition. Four different types of solvents were tried. For different amounts of solvent, different reductions in viscosity of the emulsion were observed and recorded. It was decided to add some solvent to the basic emulsion to control its viscosity.

The last step was to take this emulsion of optimal composition and see how it would assist oil recovery in a laboratory sand pack displacement experiment. Different sizes of emulsion slug were tested in two cores. The results were compared with a reference waterflood.

5. EXPERIMENTAL EQUIPMENT, MATERIALS AND PROCEDURE

5.1 EMULSIFICATION

5.1.1 Interfacial Tension

In the light of the comments observed in the literature, the Du Noüy tensiometer was chosen to measure interfacial tension between the different caustic solutions and oil. The Du Noüy tensiometer provided more versatility by enabling the investigation of the effect of oleic/aqueous phase volume ratio on the value of interfacial tension.

The principle of operation of this tensiometer is to exert a force on the interface between the two liquids via a platinum iridium ring (see Figure 10). At the point where the ring breaks through the interface, the force exerted via the tensiometer just exceedes the interfacial force between the two liquids. The interfacial tension can then be calculated by applying the proper correction factors for the equipment and for each reading (see Figure 11).

There are two types of limitations to the use of this tensiometer. First, its reliability is greatly reduced when the value of interfacial tension falls below 1 dyne/cm. For such small values, the spinning drop method is more accurate. Second, at high interfacial tensions (corresponding to low surface-active agent concentration in the aqueous phase) the interface between the two liquids is no longer uniformly horizontal. A cusp in the oil phase

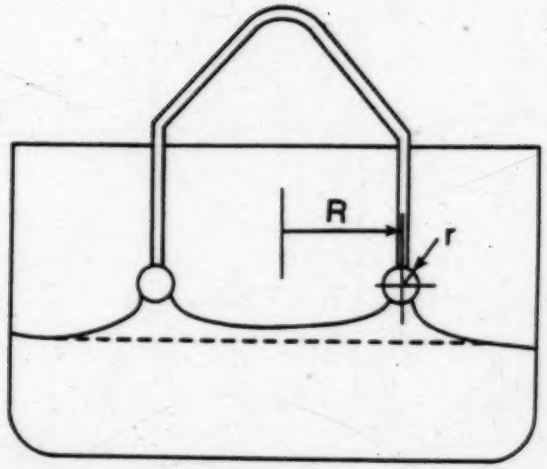

Stage 1 Interfacial Film is Stretched

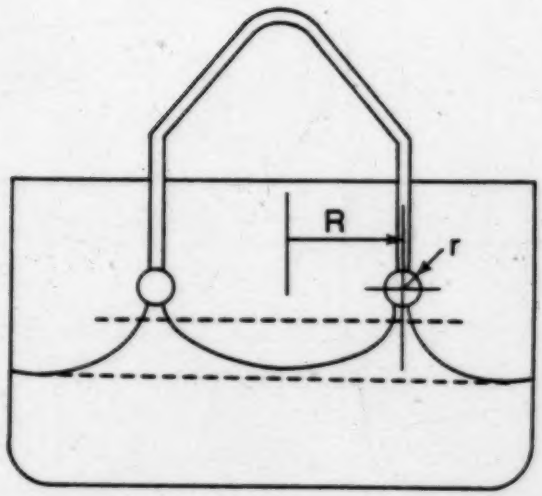

Stage 2 Film Rupture is Impending

Figure 10. Interfacial Tension Measurement

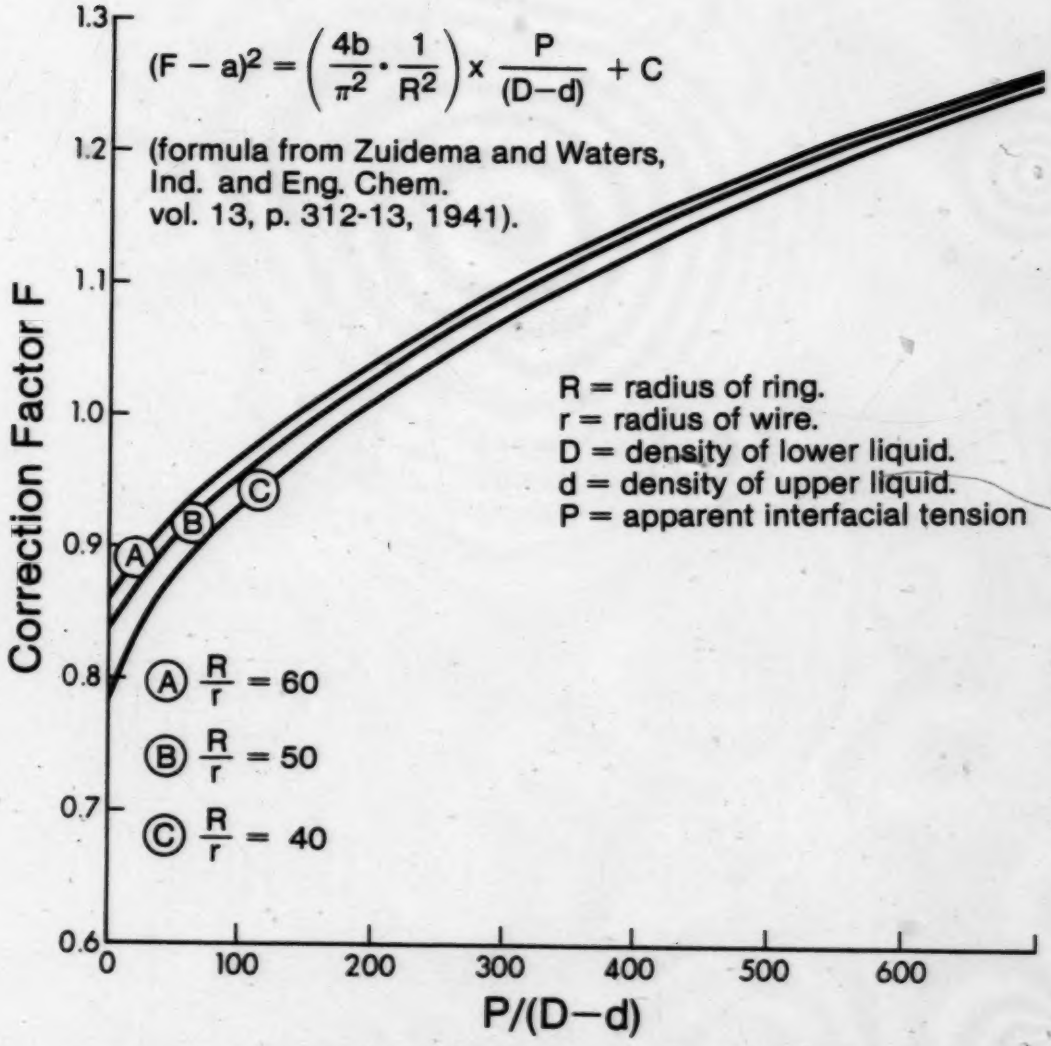

Figure 11. Correction factor for surface and interfacial tension by ring method with 6 cm ring (upward pull only) For Cat# 70535 & #70545 Kruss-Dunouy Tensiometers (Courtesy of Central Scientific International).

develops and interferes with the measurements; the platinum iridium ring tends to slide on one side of the cusp and give erroneous readings. Careful positioning of the ring is necessary for it to always remain horizontal prior to rupture of the interface. An additional problem which becomes more pronounced as the viscosity of the oil increases is the drag of the oil on the wire frame supporting the ring. This drag delays the response time of the interface to an increase in force applied; it also decreases the magnitude of that response. The result is usually an overestimate of the value of interfacial tension. Sometimes also, a film may form between the wire frame cross bar and the oil surface; it must be removed otherwise the work necessary to create that surface will be measured by the tensiometer and superimposed on the work necessary to break through the liquid-liquid interface. Interfacial tension would again be overestimated. Nevertheless, the Du Noüy tensiometer gave reproducible and reasonably accurate results in this study.

5.1.2 Emulsion Preparation

Consideration was given to classical emulsion theory with regard to the effect of mixing time and shape of the blending container. All mixtures were stirred for five minutes at high speed in a blender; the design of the blender was such that the walls were very close to the blades of the mixer as can be seen in Figure 12: the more

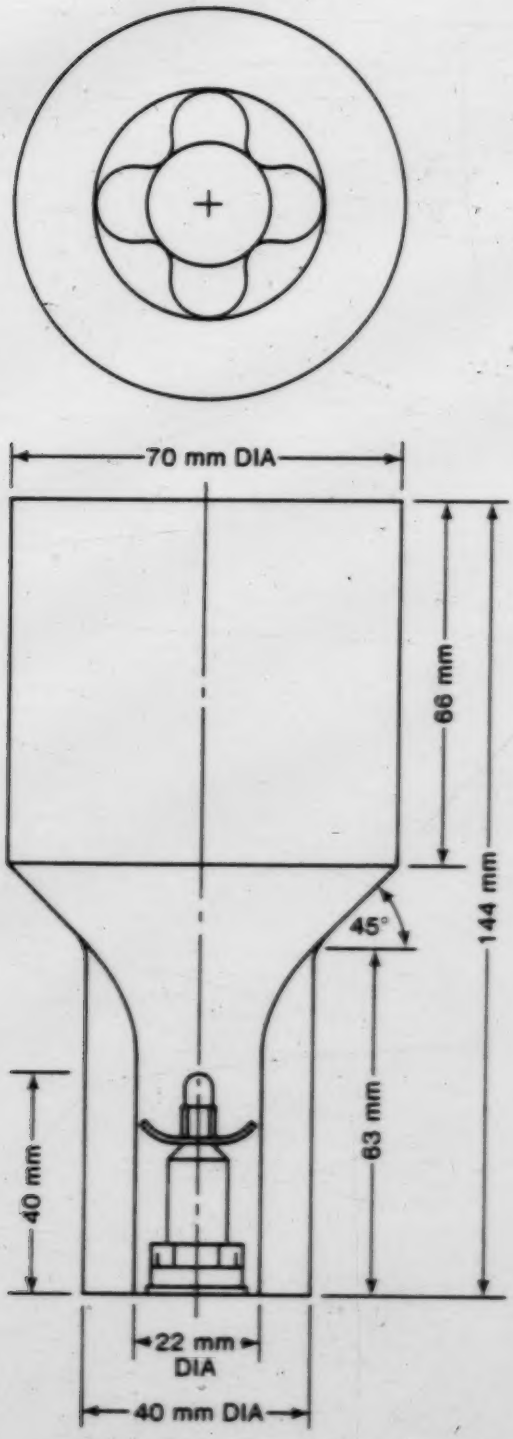

Figure 12. Cross-Sectional View of the Inner Portion of the Blending Container

intense the agitation, the better the emulsification. The container was surrounded by a jacket through which distilled water was circulated; this minimizes the effect of heating which inevitably occurs during mixing and affects the properties of the emulsion formed. Table B-2 (Appendix B) provides the values of temperature before and after mixing for different combinations of crude and caustic solution.

Because oil would stick to the sides of a beaker, volumes could not be measured accurately. Therefore, the oil had to be weighed. Table B-1 (Appendix B) reports sample measurements. Oil density was known from previous calculations and used to determine the corresponding volumes.

A syringe was filled with oil and emptied prior to the start of the experiments so that the amount removed from the beaker with the syringe was exactly the amount put in the emulsion. Preparation procedure was as follows:

1. 100 ml of 1.0 percent by weight (0.25 M) sodium hydroxide solution was diluted to 1000 ml of 0.10 percent by weight (0.025 M) sodium hydroxide solution.
2. 200 ml of crude were weighed; the weight was recorded.
3. The weight of the amount of crude to be blended was determined.
4. The volume of solution required was measured by pipetting it in a beaker.
5. The solution temperature was recorded.
6. First, the liquid with the largest relative volume was

poured into the blender.

7. If this liquid was oil, it was poured until the scales indicate the correct amount has been added. For the last ml, a syringe was used.
8. The liquid was agitated by putting the blender on 'blend'.
9. The other liquid was poured in.
10. After the last drop was added, 5 minutes of blending were counted with a stopwatch.
11. The blender was stopped. A drop of emulsion was put in water, and a drop in toluene. An oil-in-water emulsion will be soluble in water; a water-in-oil emulsion will be soluble in toluene.
12. The emulsion was poured into a jar and labelled.
13. Emulsion temperature was measured.
14. It was left to stand 24 hours.
15. A sample of the water-in-oil emulsion was distilled.
16. The pH of each phase was measured (when possible).
17. If the emulsion was stable, its viscosity was measured.

The phase with the largest relative volume was placed in the blender first to ensure a more homogeneous mixing of the smaller volume phase. When more than two phases were mixed, the oleic phases were placed in first and the aqueous phase last. The consistency of procedure was perceived as a step toward reproducibility of results. The basic emulsion (92 percent crude , 8 percent solution at 0.10 percent sodium hydroxide by weight (0.025 M) was prepared in batches

of 200 ml at a time, following exactly the procedure for all previous emulsions.

The mixtures were prepared as follows:

1. The percentage of each component to be blended was determined: emulsion, crude oil, and distilled water.
2. The percentage distilled water was converted to a volume. This volume was pipetted in a beaker.
3. The percentage emulsion was converted into a weight, knowing the density.
4. A beaker of emulsion was weighed and its weight was recorded.
5. The emulsion was poured in the blender. To ensure exact volume was added, a syringe was used for the last ml.
6. Steps 3 to 6 were repeated for the crude oil.
7. The blender was switched to "blend".
8. The distilled water was poured in.
9. The last drop was added as the stopwatch was started.
10. Five minutes were counted and the blender was stopped.
11. The mixture was poured into a jar.
12. The mixture temperature was measured.
13. The jar was labelled.
14. The mixture stood for 24 hours before testing it.

The order in which the three components were placed was maintained throughout. Crude was added to the mixture while the latter was at rest. The distilled water insured uniform mixing by passing through both layers and reaching the rotating blades. The water was always poured at the center

of the blending container, above the blades.

The pre-mixing effect was therefore retained to a certain extent. This effect is always beneficial to emulsion stability. In this case high viscosity of the emulsion and of the crude oil render pre-mixing less effective. The composition of each mixture is listed in Table B-5, Appendix B.

It is recognized that the manner in which an emulsion is prepared will influence its stability to a large extent. Temperature, rotating speed, type of blades, size of batch prepared and solution composition are determining factors.

5.1.3 Microscope Observations

The apparatus used was a Wetzlar microscope. Useful accessories included an ultraviolet light source and a camera mounted in parallel.

Ultraviolet light assisted in determining the nature of the phases under scrutiny. Since oil appears olive green under such light while water becomes black, it was then possible to determine whether a mixture was an oil-in-water or a water-in-oil emulsion.

The camera permitted taking pictures under normal light only. These pictures were used qualitatively to obtain an idea of the appearance of the emulsion or to follow an emulsion and see whether it destabilized with time.

For quantitative studies such as drop size distribution, all pictures were taken at the same high

magnification and enlarged to 8 in. by 10 in. prints. The procedure used was as follows. One drop of crude was diluted 50 times with a suitable solvent and placed on a special glass slide and under a cover slip. When a representative sample was found, the microscope was first focused on the smaller drops and a picture was taken. Several pictures were then taken at different depths of field; each time a larger drop size was in focus. When the largest visible drop had been photographed, the frame was moved to another spot and the process was repeated until the number of drops photographed was judged sufficiently large for the population to be representative.

The film was then developed into 8 in. by 10 in. prints. On each print, the drops in focus were circled with ink. The pictures were then sent for bleaching and came back absolutely white except for the ink rings. All rings were filled in and the pictures were sent through an image analyser to determine the surface area of each drop. Then using a computer program the arithmetic mean diameter and standard deviation were obtained.

One problem attached to these observations pertains to the nature of the liquid under consideration. Because the lamella of fluid is very thin and trapped between two large glass surfaces, the effect of preferential wetting will be quickly felt. Since glass is oleophobic, dispersed water droplets tend to gather on the glass surface and to coalesce among themselves. This was observed on a few occasions but

it was by far the exception and not the rule.

5.1.4 Rheological Properties

The appparatus used was a Weissenberg rheogoniometer. This versatile viscometer allows measurement of shear stresses and shear rates over a very wide range. Shear rates can be selected with a gearbox and communicated to a conic bottom platen; there are 60 different shear rates to choose from, and 7 different torsion bars. The Weissenberg rheogoniometer is a precision cone and plate arrangement. The tip of the cone is truncated to avoid damage by abrasion to the top flat platen. This platen can be moved vertically and positioned at a distance from the bottom cone such that it would be just touching the imaginary tip. Given the angle of the cone, the gap between the two platen at the center of is 25,000 nanometers (25 microns). The width of this gap is determined by a calibrated transducer.

A calibration curve of shear stress versus voltage output was established using a Can-Am Newtonian calibration fluid with a viscosity of 0.950 Pa·s (950 cp) for three different shear stress transducer attenuations (see Appendix F, Figures F-1 to F-4).

A new set of calibration curves must be obtained when the torsion bar is changed. An appropriate calibration fluid must be used. If the torsion bar is designed to measure smaller shear stresses, the calibration fluid must have a lower viscosity. The chart recordings could then be

interpreted and the plot of shear stress versus shear rate yielded the rheological behaviour of the fluid under consideration. All measurements were recorded in a controlled environment at 25°C.

Shear rates are both exact and constant because of the gearbox selection feature. By setting the rheogoniometer and the electric motor on two separate tables, the amount of vibrations transmitted to the bottom platen is kept to a minimum. Shear stresses are transmitted by the top platen to a transducer; the current generated is then plotted on a chart recorder.

The Weissenberg rheogoniometer has many advantages over other viscometers. It provides the largest array of measurable shear stresses and shear rates. Each shear rate is known and constant during a run. Other viscometers, such as the Brookfield, have spindles of irregular shape where the rate of shear will be different in different locations. The Weissenberg also requires very small amounts of sample compared to other viscometers which often need 500 ml or more to provide an unbiased reading. Time is also saved during the cleaning of the apparatus and changing of the sample.

5.2 SAND PACK DISPLACEMENTS

A layout of equipment set-up can be seen in Figure 13. The core holders were made of two and a half inch nominal size stainless steel pipe. They came in two lengths: 0.609

m (2 ft) and 1.22 m (4 ft), equipped with flanges. Inlet and outlet ends were covered with cintered metal screens to induce a more uniform injection fluid distribution. The material used was a 70 to 140 mesh Ottawa sand. The crude oil and emulsion injected passed through a Millipore filter block to remove the solid impurities the fluids may contain. The average sand pack porosity was about 41 percent; the average permeability was about 13.5 Darcies.

5.2.1 Packing the Core

It was decided to use the following wet packing procedure. The core holder was closed at one end with a flange; water and sand were added alternately so that the sand poured through the open end of the core holder held in the vertical position would always fall through a small head of water. Once the sand pack was completed, it was vibrated for an hour to allow sand grains to settle and form a tighter pack.

The advantage of this method over dry packing is that it reduces the tendency of the sand grains to segregate according to weight. A gradation of particles would then occur between one end of the core and the other, when in fact what is sought is a uniform distribution of all particle sizes. Wet packing also removes the need for evacuating the dry sand pack and saturating it with water. Wet packing eventually saves both time and effort without jeopardizing the properties of the resulting sand pack.

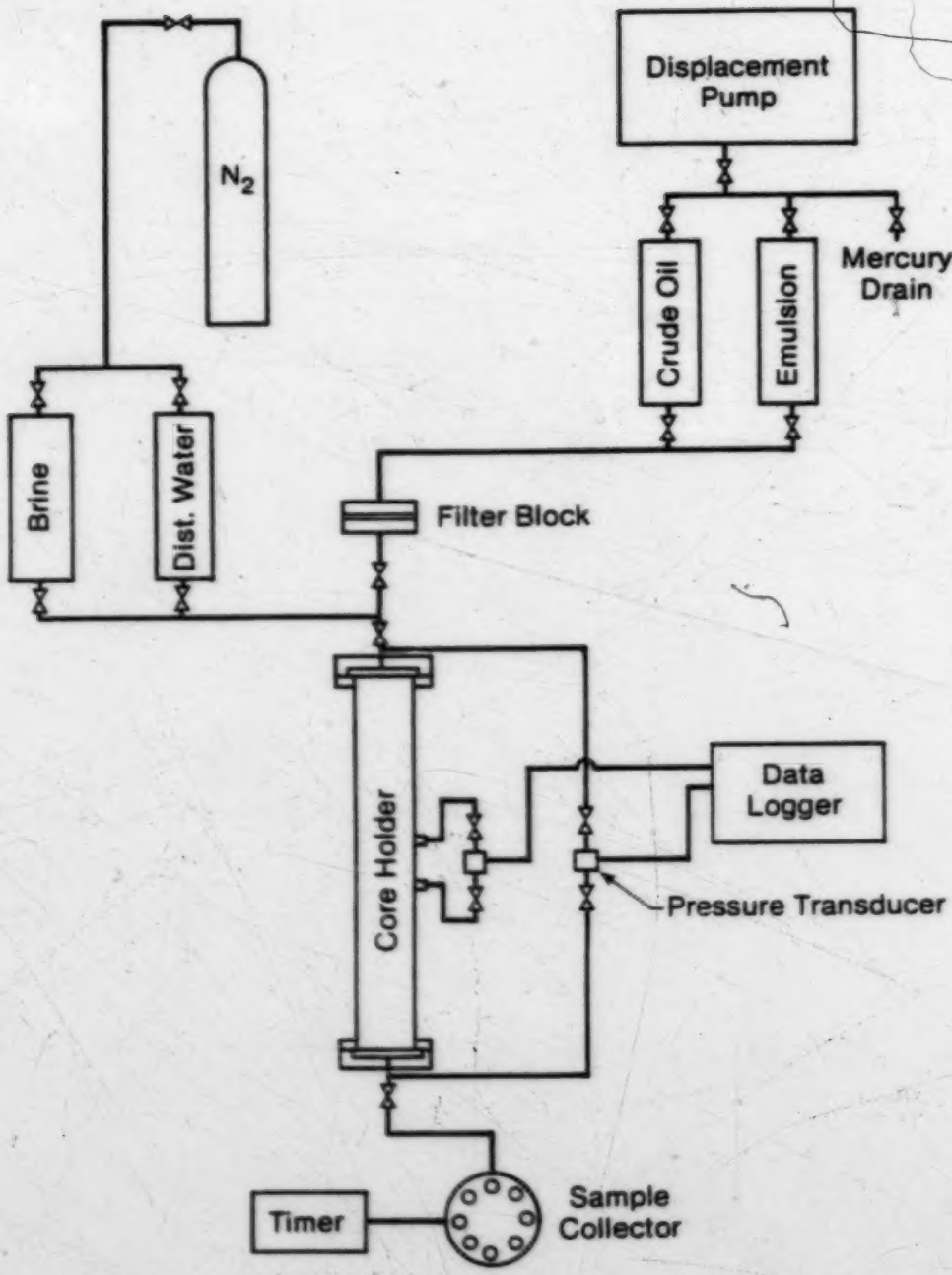

Figure 13 EQUIPMENT LAYOUT

5.2.2 Determination of Permeability

The sand pack was then ready for testing and the first property to be measured was permeability. By flowing through at a constant rate the same distilled water that was used for packing, and measuring the pressure drop transmitted to a data logger by a pressure transducer, the absolute permeability of the sand pack was calculated using Darcy's equation.

5.2.3 Determination of Porosity

A 5 percent by weight sodium chloride brine was injected into the sand pack. Fluids at the outlet were collected in 50 ml glass centrifuge tubes and analysed for salt content using an Abbé refractometer. The cumulative volume of effluent produced was then plotted against brine concentration, yielding a characteristic S-shaped curve (see Figure 14). By balancing graphically the areas above and below the curve the pore volume was determined and porosity calculated accordingly. Data for each sand pack is recorded in Table G-4, Appendix G. Graphical representation of the results for cores #4, 5, and 6 is presented in Figure G-1, Appendix G.

5.2.4 Displacement Procedure

After the sand pack properties had been determined, heavy oil was injected to displace the brine by drainage via a positive displacement Ruska pump. The sand pack was held

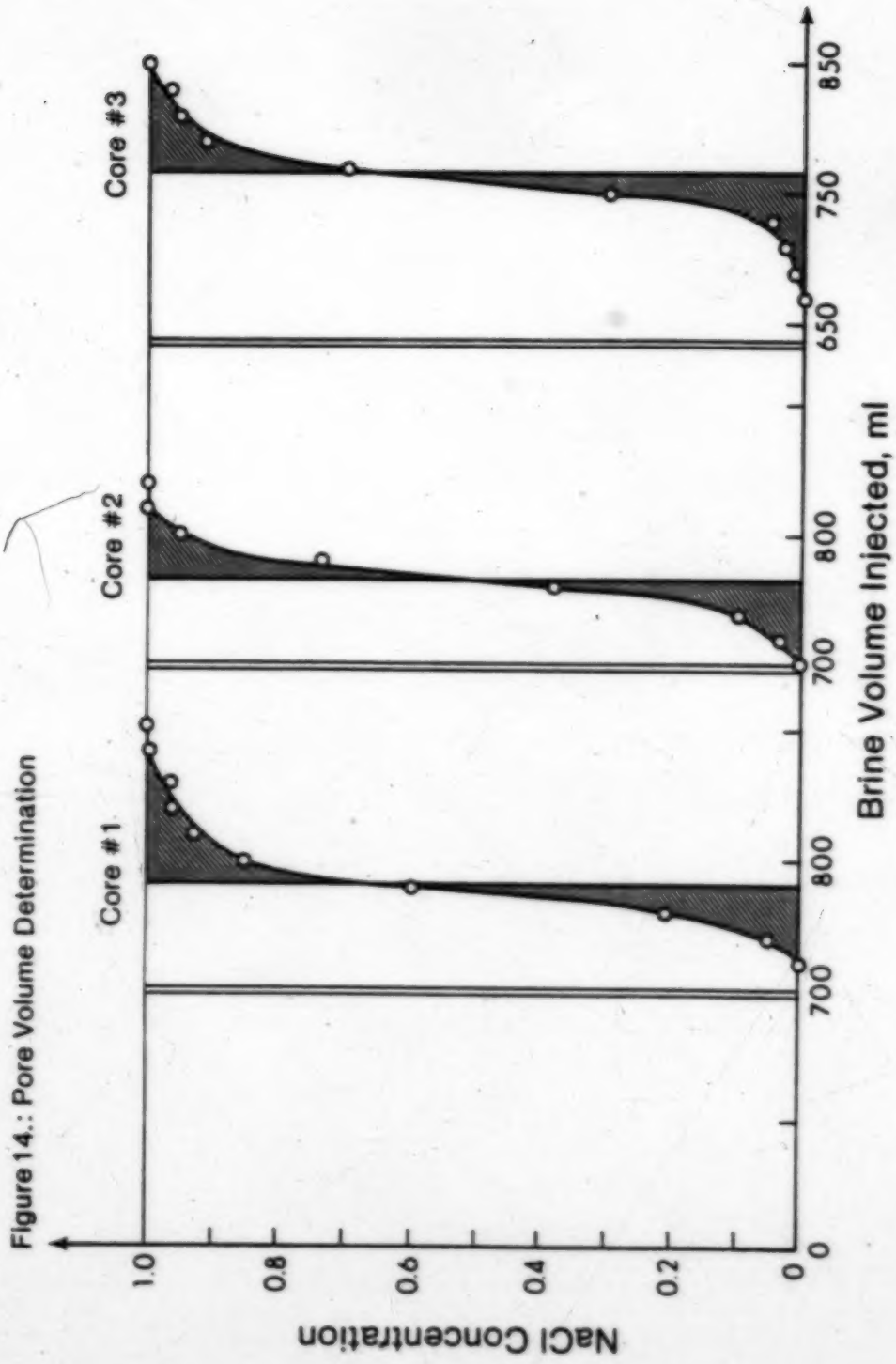

Figure 14.: Pore Volume Determination

vertical and heavy oil was injected at the top; oil being lighter than brine, the interface between the two liquids during displacement was as horizontal as it could be, ensuring an efficient and stable displacement. The effluent was collected in 2000 ml graduated cylinders and drainage was continued until the amount of aqueous phase produced represented less than 2 percent of the effluent. The brine was then at its irreducible saturation. The volume of oil in the sand pack could be calculated knowing the pore volume. Initial sand pack conditions are shown in Table G-3, Appendix G.

The emulsion slug was then injected in the porous medium in the same manner and driven by a suitable waterflood. When this water broke through, the emulsion flood was continued and the oil production history determined through analysis of effluent samples collected at regular intervals in centrifuge tubes. The experiment was stopped when the oil fraction collected in the effluent dropped below 5 percent. Oil recovery from various emulsion floods were compared with that for a standard waterflood conducted at the same injection rate.

6. DISCUSSION OF RESULTS

6.1 INTERFACIAL TENSION

Three series of runs were performed at three different volume ratios. In all three series, it was observed that the interface between the two liquids was cusped for sodium hydroxide concentrations of 0.00 to 0.05 percent by weight (0.00 to 0.0125 M). At higher concentrations, the interface was horizontal.

A large decrease in interfacial tension was noticed in each case as sodium hydroxide concentration increased to 0.10 percent by weight (0.025 M). Surface-active agents present in the oil have reacted with sodium hydroxide in the water to form soaps at the interface between these two liquids. Presence of small amounts of these soaps lowered interfacial tension considerably.

In Figure 15 it can be noted that interfacial tension is very low and constant for all concentrations higher than 0.05 percent by weight (0.0125 M). The oil to caustic solution volume ratio is one to three.

Figure 16 shows that even if some data scattering occurs around the minimum, the trend at higher concentrations is toward increasing interfacial tension at a one to one volume ratio. Figure 17 shows that even if there is a minimum value at 0.10 percent sodium hydroxide by weight (0.025 M), the interfacial tension keeps dropping as concentration volume increases, for an oil to caustic

Figure 15. Interfacial Tension between Eyehill Crude Oil and Caustic Solution.

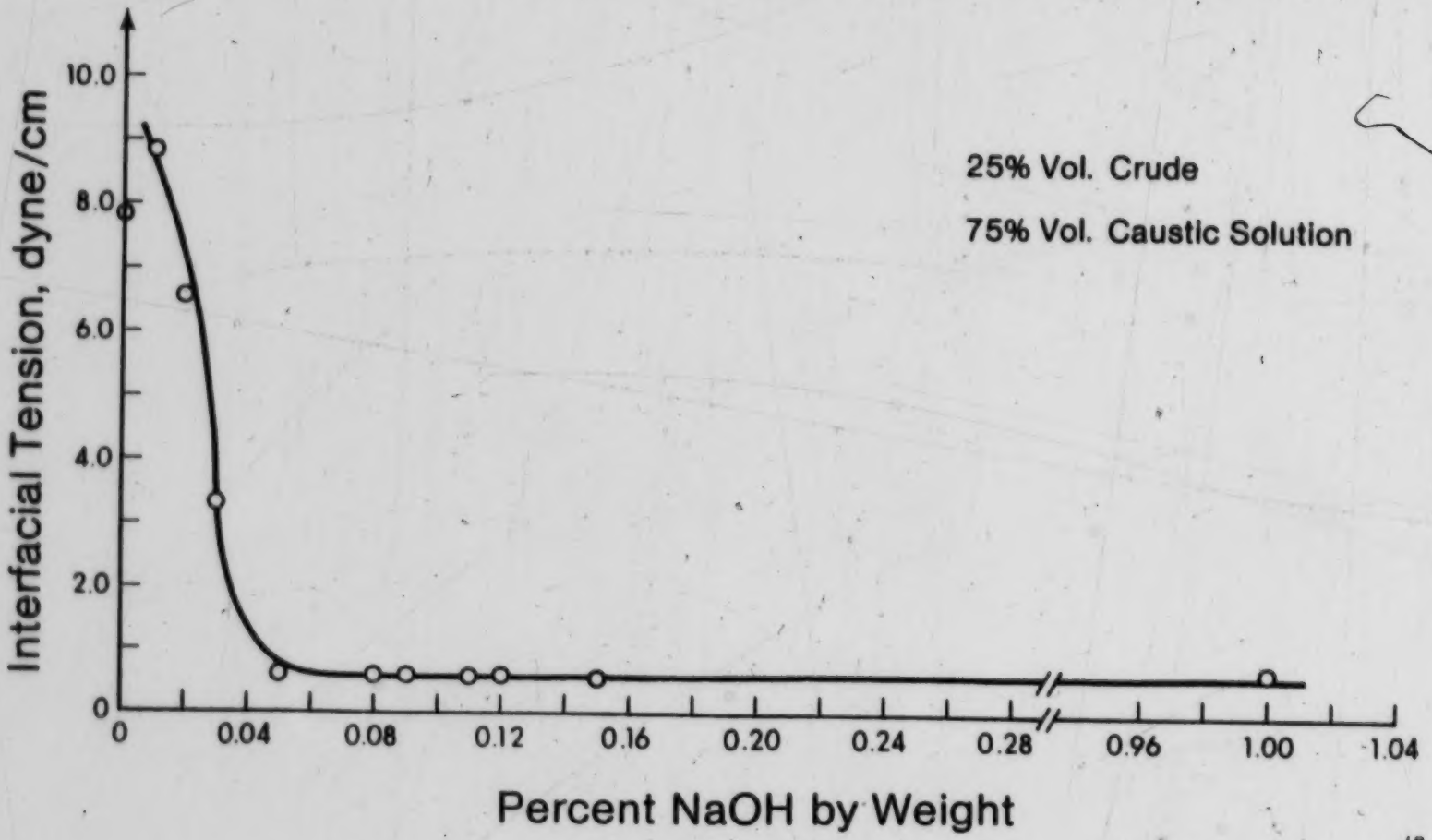

Figure 16. Interfacial Tension between Eyehill Crude Oil and Caustic Solution.

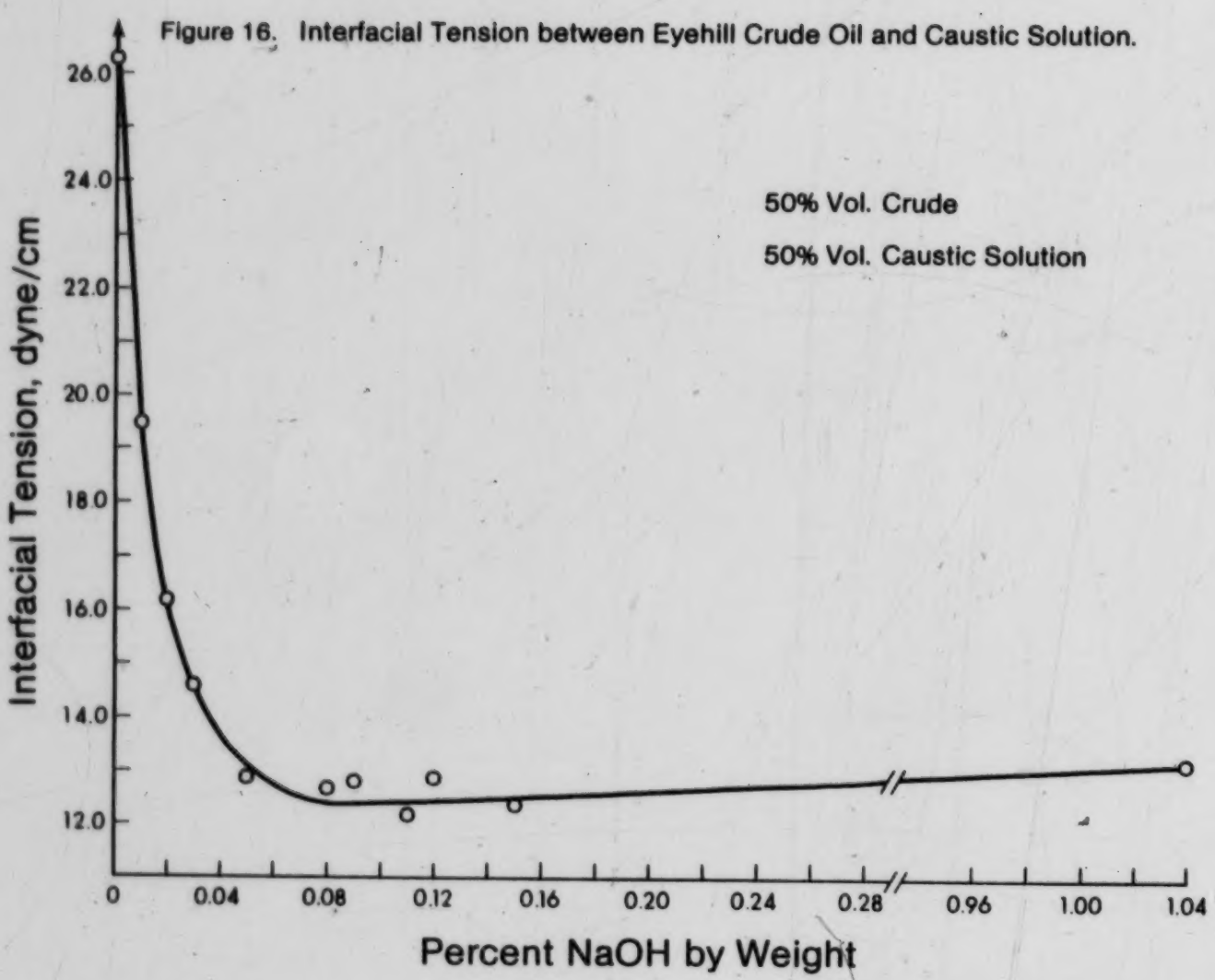

Figure 17. Interfacial Tension between Eyehill Crude Oil and Caustic Solution.

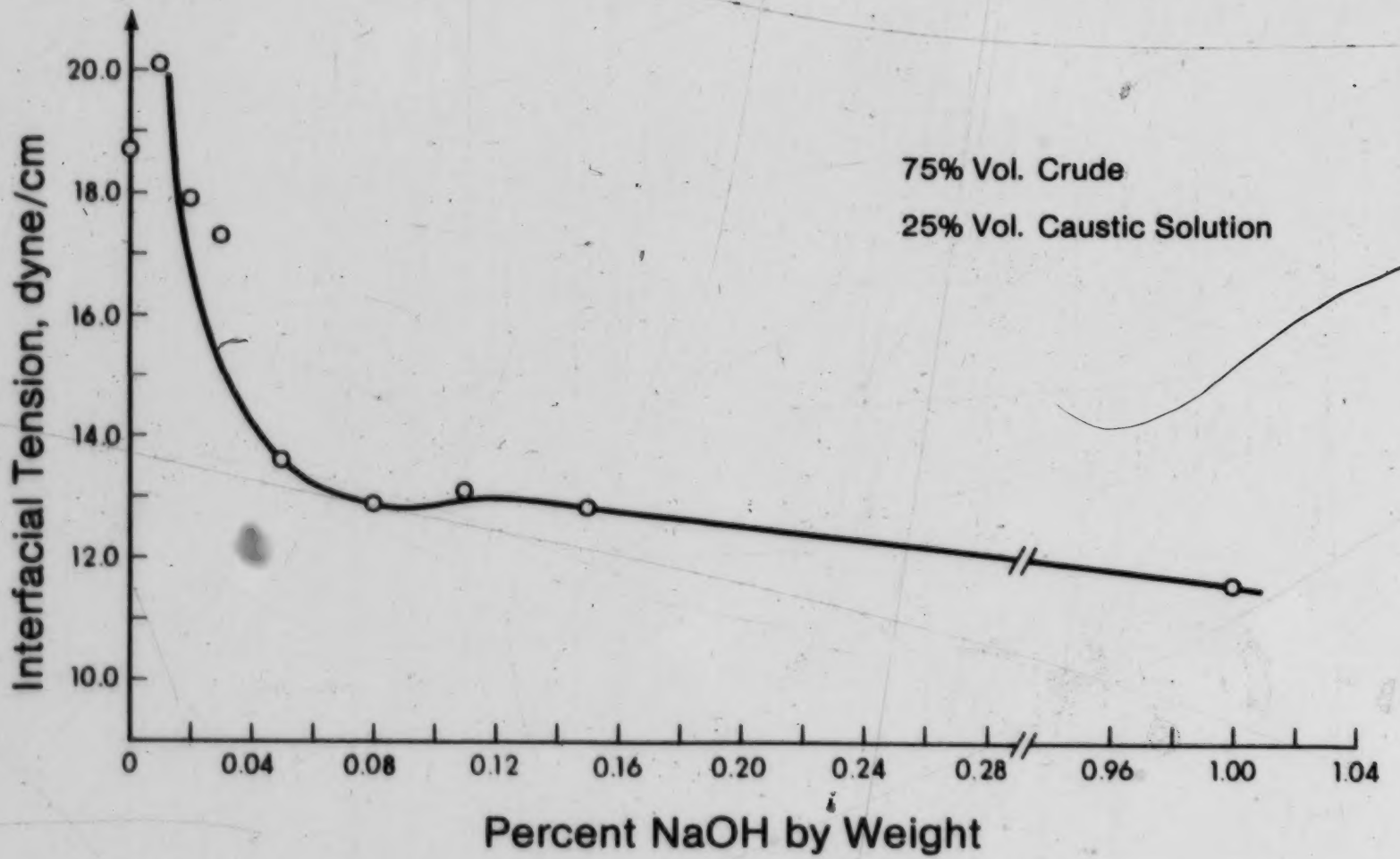

solution ratio of three to one.

Figures 15 and 17 show an anomalous observation: interfacial tension at 0.010 percent (0.0025 M) is higher than at zero percent sodium hydroxide concentration. These runs were repeated a maximum of five times and yielded consistent values. The mechanism for this peculiar behaviour was not elucidated. It is generally conceded that the reaction of surface-active agents with caustic solutions to form soaps lowers the interfacial tension. Given a fixed interfacial area, the higher the caustic concentration is, the more soaps are generated by reaction and the lower the interfacial tension becomes. Similarly, the lower the caustic concentration is, the larger the interfacial tension should be. Ultimately, when no caustic is added, the interfacial tension should be at its highest value. This observation is verified in Figure 16 but not in Figures 15 and 17.

Symonds (1980) reported that the interfacial tension between caustic solutions and the Wainwright crude passed through a minimum and then increased with increasing caustic concentration. Figure 15 shows that Symonds' observations are duplicated only when one volume of crude oil is used with three volumes of caustic solution.

To put into better perspective the variation of interfacial tension values with changes in crude to caustic solution volume ratio, a cross plot of Figures 15, 16, and 17 was performed. For each caustic concentration,

interfacial tension was plotted as a function of volume of crude used (Figure 18). A family of S-shaped curves was obtained, indicating that interfacial tension was a strong function of crude to caustic solution ratio.

For concentrations below 1.00 percent by weight (0.25 M) caustic, all the curves follow a similar pattern. At all concentrations, the measurement of interfacial tension is a strong function of the relative amounts of crude oil and caustic solution utilized. The caustic concentrations exhibiting the lowest interfacial tensions are:

* 25 percent crude oil by volume: 0.10 percent caustic by weight (0.025 M)
* 50 percent crude oil by volume: 2.00 percent caustic by weight (0.50 M)
* 75 percent crude oil by volume: 1.00 percent caustic by weight (0.25 M)

Caustic concentrations between 0.05 and 0.15 percent (0.0125 and 0.0375 M) produce similar curves within an interfacial tension range of ± 0.50 dyne / cm for a crude fraction of 75 percent (see Figure 18). There is therefore allowance for possible fluctuation in caustic concentration. On the other hand, the curves for caustic concentrations between 0.01 and 0.05 percent (0.0025 and 0.0125 M) do not fall within any narrow range. Similarly, the curves for 1.00 and 2.00 percent caustic solutions are very different and do not allow any fluctuation in caustic concentration without a drastic change in interfacial tension. As a matter of fact,

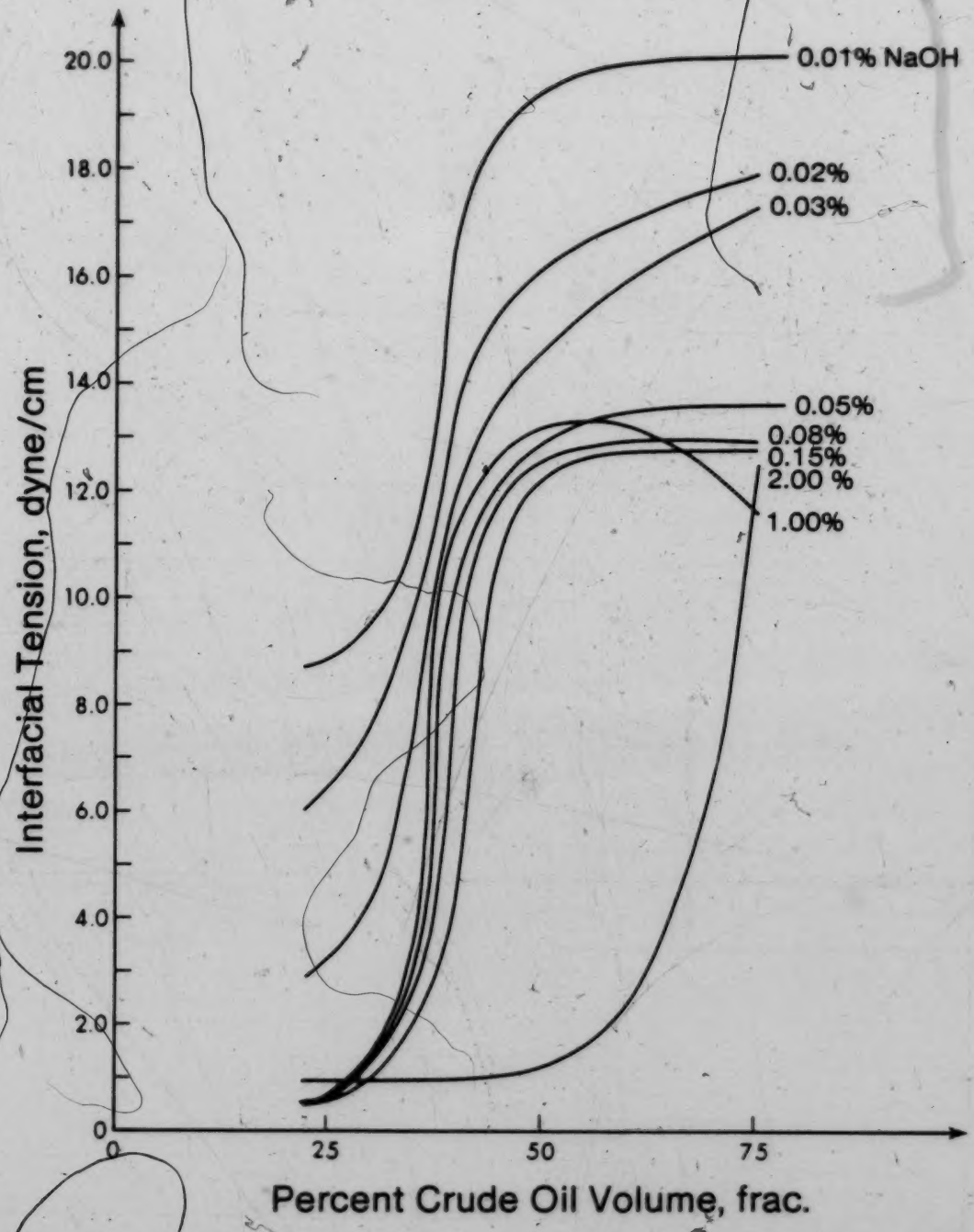

Figure 18. Interfacial Tension between Eyehill Crude Oil and Caustic Solution.

the values of the interfacial tension for the 2.00 percent solution at 25 and 75 percent crude oil by volume fall within the range of the 0.05 to 0.15 percent solution. In other words, at these oil fractions there would be no advantage in using a 2.00 percent instead of a 0.10 percent caustic solution.

In addition, the stable emulsions contain at least 90 percent crude by volume, and while the 0.05 to 0.15 percent caustic (0.0125 to 0.0375 M) curves seem to flatten after the 50 percent oil by volume mark, the 2.00 percent caustic (0.50 M) curve shows a rapid increase in interfacial tension.

Similar observations were made by McCaffery as reported by Rubin and Radke (1980). As reported in the literature review, he noted that interfacial tension depended greatly on the phase volume ratio. For a ratio of three volumes of caustic solution to one volume of crude oil where interfacial tension did not increase with increasing caustic concentration, the results are in agreement with those of MacKay et al (1978).

Other observations were reported by Rubin and Radke (1980). They found interfacial tension was also a function of time, ratio of interfacial area to oleic phase volume, and adsorption/desorption rate constants. All these factors can have a sufficiently large effect to cause variation of interfacial tension values by two to three orders of magnitude. Figures 5, 6, and 7 from Rubin and Radke all

indicate that as the amount of oil used decreases (i. e. as the phase volume ratio increases) the interfacial tension between the two liquids increases. The trend observed in Figure 18 is the exact opposite; interfacial tension increases as the amount of oil used increases. No explanation is given for that behaviour. It should be noted, however, that Rubin and Radke used mineral oil as the oleic phase and that they used a known amount of oleic acid as the surface-active agent. The Eyehill crude, by comparison, is a complex mixture of hydrocarbons and may contain different acids in different concentrations the combined action of which would be responsible for the observed behaviour. In both instances interfacial tension is shown to be a strong function of phase volume ratio.

6.2 EMULSION PREPARATION

The single most important factor was certainly the high connate water content of the crude; it decreased the ability of the crude to accept more water coming from the sodium hydroxide solution. Table B-3 (Appendix B) shows that the water content of the W/O phase is (with minor exceptions) around sixty percent and does not fluctuate significantly when the fraction of crude incorporated in the preparation increases from ten to one hundred percent. Unstable emulsions separated readily into two phases. A smaller volume of solution has a better chance of forming a single phase emulsion than a larger volume.

The curve in Figure 19 indicates that up to 85 percent crude, the volume of crude utilized equals approximately the volume of water-in-oil emulsion formed. This means the crude refuses to accept water coming from the caustic solution. The resulting W/O emulsion was merely a churning of the original crude with the fifty nine percent connate water it contained.

Either free water was produced along with the oil and connate water emulsion, or the crude was produced as an emulsion and part of the connate water separated with time. Upon shaking, the water recombined with the oil and the resulting emulsion showed no further acceptance of water coming from the caustic solution. Alternatively, when some of the connate water separated with time, the resulting crude could accept a limited amount of caustic solution as testified by the question marked data points in Figure 19.

The 70 percent crude oil emulsion which seemed to be stable after the first series of preparations (see Figure 19) was shown to separate into two phases. A third preparation was conducted which confirmed the instability of this emulsion and the reproducibility of emulsion preparation by this method. The striking phenomenon was that for small volumes of water-in-oil emulsion, blending with caustic solution did not result in an oil-in-water emulsion. Instead, the original emulsion remained as water-in-oil and excess caustic solution was left unused. Emulsion theory would have predicted an emulsion inversion.

Figure 19. Effect of Crude Content on W/O Emulsion Formation

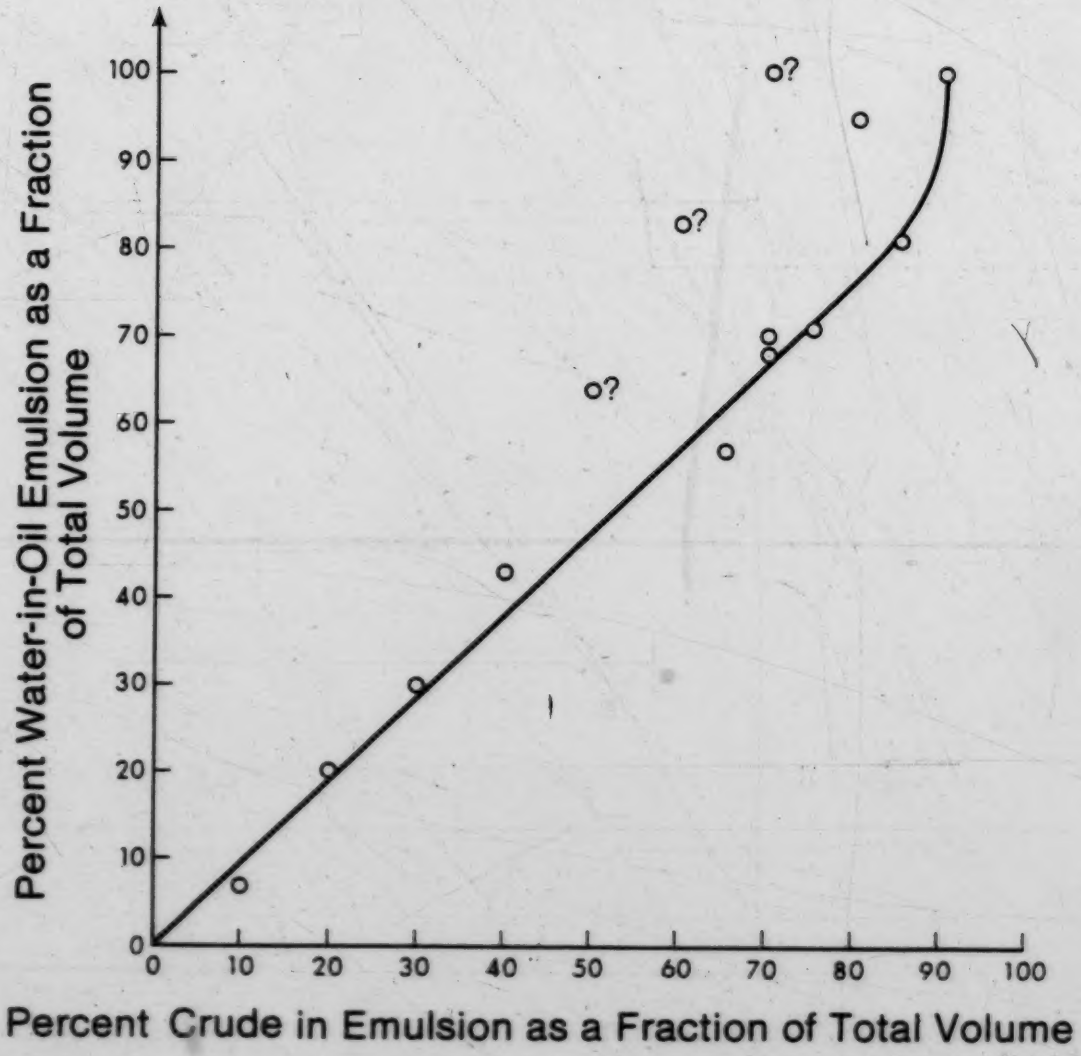

It seems that for this petroleum emulsion, the type in which it occurs (i. e. water-in-oil) is its most stable arrangement. It will not abandon this arrangement under agitation or addition of electrolyte or application of heat.

The only way to make the crude comply with emulsion theory would be to remove the connate water it contains by vaccuum distillation. Then emulsion inversion will be observed upon addition of excess dispersed phase liquid. However, the nature of the original oil will have been altered significantly in the process because the ions present in the connate water would transfer as solids to the oil phase upon vaccuum distillation, as mentioned earlier. Distillation of the water-in-oil phase confirmed that caustic solution and crude did not mix very well even if the consumption of sodium hydroxide increased as the amount of oil present increased.

As the crude content increased, visual observation revealed that the consistency of the water-in-oil phase changed abruptly from that of a gel (up to 50 percent crude) to a less viscous state (60 percent and up).

The difference in pH between the two phases was fairly large(see Figure 20). The oil-in-aqueous solution curve shows a progressive decrease in pH with increasing percent crude oil - above 30 percent crude by volume. This can be related to the caustic consumption by oil. The aqueous solution-in-oil curve exhibits a downward sloping trend but there is much scatter in the readings. Tabulated values of

Figure 20.

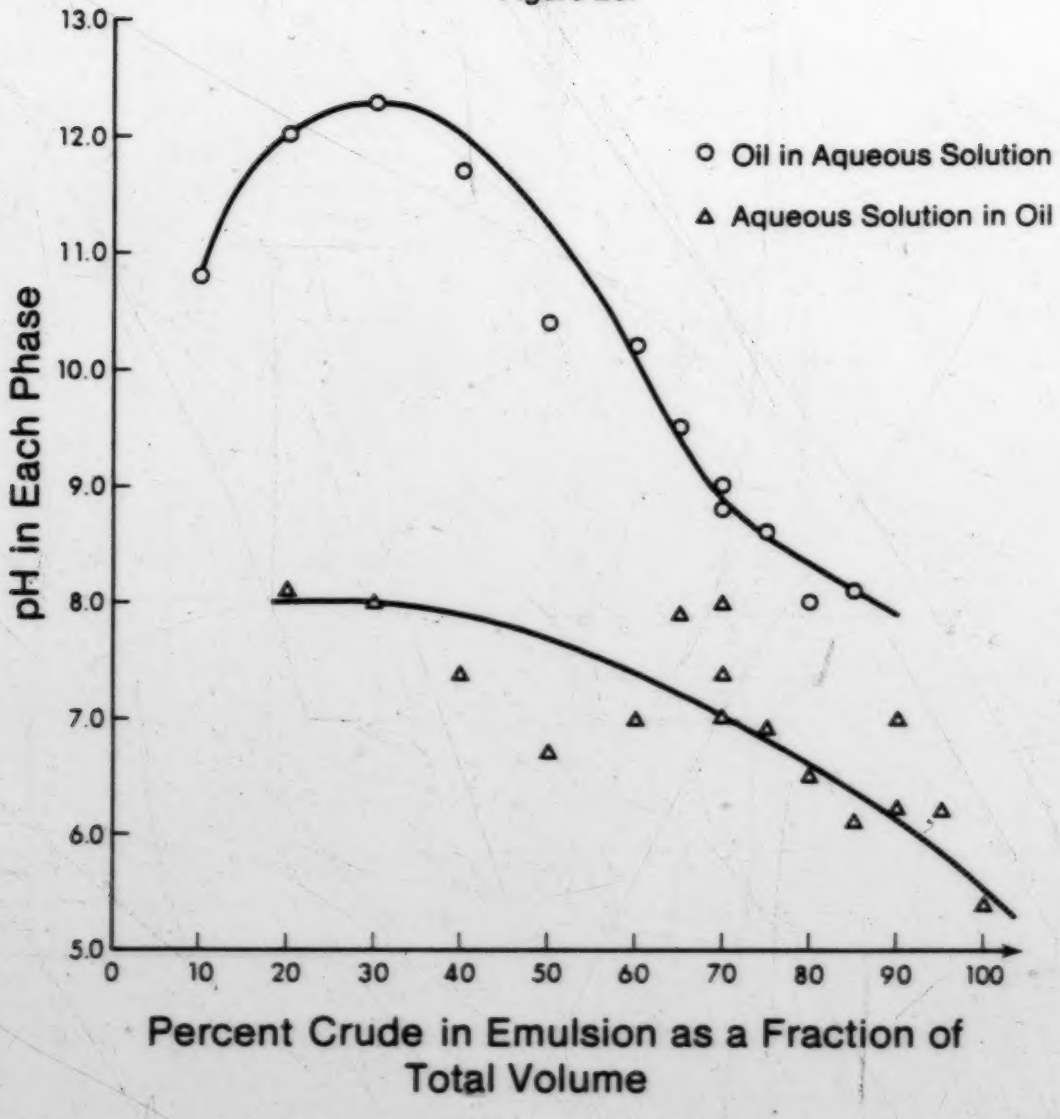
13.0
12.0
11.0
10.0
9.0
8.0
7.0
6.0
5.0
pH in Each Phase
0
10
20
30
40
50
60
70
80
90
100
Oil in Aqueous Solution
Aqueous Solution in Oil
Percent Crude in Emulsion as a Fraction of Total Volume

pH for Figure 20 are listed in Table B-4 (Appendix B).

An emulsion was prepared using 10 percent distilled water instead of 10 percent of 0.10 percent by weight sodium hydroxide solution (0.025 M) in an attempt to determine the role of caustic in emulsion stability. The distilled water and crude oil mixture proved to be of low stability and less homogeneous than the emulsion prepared with caustic.

It was observed that all emulsions containing more than 90 percent crude were single phase emulsions. A search was conducted between 85 percent crude (two phases) and 90 percent crude (one phase) emulsions to determine the point at which the first single phase emulsion could be formed. The 87 percent crude emulsion was prepared twice and came out as one phase in each case. But the 86 percent crude mixture behaved differently (see Table 1). Out of the three samples prepared, one exhibited large drops of caustic solution on the walls of the container-twenty four hours after preparation-, the other a very shallow caustic solution zone at the bottom, and the third, two distinct phases. This emulsion was then regarded as being on the very border between stable and unstable preparations. It was classified as unstable. Therefore stable water-in-oil emulsions contain at least 87 percent crude (35.6 percent oil). The 100 percent crude emulsion (41.0 percent oil), prepared one month earlier exhibited black pits on the wall of the container as a sign of instability.

Optimal Composition Selection

TABLE 1

Percent Crude	Emulsion Temperature,C	Number of Phases
86.0	30.0	2
86.0	30.5	2
86.0	32.0	2
87.0	30.5	1
87.0	30.0	1

Water extraction confirmed the stability of 90 percent crude (one-and-a-half months old) and 95 percent crude (one month old) emulsions. Distillation showed the water content was the same at the top and the bottom of the container (i.e. no separation occurred). Results of these water extractions are shown in Table D-1, Appendix D). The percentage water for the 90 percent crude emulsion was consistently lower than a-month-and-a-half earlier (57 against 65 percent); the 95 percent crude emulsion gave comparable results one month apart (61 versus 60 percent).

Since a 50 percent variation was allowed in the sodium hydroxide concentration, (see Paragraph 5.1.1 Interfacial Tension) the same margin of safety was allowed for the caustic solution content. The maximum amount of caustic solution the emulsion may contain was 13 percent. It was determined that an emulsion containing 8 percent of 0.10 percent by weight (0.025 M) caustic had an appropriate margin of safety against phase separation. Confirmation of the optimality of the 92 percent crude and 8 percent caustic solution at 0.10 percent concentration (0.025 M) was obtained through continuous testing as shown in Table D-2, Appendix D.

The formation of extremely small water droplets upon mixing could have been predicted from emulsion theory. The combination of a narrowing of the container close to the blades and a very large difference in viscosities accounted for the difference in velocities necessary to the creation

of a large interface between the two liquids.

The W/O emulsions formed can all be classified as "mousses", following Berridge et al (1978). This seems to indicate the asphaltene content may be high. Oil analysis showed an asphaltene content of 11.6 percent by weight. The analysis was conducted in accordance with the procedure reported by Speight (1970). Asphaltene content may dictate the nature of the interfacial film formed and hence, emulsion stability.

Appendix A contains a water analysis report from the Department of Agriculture on the connate water produced with the Eyehill crude. This report revealed a large quantity of solids and ions in the water. These solids and ions would also contribute to the emulsion stability by playing a role in the formation of the interfacial film.

6.3 MICROSCOPE OBSERVATIONS

Several emulsions were studied as they aged. These results are reported here along with comments.

6.3.1 Crude Oil

Crude oil appeared as a mass of medium-size water drops embedded in the oil (see photograph in Figure 21). Observation under ultraviolet light confirmed that the oil was the continuous phase.

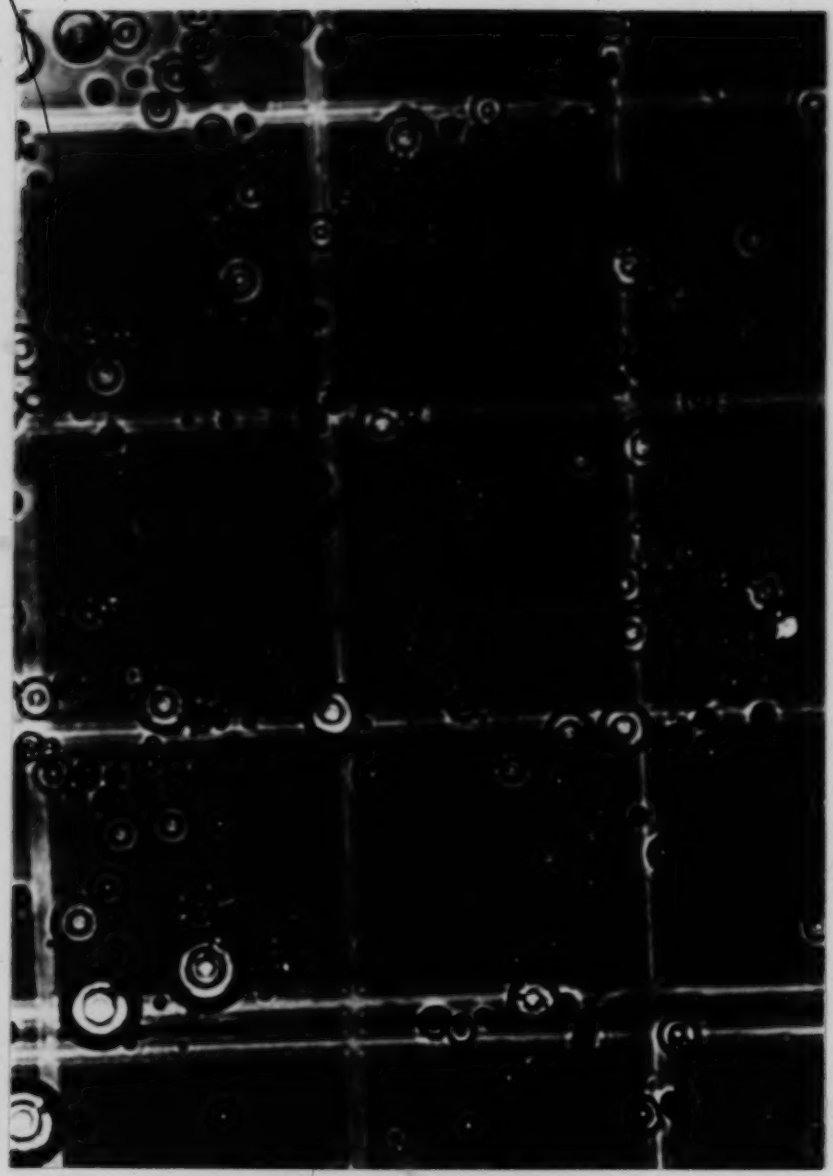

Figure 21. Original Eyehill crude-no stirring 1400x

6.3.2 Crude Oil with a Drop of Sodium Hydroxide Solution

A drop of sodium hydroxide solution was added to a drop of crude and the reaction between the two was observed under the microscope. Before the drop was added, water drops moved freely past one another. After the addition, the water drops tied into chains and became immobile.

Under the cover slip, the sodium hydroxide solution formed large drops. The oil seemed to absorb the solution by sudden movements. No new water drops were observed forming but some drops on the edge of the envelope remained in direct contact with the solution. Some isolated drops of crude surrounded by caustic solution became increasingly crowded with small water drops, acquiring the gel-like look of the emulsions while the bulk of the crude retained its original medium-size water drops.

The caustic solution was certainly lowering the oil-water interfacial tension but the time it took for the caustic to take effect was far greater than the time allowed for emulsification during the standard runs (five minutes). It could be that a parameter other than the presence of caustic played an important role during emulsification.

6.3.3 100 Percent Crude Oil Emulsion

To prepare a 100 percent crude oil emulsion, the original Eyehill crude containing fifty nine percent water in the form of dispersed drops was stirred for five minutes. This action resulted in a decrease in water droplet size

(see Figure 22). Some larger-size water drops were observed in a mass of flowing gel-like substance which could very well be described as very small water drops in oil. An emulsion different from the original crude could have formed during the blending process in the absence of sodium hydroxide. The drops formed by addition of sodium hydroxide under the microscope (Paragraph 6.3.2) were not as small as these.

6.3.4 90 Percent Crude Oil Emulsion

To obtain a 90 percent crude oil emulsion, nine volumes of crude containing fifty nine percent connate water were blended with one volume of sodium hydroxide solution containing 0.10 percent caustic by weight (0.025 M); (see Figure 23). All the water drops were about the same size and were attached to patches of a gel-like substance. A patch was isolated and appeared to be essentially oil under the ultraviolet light. If it contained water drops, these were either too small to reflect light or too numerous to be singled out. Under the pressure of the microscope lens on the cover slip, the gel-like substance would move and return to its initial position upon release of pressure. This resilient substance would not break.

6.3.5 70 Percent Crude Oil Emulsion

Blending seven volumes of Eyehill crude with three volumes of caustic solution containing 0.10 percent sodium

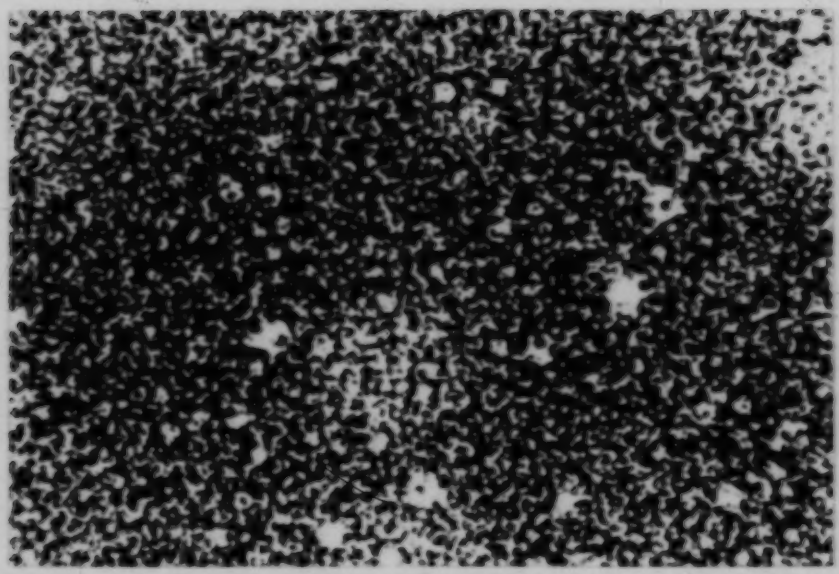

Figure 22. 100% Eyehill crude after 5 min. stirring 1750x

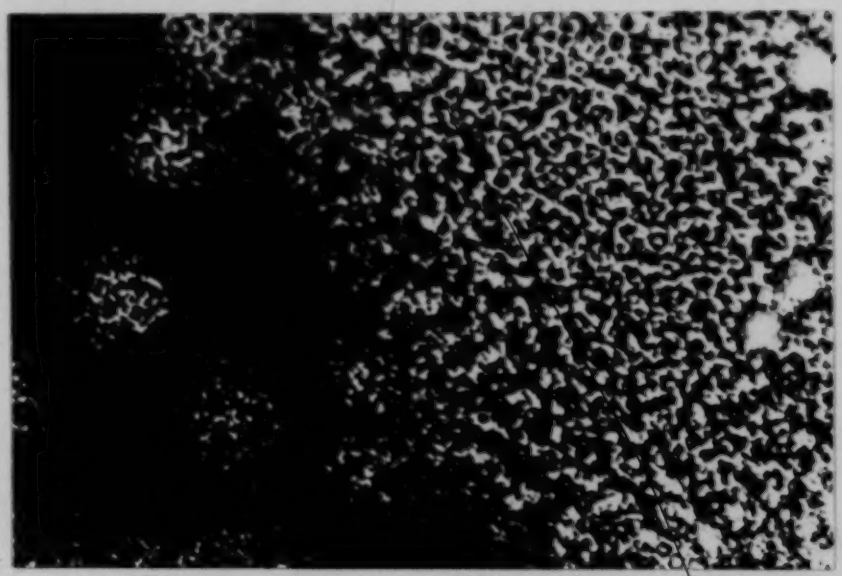

Figure 23. 90% Eyehill crude 10% NaOH solution 1750x

hydroxide by weight (0.025 M) resulted in a 70 percent crude oil emulsion. This emulsion was unstable and readily separated into a water-in-oil emulsion and an aqueous phase. The water-in-oil emulsion was observed under the microscope. Undiluted or with Varsol as a solvent, the same gelatinous substance could be seen. Two pictures were taken; (see Figures 24 and 25).

As noted previously, the microscope study confirmed that the initial oil was already an emulsion. As this emulsion was agitated, the water drops must have decreased in size.

It became apparent that the possibility for this substance to accept additional water or even caustic solution was very limited. As the water drops decrease in size, the sum of their surface area increases, taking the ability of the oil to remain the continuous phase to its limit. It was not until the crude oil formed 87 percent by volume of the emulsion mixture that the totality of the water and caustic solution was merged to form a single phase stable emulsion.

6.4 Aging of Emulsions

Rubin and Radke (1980) reported a variation of interfacial tension with time. Earlier, McCaffery (1976) investigated the aging behaviour of some Wainwright crude oils against caustic solution and reported a very large

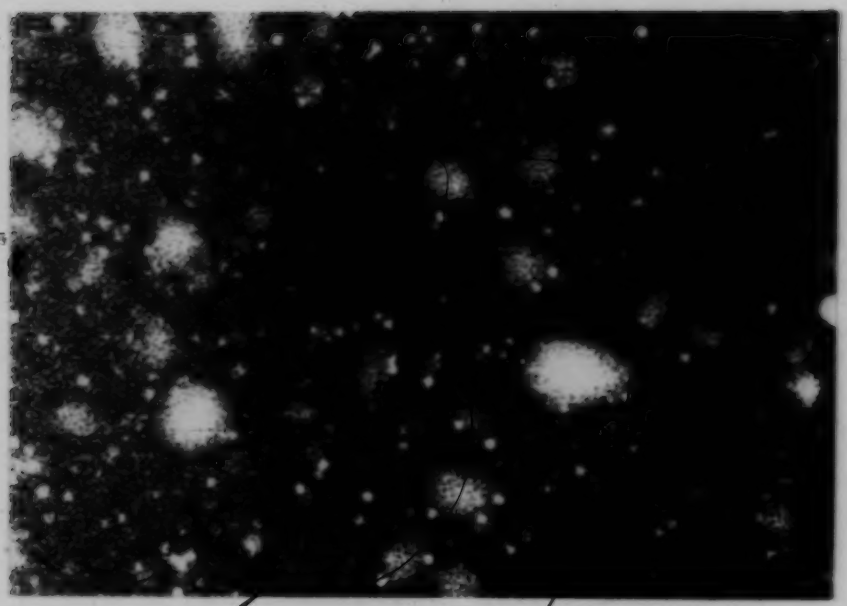

Figure 24. 70% Eyehill crude 30% NaOH solution 700x

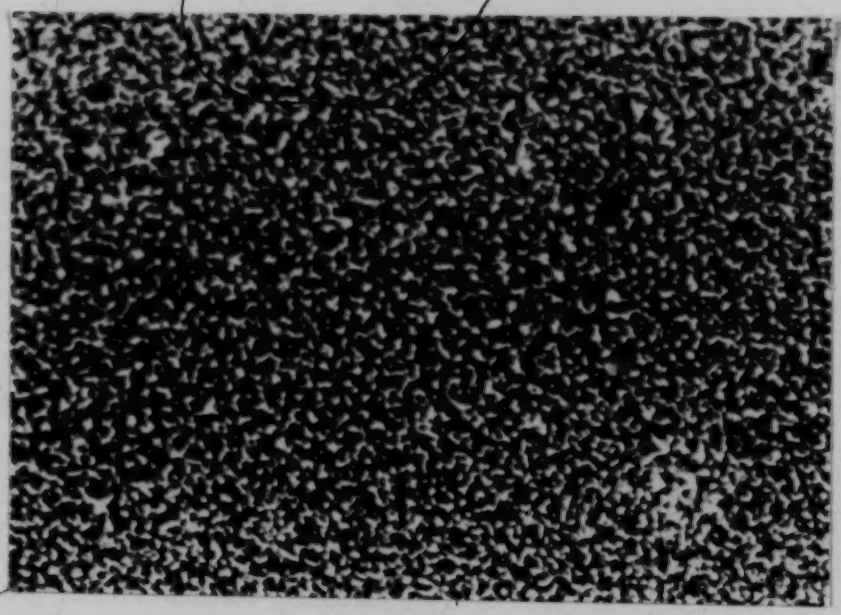

Figure 25. 70% Eyehill crude 30% NaOH solution 1750x

increase in interfacial tension with time. If such changes occurred at the interface between the two liquids, then the behaviour of the emulsion would change, independent of whether it was stable or not. With time, oxidation of the crude is also likely to occur, resulting in an increase in emulsion viscosity. Aging would also occur in-situ and it would be useful to predict what changes would take place and whether these changes would affect emulsion stability.

There are several common methods of determining emulsion stability. Zeta-potential provides a measure of the stability of an emulsion. However, the method requires a conductive continuous phase to be effective: it should work for oil-in-water emulsions but not for water-in-oil emulsions which are the object of this study. Other investigators, both in the laboratory and in the field, have used zetameters to measure the stability of petroleum emulsions and obtained random predictions or inconclusive results. Use of zetameters to predict emulsion stability comes from the field of biology where it has been quite successful; it seems however that the method cannot be applied directly to petroleum emulsions. Visual observation of an emulsion can sometimes reveal a creaming or flocculation phenomenon. In this case however, because of the very high viscosity of the continuous phase, these mechanisms cannot be observed within any reasonable time span.

Another method consists of using photographs of the emulsion to determine the drop size distribution of the water drops. A change in drop size over a time interval means coalescence of the drops and thus instability. But the drops were so small and numerous in all the emulsions prepared that their measurement was not technically feasible.

The original preparations were observed for signs of instability. It should be realized that instability is much more difficult to detect for heavy oils than for conventional oils. Because of high viscosity and almost equal densities, gravity segregation is very unlikely to occur within a reasonable time frame at room temperature. Because of the extremely small droplet size, coalescence can only be appreciated under the microscope once the droplets are in the visible range. The problem is further compounded by the fact that it has not been possible to dilute these emulsions by any solvent, for easy observation under the microscope. All of the reported observations are therefore only qualitative in nature.

6.4.1 75 percent Crude Oil Emulsion

Three volumes of Eyehill crude were blended with one volume of caustic solution containing 0.10 percent sodium hydroxide by weight (0.025 M); see photographs in Figures 27 and 28. Oil separated at the surface and formed a film. Below it the W/O phase retained its mobility but a dark band

developed on the walls of the container thereby showing a certain degree of instability.

6.4.2 Crude Oil

Drop size distribution analysis was performed on the wellhead crude at a one year interval. Following the method described in Chapter 4 (Paragraph 4.1.3), the surface area distribution was obtained (see Figure 26) and the average drop diameter calculated (see Table C-1, Appendix C).

In 1981 the drop size was uniform throughout the sample with an average value of 7770 nanometers (7.77 microns). In 1982, even though no change in the appearance of the sample had occurred, separation of the oil and water had begun. The top of the sample had become oil-rich and contained smaller water droplets (average diameter: 1690 nanometers or 1.69 microns). The bottom of the sample showed more water drops of larger size (average diameter: 9840 nanometers or 9.84 microns).

Figure 26 shows the surface distribution for the crude in 1981 (solid line) and for the top of the sample in 1982 (dashed line). The distribution is seen to shift from smaller amounts of larger surface area drops to larger amounts of smaller surface area drops. The equivalent percentage reported on the vertical axis is the fraction of the total number of drops falling within a drop surface area interval. Because these fractions or percentages were applied to intervals of vastly different sizes it became

Figure 26: Effect of Time on Drop Size Distribution

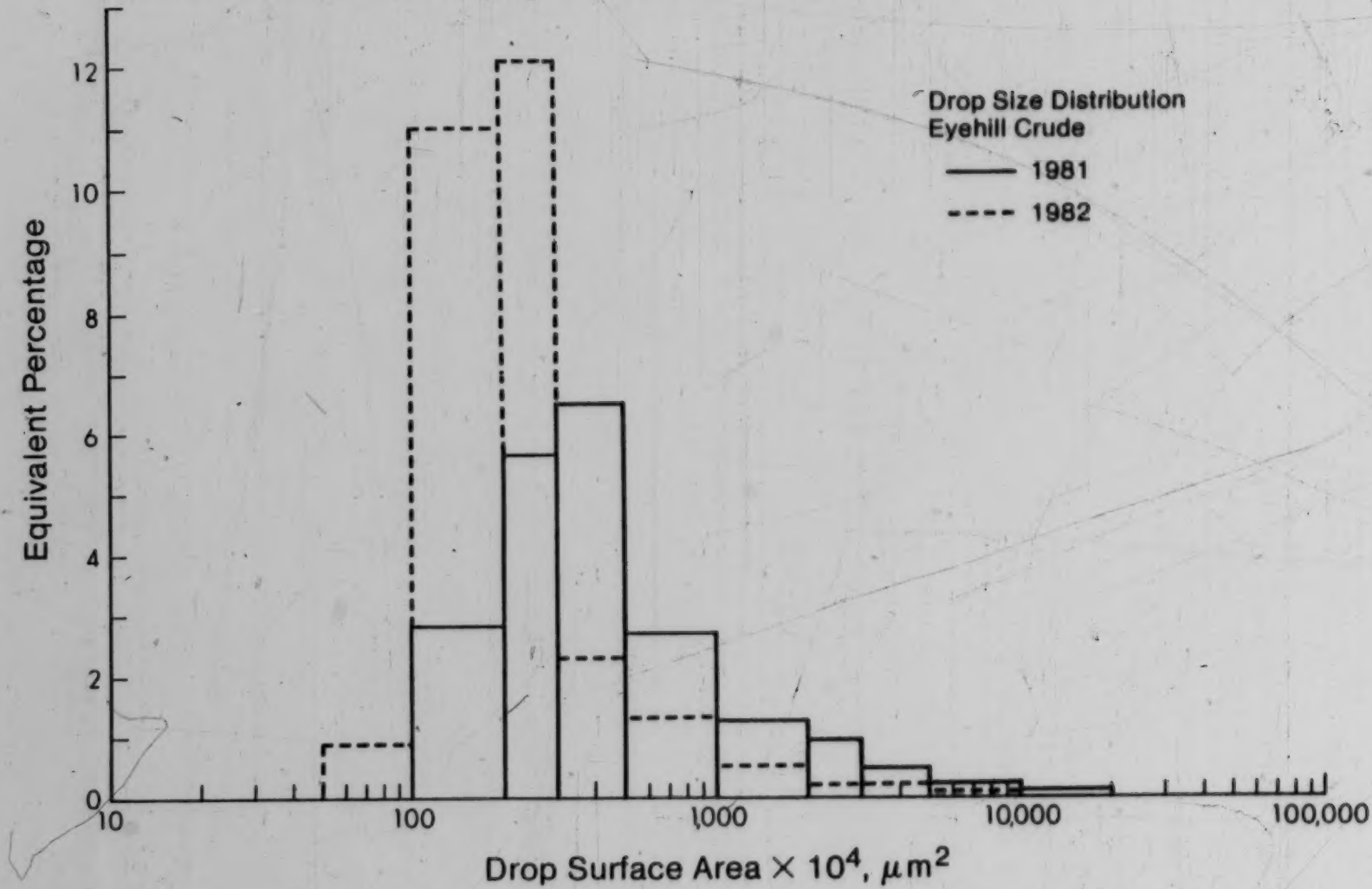

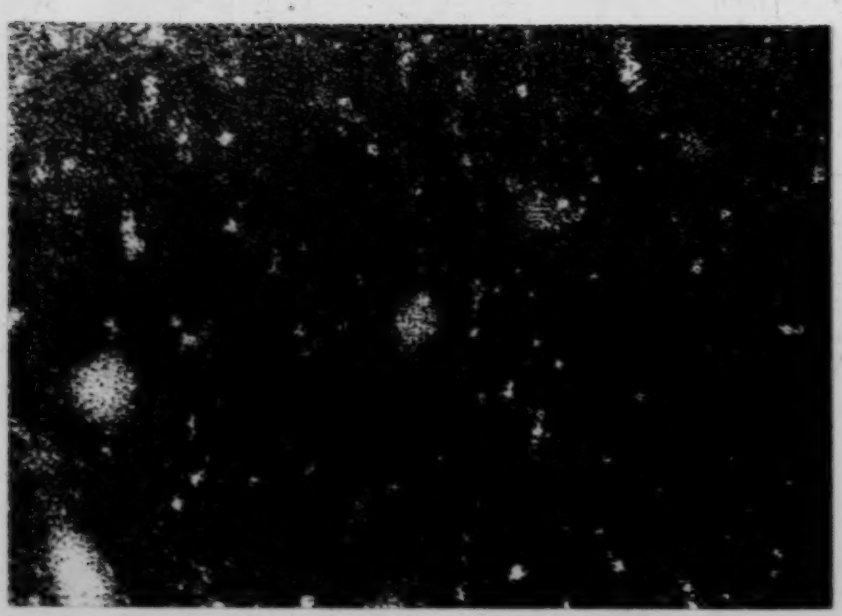

Figure 27. 75% Eyehill crude 25% NaOH solution 175x one month after preparation

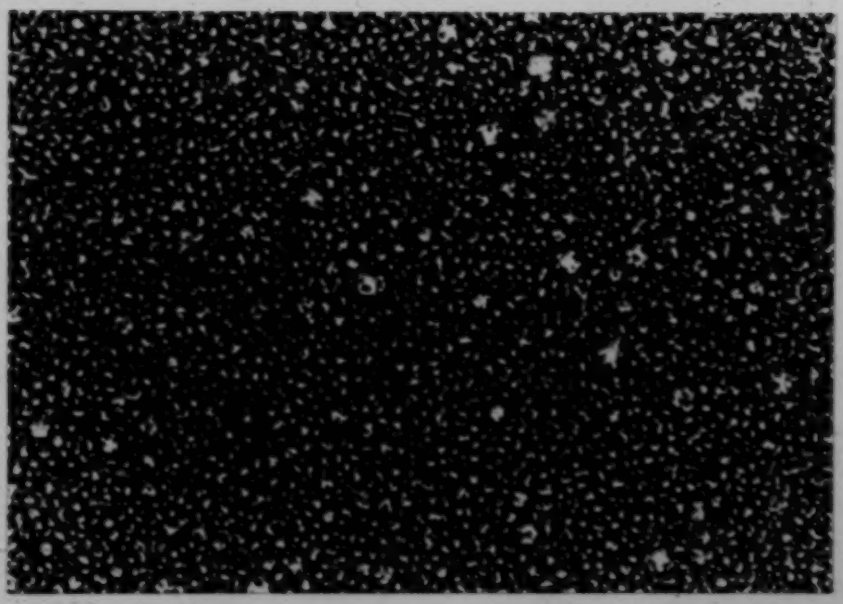

Figure 28. 75% Eyehill crude 25% NaOH solution 1750x one month after preparation

necessary to correct these values so that the area under each bar of the graph was a true reflection of the cumulative surface areas observed within the surface area interval under consideration.

In conclusion, the wellhead crude emulsion showed signs of instability over a period of a year. Single phase emulsions exhibited no visible sign of instability. The 100 percent crude oil emulsion showed signs of instability even though it was a single phase. It seemed that the absence of caustic was responsible for this behaviour; caustic clearly played a role in the long term stability of the emulsions. Mechanical agitation by itself was not sufficient to ensure stability through significantly smaller drop size. High viscosity was not a barrier to phase separation but simply slowed the process.

6.5 RHEOLOGICAL PROPERTIES

To predict the behaviour of the emulsions it was necessary to gain some insight into their flow properties. Some emulsions were studied as such; others were tested after blending with various amounts of distilled water and crude oil. The composition of each of the different mixtures is shown in Table B-5, Appendix B. Some mixtures came out as a single phase, others as two phases. The number of phases and nature of each phase is shown for each mixture in Table D-4, Appendix D. The results were plotted on a ternary diagram (Figure 29). All phases were

determined at the points indicated in the graph. Therefore, the dotted lines separating the regions are only indicative of the different areas. On a narrow strip joining the Emulsion and Crude Oil apexes, resulting mixtures are single phase. Mixtures 6, 16, and 25 are in the regions where both a W/O emulsion and free oil were observed. Mixtures 5, 9, and 11 are in regions where three phases (water, W/O emulsion, and oil) were noted. All the other mixtures were in a two-phase region (i. e. water and W/O emulsion). This graph shows that the chosen emulsion (92 percent crude, 8 percent caustic solution) mixes with distilled water to a limited extent. Such behaviour has an impact on the quantity of aqueous phase present in the W/O emulsions. Samples of this phase were extracted from each mixture and the water content was calculated and tabulated as percentages in Table D-3, Appendix D. These values were then plotted in Figure 30. The maximum variation in water content from one emulsion to another was found to be 15 percent. The diagram was separated into three zones arbitrarily but no definite pattern of water content as a function of mixture composition emerged. Comparison with the graph in Figure 29 failed to show any correlation with the number of phases. It remains unclear why the water content of W/O emulsions was not linked to mixture composition or number of phases present. It would have been logical to expect larger water contents for mixtures prepared with increasing amounts of distilled water.

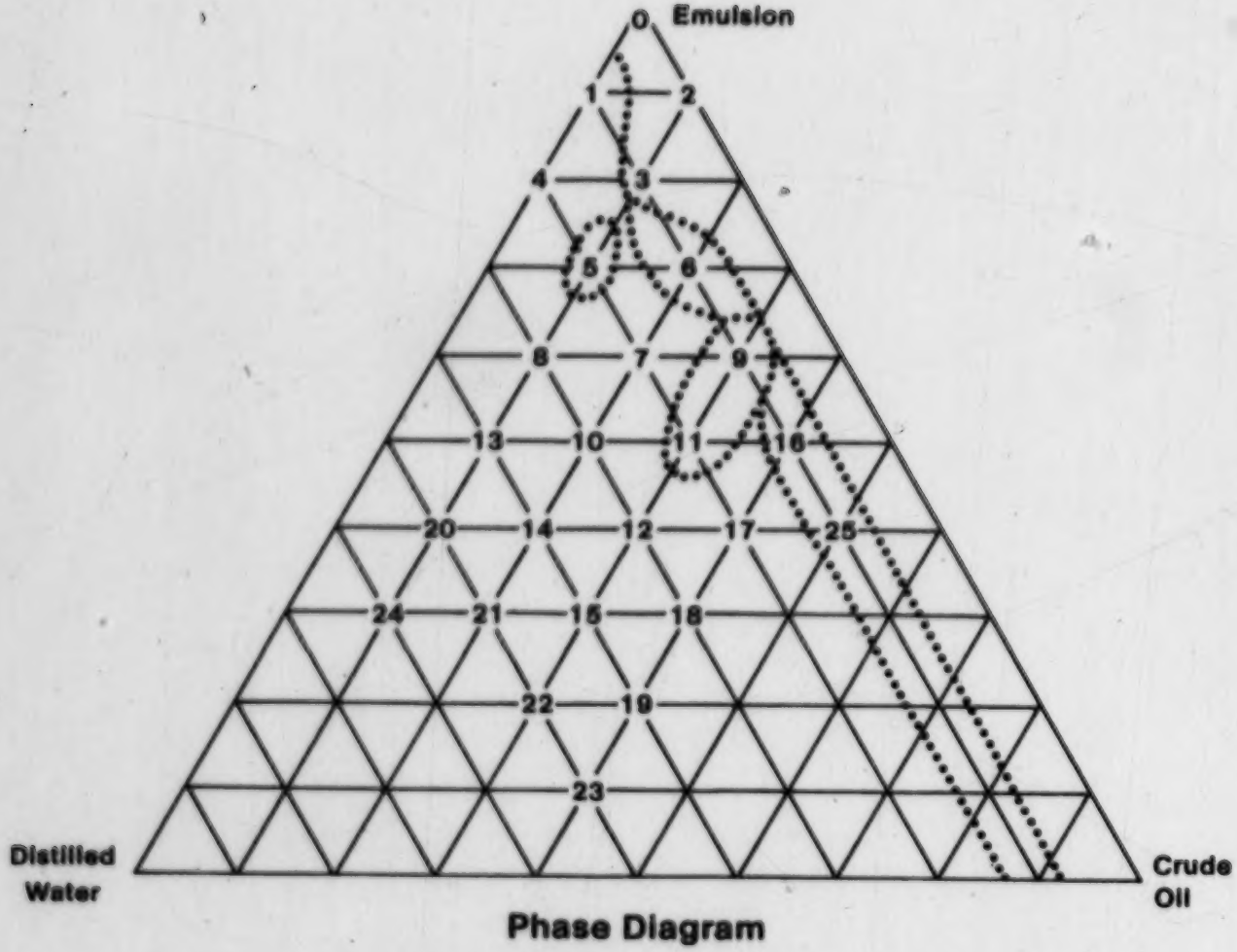

Figure 29. Sample Composition

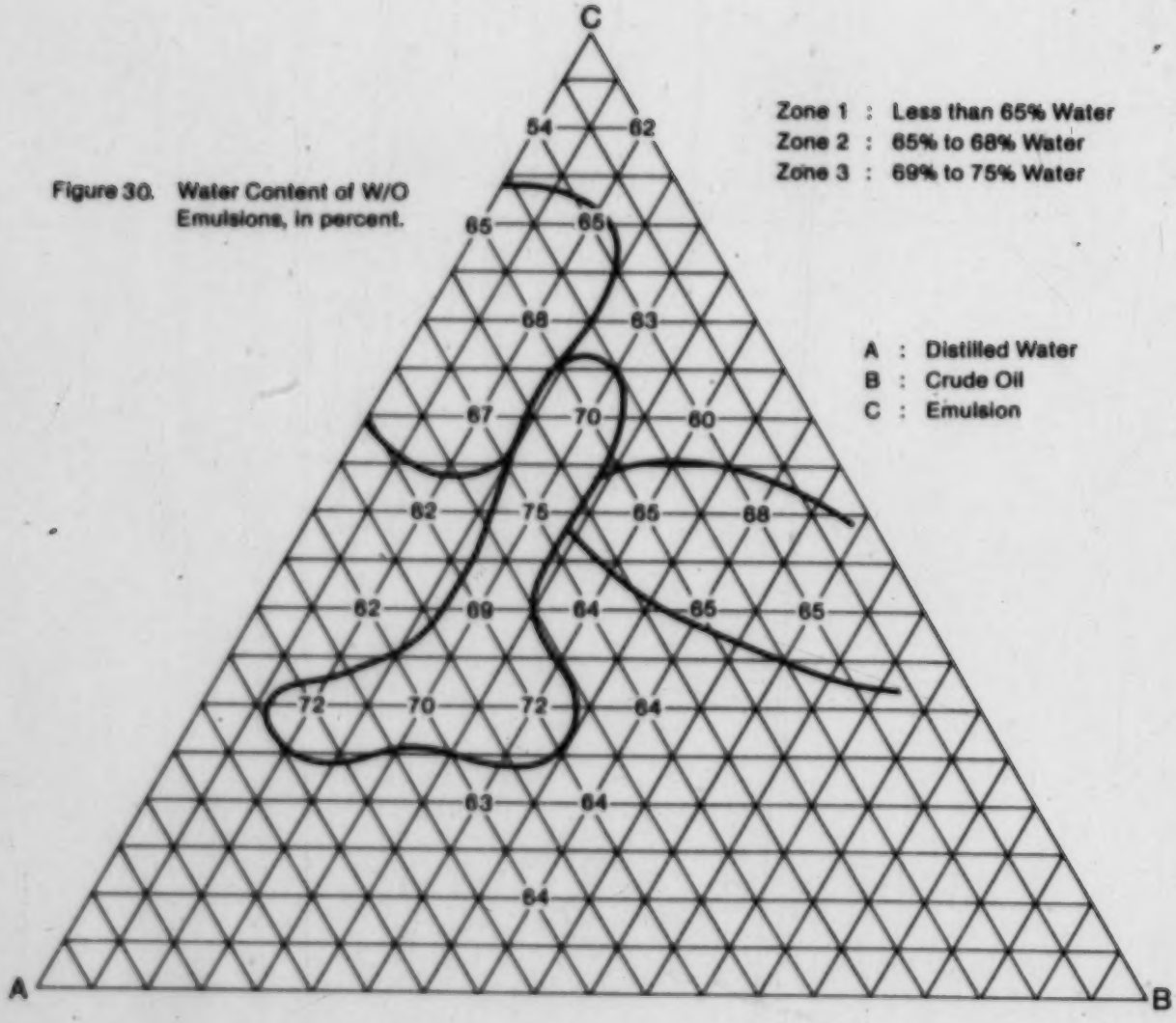

Figure 30. Water Content of W/O Emulsions, in percent.

Zone 1 : Less than 65% Water
Zone 2 : 65% to 68% Water
Zone 3 : 69% to 75% Water

A : Distilled Water
B : Crude Oil
C : Emulsion

The rheology of the W/O phase of each mixture was then studied separately. Data for the original Eyehill crude is reported in Table E-1, Appendix E. Apparent viscosity data for most mixtures is shown in Table E-2, Appendix E. Shear stress and shear rate data are shown in Table F-1, Appendix F. Some emulsions were investigated over a wide range of shear rates. As the viscosity increased from mixture to mixture, the number of possible measurements decreased. Only those samples with four or more readings were graphed. These graphs on log-log scale show that most mixtures (see Figure 31) including the optimal emulsion (Figure 32) seem to follow a power law fluid model with exponent smaller than 1.0 (pseudoplastic fluids). Value of the flow index and consistency index were calculated using a linear regression technique (see Table F-2, Appendix F). Sample 6 does not follow a power law fluid model and starts to exhibit a different behaviour for shear rates approximately greater than 10 reciprocal seconds (Figure 33). Attempts were made to plot the data for samples 5, 6, and 11 on different scales (Figures 34; sample 5 only in Figure 35) with inconclusive results. Similar attempts were made for samples 6 and 11 (see Figures F-9 and F-10, Appendix F). It was concluded however, that all W/O emulsions studied here were non-Newtonian.

The rheology of such fluids is defined by a consistency index, K, and a flow index, n, such that

$$\tau = K \cdot \sigma^{n} \qquad (7)$$

Figure 31.

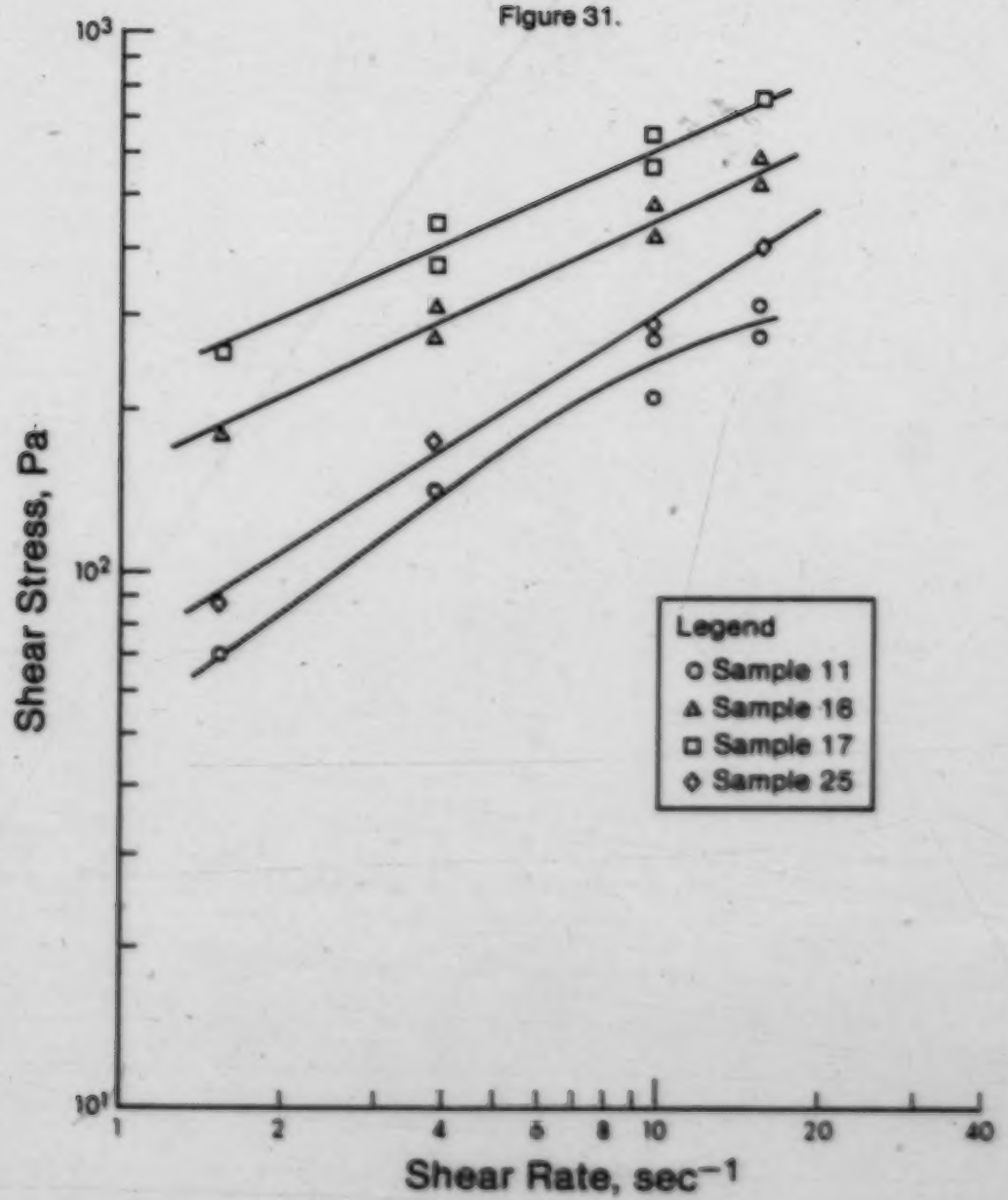
Shear Stress, Pa
10^3
10^2
10^1
1
2
4
5
8
10
20
40
Shear Rate, sec^{-1}
Legend
Sample 11
Sample 16
Sample 17
Sample 25

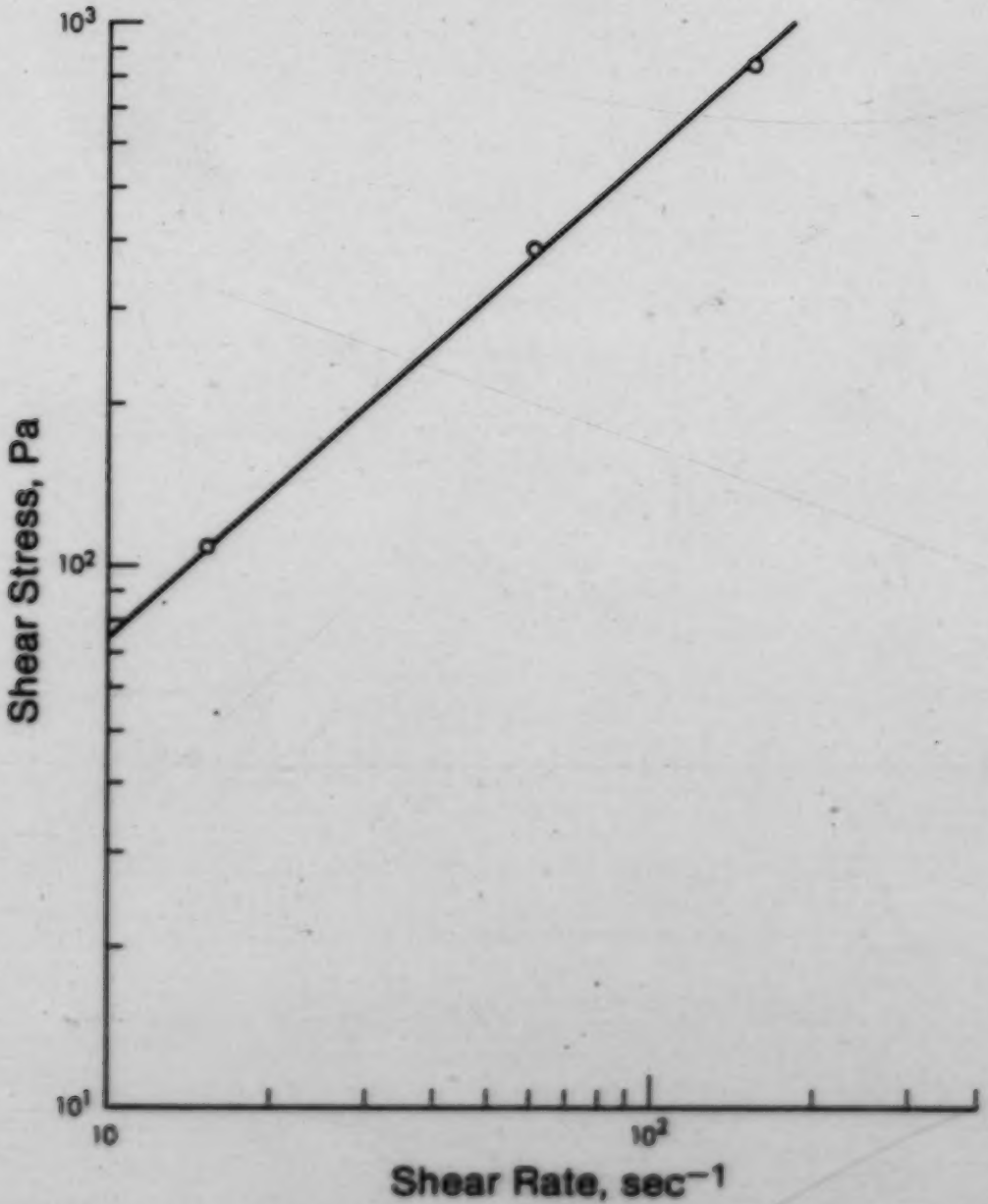

Figure 32. Optimal Emulsion Rheology.

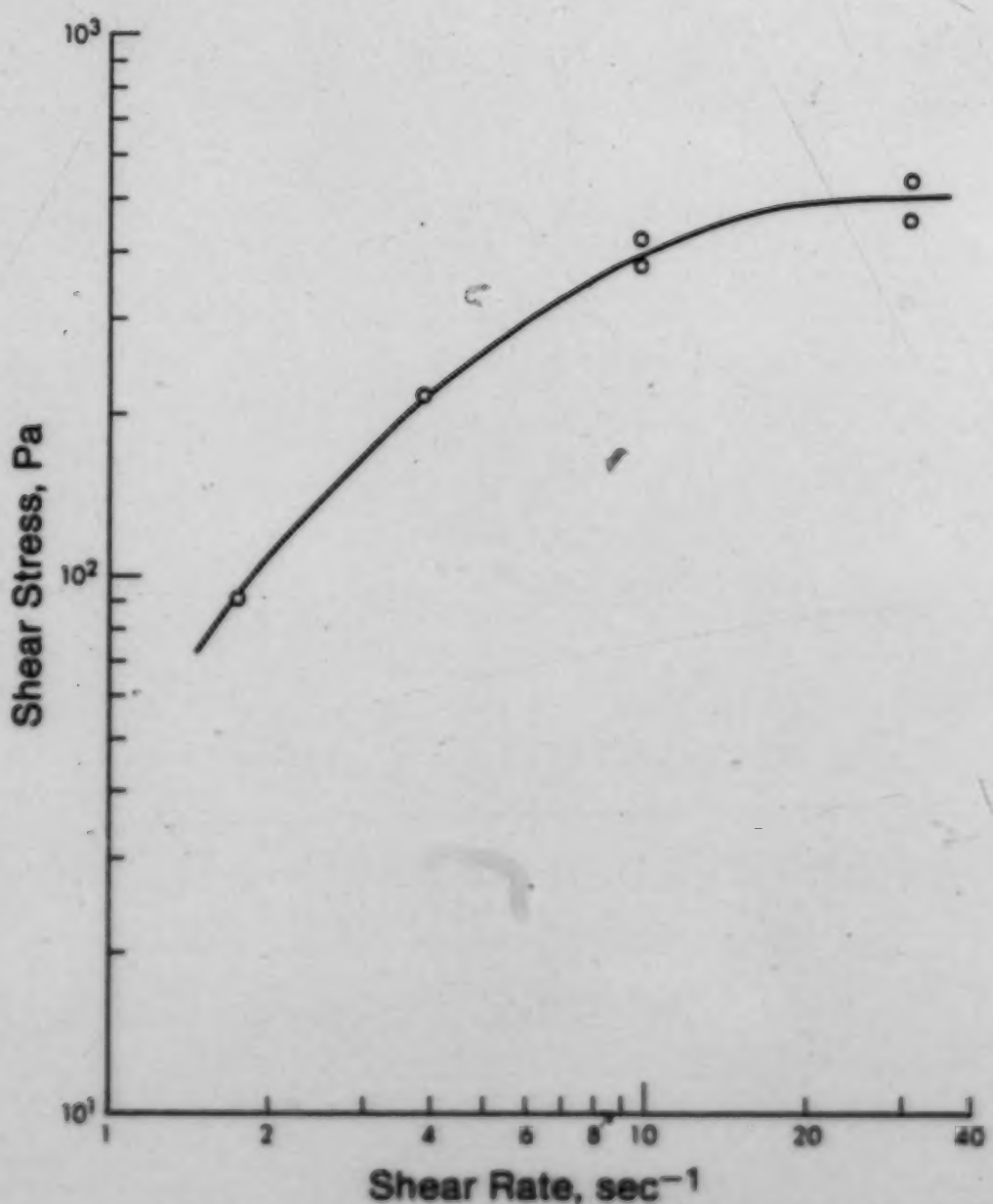

Figure 33: Sample 5 Rheology: Log-Log Scales.

Figure 34: Rheological Behavior; Semi-log Scales.

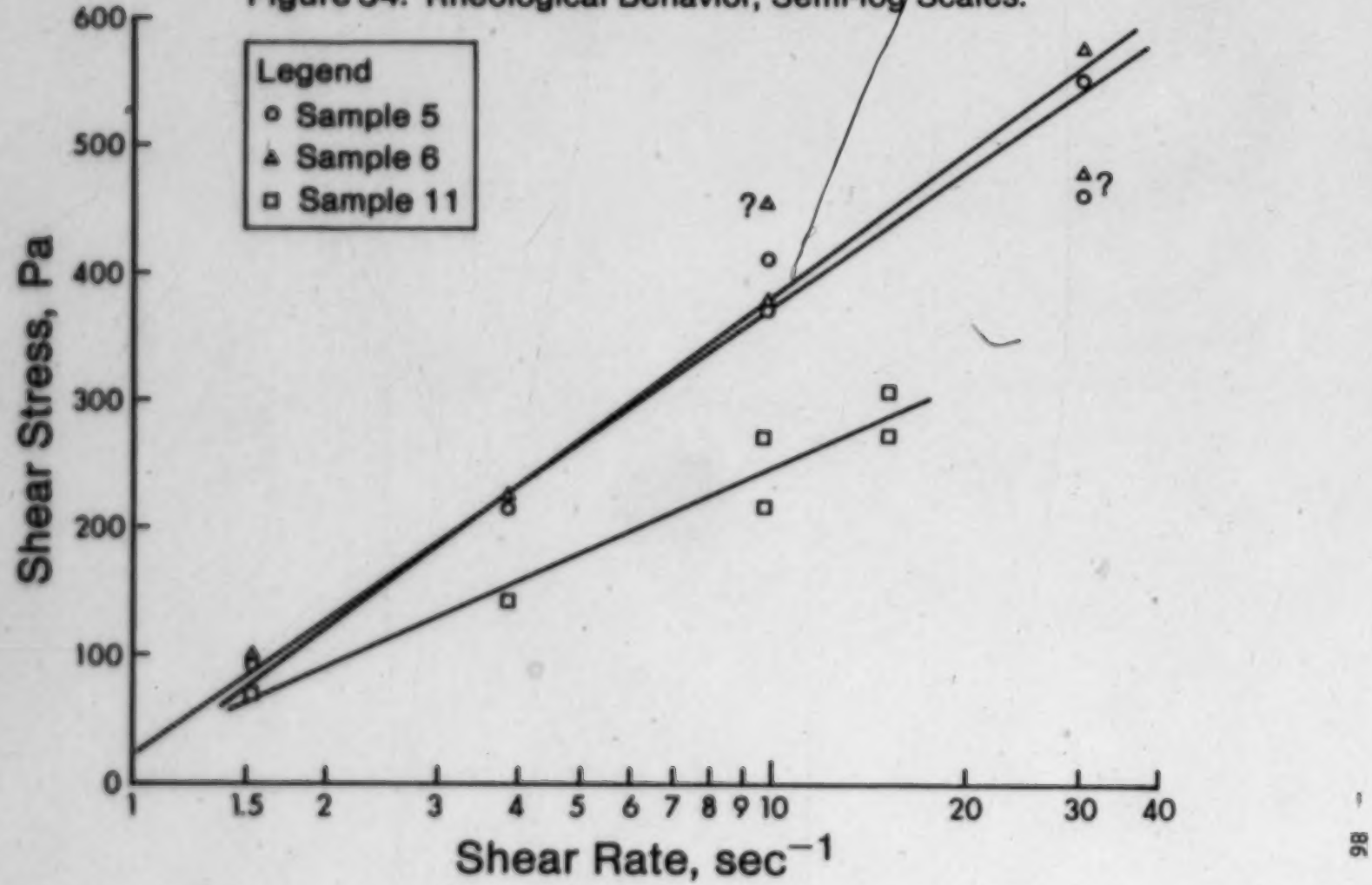

where τ is the shear stress in pascals, and σ is the rate of shear in reciprocal seconds. For fluids such as the optimal emulsion (Figure 32) one set of K and n values is sufficient to describe its rheology for a wide range of shear rates. For others-such as mixtures 5, 6, and 11-the shear stress versus shear rate relationship does not plot as a straight line. Nevertheless, the curve could be approximated by a series of straight lines. For each segment, one set of K and n parameters would describe the flow properties over a small range of shear rates. Hence mixtures 5, 6, and 11 were not totally different in behaviour from other non-Newtonian mixtures. Linear regression analyses indicated that the consistency index of samples 16 and 17 was extremely high (see Table E-2, Appendix E).

It should be noted that the evaluation of the flow index n, and of the consistency index K, is dependent upon the equipment with which shear stress and shear rate are measured. The parameters obtained using the rheogoniometer would have to be corrected prior to predicting emulsion behaviour in a porous medium. Still another set of values for n and K would be required to describe emulsion flow in a pipe. Flow and consistency indexes are model-dependent.

Apparent viscosity was then plotted as a function of shear rate for samples with four or more readings (Figure 36). All the curves show decreasing viscosity with increasing shear rate. Samples with the highest viscosity at low shear rates show the greatest decrease in apparent

Figure 35. Sample 5 Rheology; Arithmetic Scales.

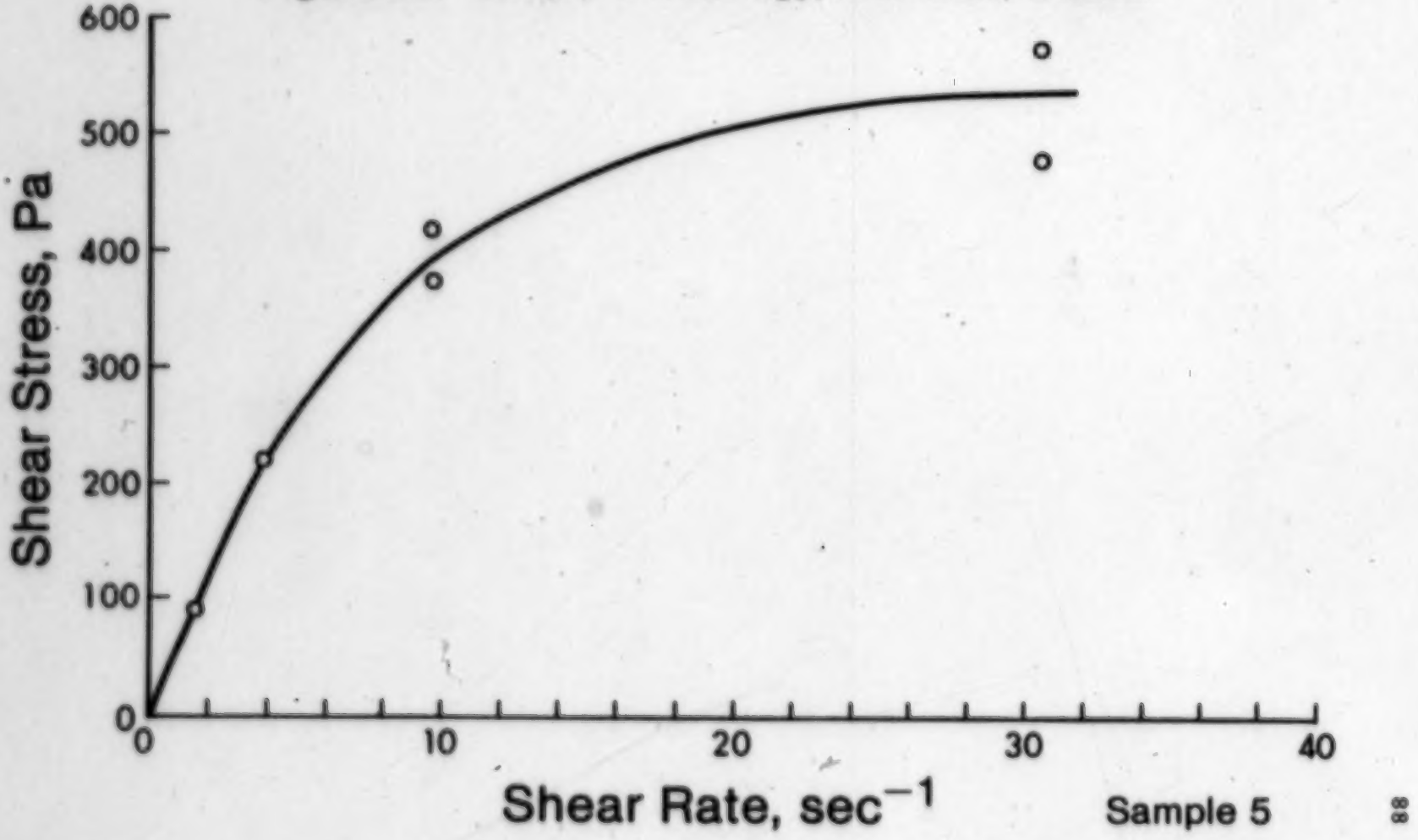

Figure 36.

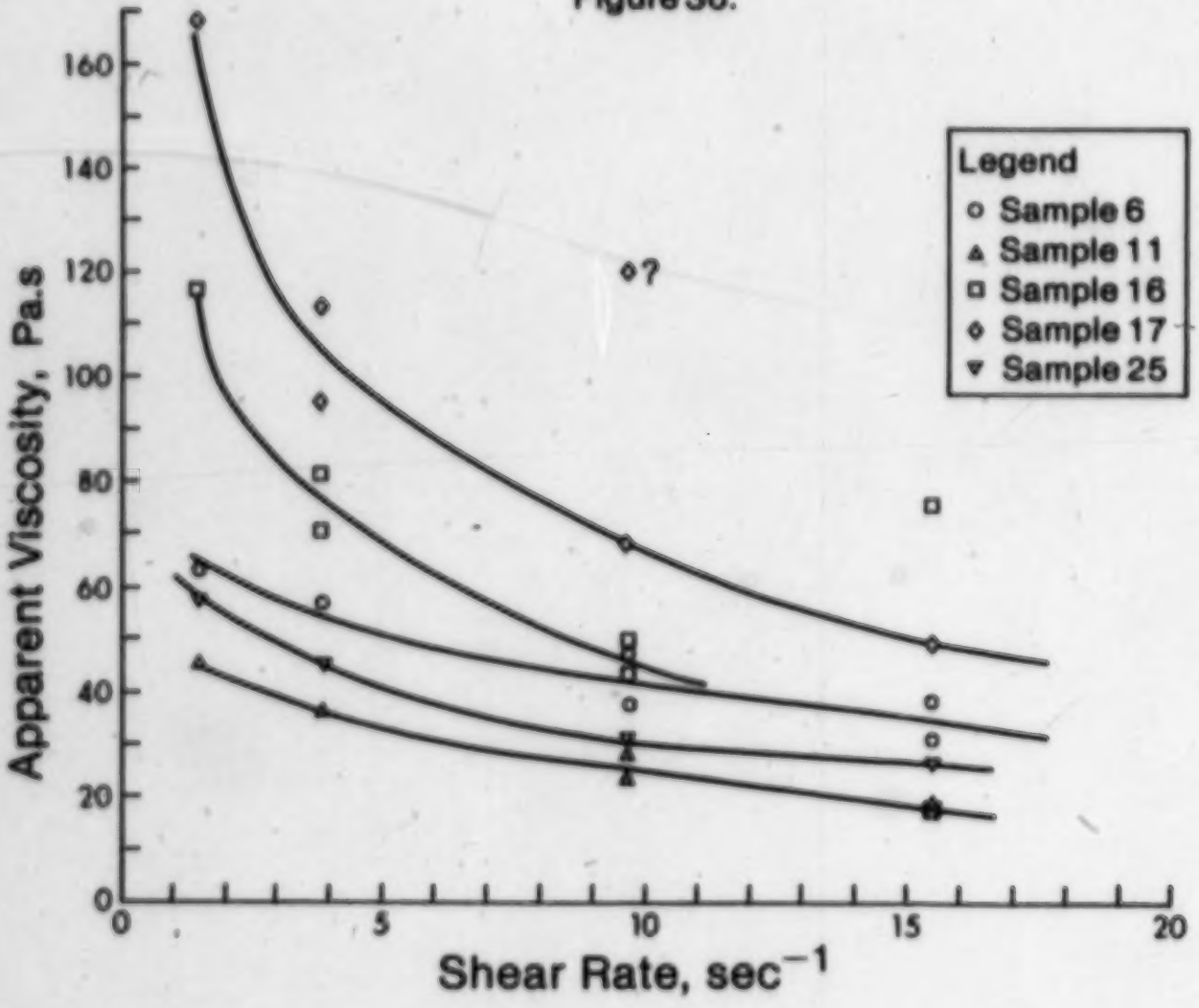
Apparent Viscosity, Pa.s
160
140
120
100
80
60
40
20
0
0
5
10
15
20
Shear Rate, sec^{-1}
Legend
Sample 6
Sample 11
Sample 16
Sample 17
Sample 25

viscosity . For shear rates greater than approximately 10 reciprocal seconds, the rate of decrease of apparent viscosity with shear rate seemed linear and identical for samples 6, 11, 17, and 25. Samples 5, 9, and the optimal emulsion also exhibit linear decreases in apparent viscosity beyond some high shear rate as shown in Figures 37 to 39. This shear rate is not the same for all mixtures. Such behaviour is commonly observed with emulsions. The change in rate of decrease of apparent viscosity could be an indication of a change in structure of the macroemulsion. Water droplets which could remain as aggregates at low rates of shear became gradually dispersed at higher rates until no further dispersion could occur. Some samples showed time-dependent behaviour at high shear rates. Shear stress would start at some high value and then drop in a hyperbolic fashion, duplicating to some extent the shape of the apparent viscosity curves. Initial and final values of shear stress for these samples are reported in all tables and graphs. In the tables both values of shear stress are listed; in the graphs both values of shear stress are plotted at the same shear rate.

Three sets of ternary diagrams were determined at three different shear rates. Their purpose was to assist in predicting how the optimal emulsion would behave as it encountered varying amounts of crude oil and/or water in the reservoir. Distilled water was used throughout to provide a reference data base. The single most important result was

Figure 37. Optimal Emulsion Rheology

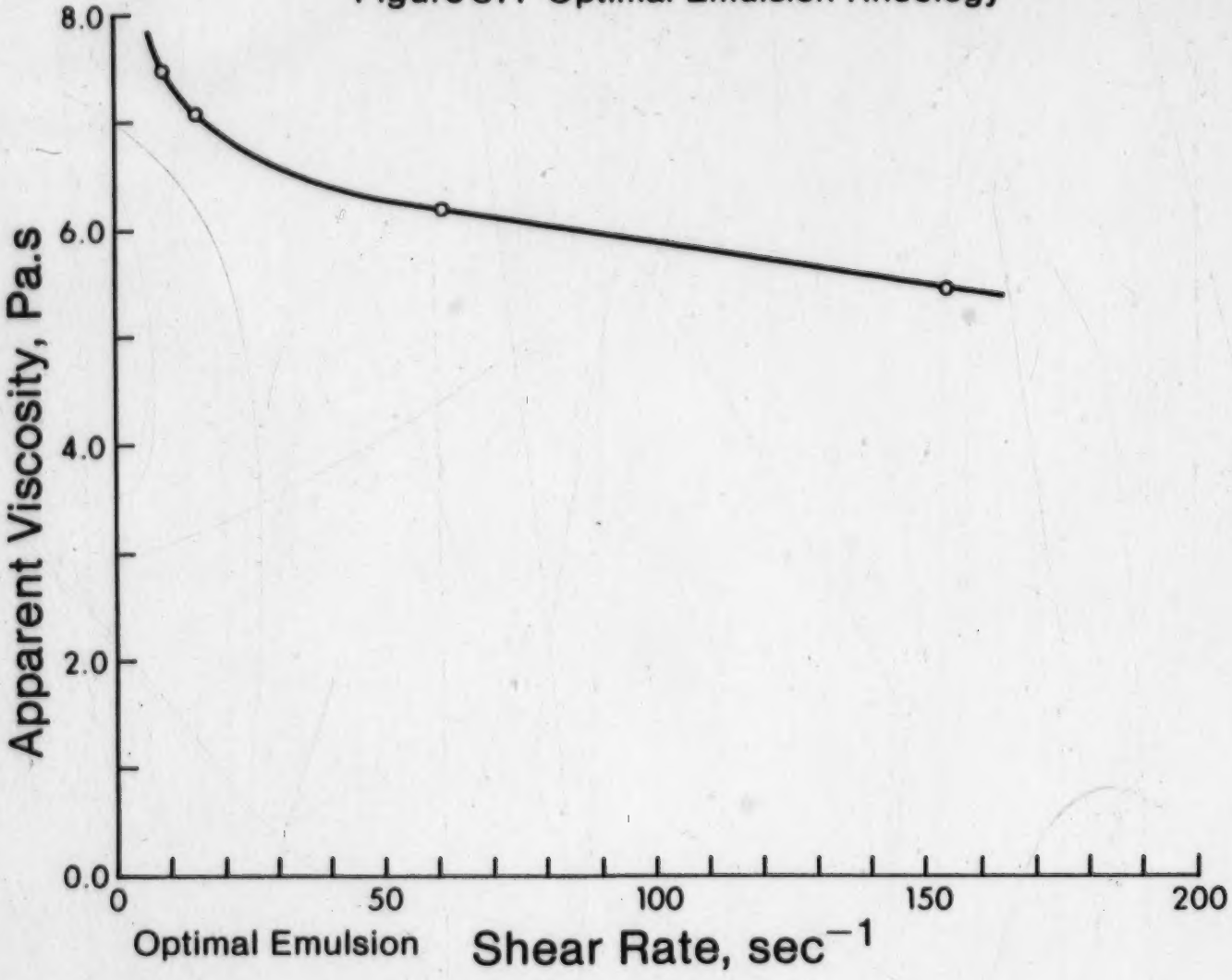

Figure 38. Sample 5 Rheology

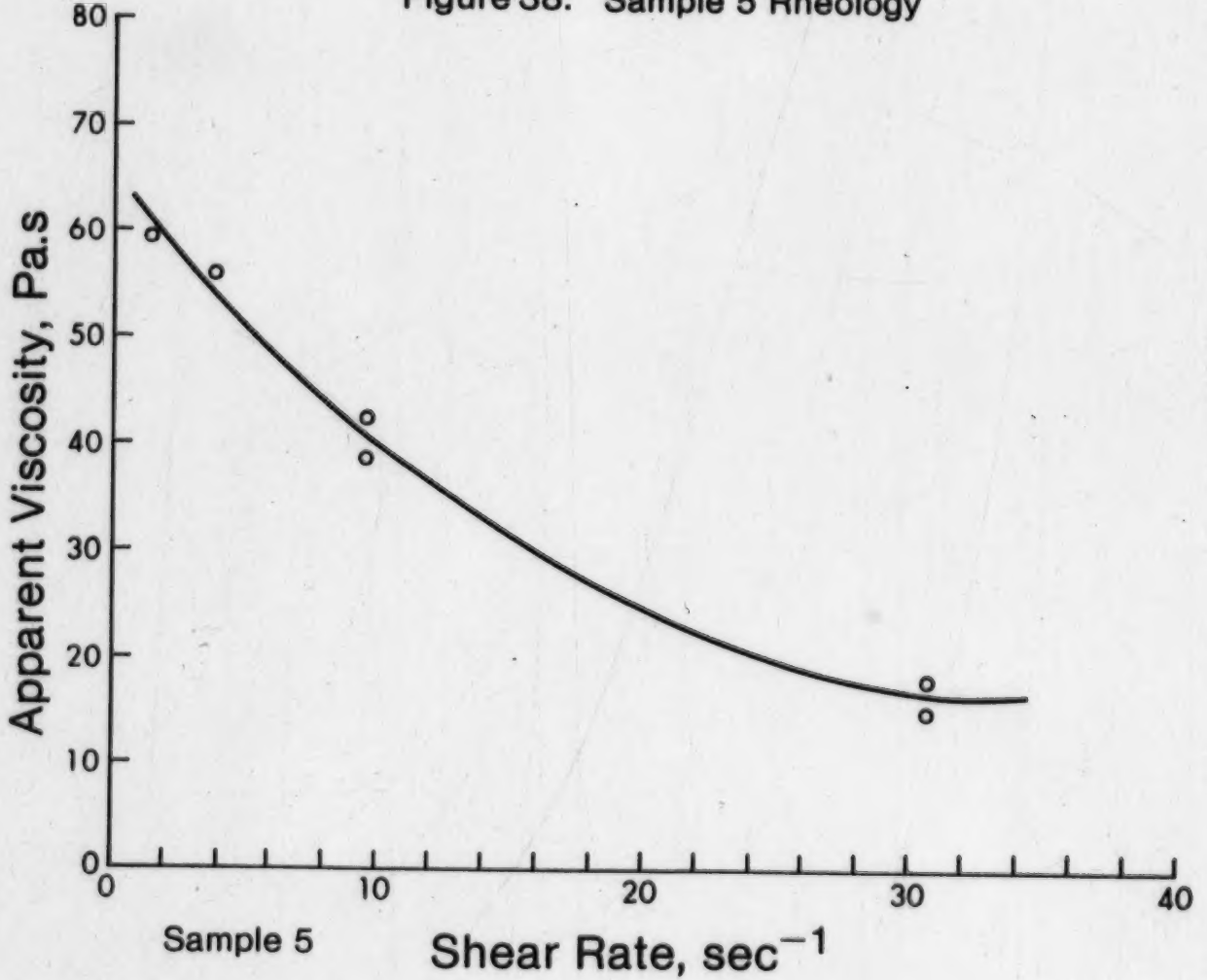

Figure 39. Sample 9 Rheology

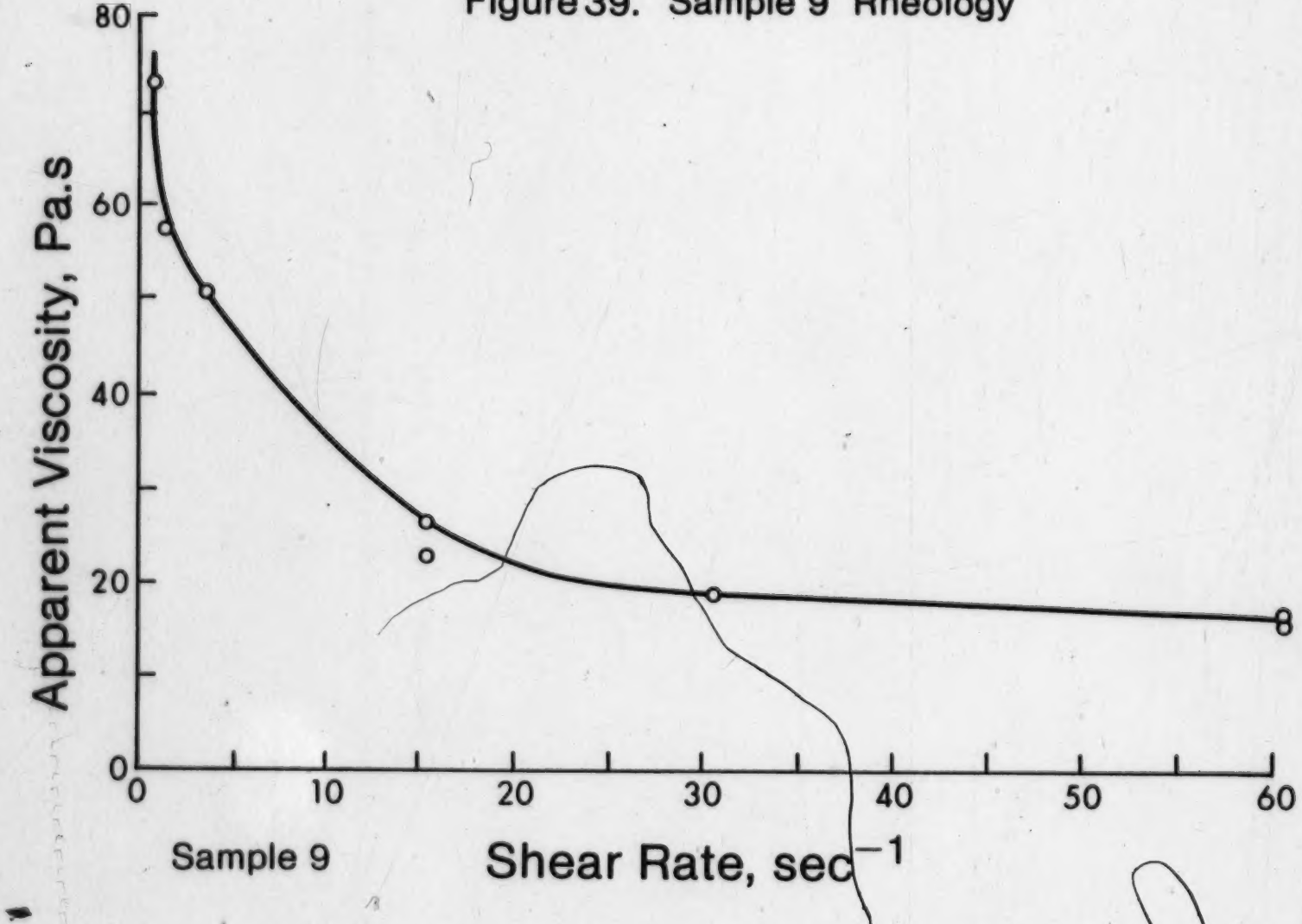

that mixtures prepared with at least 30 percent water most likely resulted in a gel or otherwise very high viscosity W/O phase (100+ Pa·s or 100000+ cp). This can be seen in Figures 40 to 42. Also, resulting mixtures all had apparent viscosities far higher than any of the three basic components (emulsion, distilled water, crude oil). Zones of similar apparent viscosity were not continuous. It was therefore not possible to say for example that for a fixed water content, any combination of emulsion and crude oil would yield moderate viscosities (relatively speaking).

Note that preparation #5 in Figures 40 to 42 had substantially lower apparent viscosity than its neighbors-for the same distilled water content. Other three-phases mixtures are preparations #9 and #11 and it can be seen on all three apparent viscosity charts that their apparent viscosities were systematically lower than those of the surrounding mixtures. There seems to be some peculiarity attached to three-phase mixtures for this particular crude oil. As a reminder, by three-phase mixture is meant a preparation where after thorough mixing in accordance with the procedure developed in Chapter 5, three distinct layers (oil, emulsion, and water) were observed.

Finally, among preparations in which two phases resulted, emulsion-water mixtures showed substantially higher apparent viscosities in the W/O phase than did their emulsion-oil counterparts on all three viscosity charts.

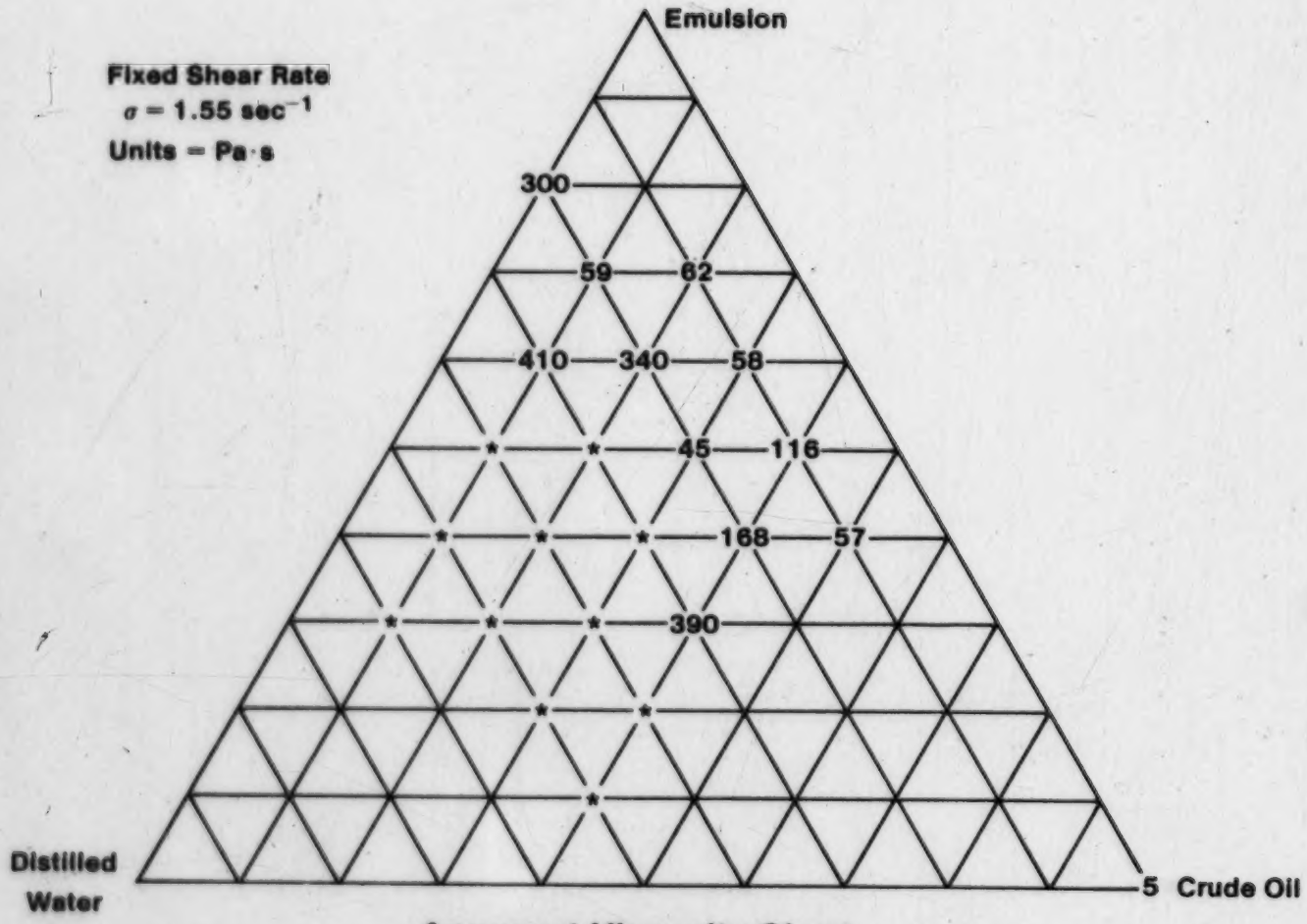

Apparent Viscosity Chart

Figure 40.

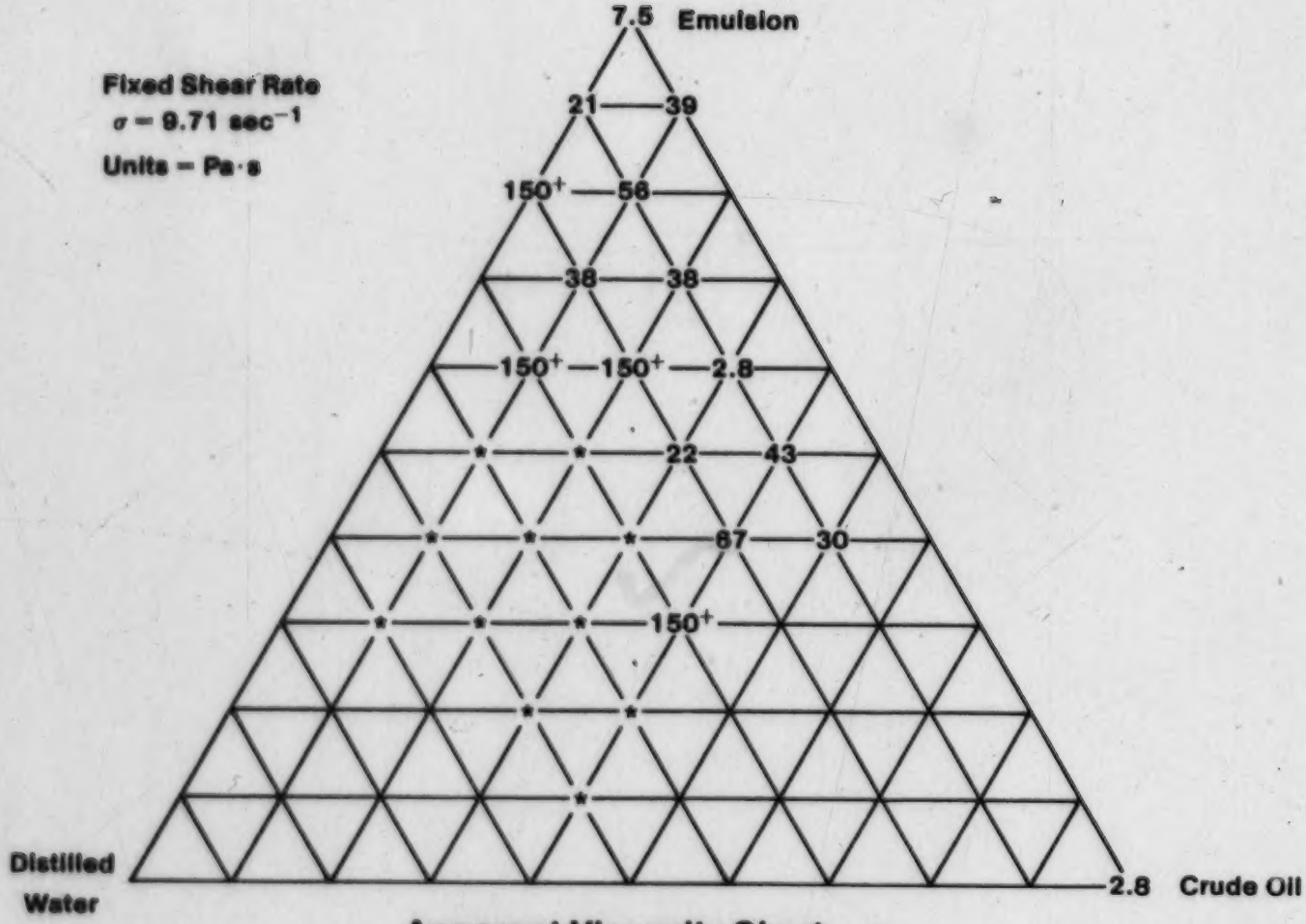

Apparent Viscosity Chart

Figure 41.

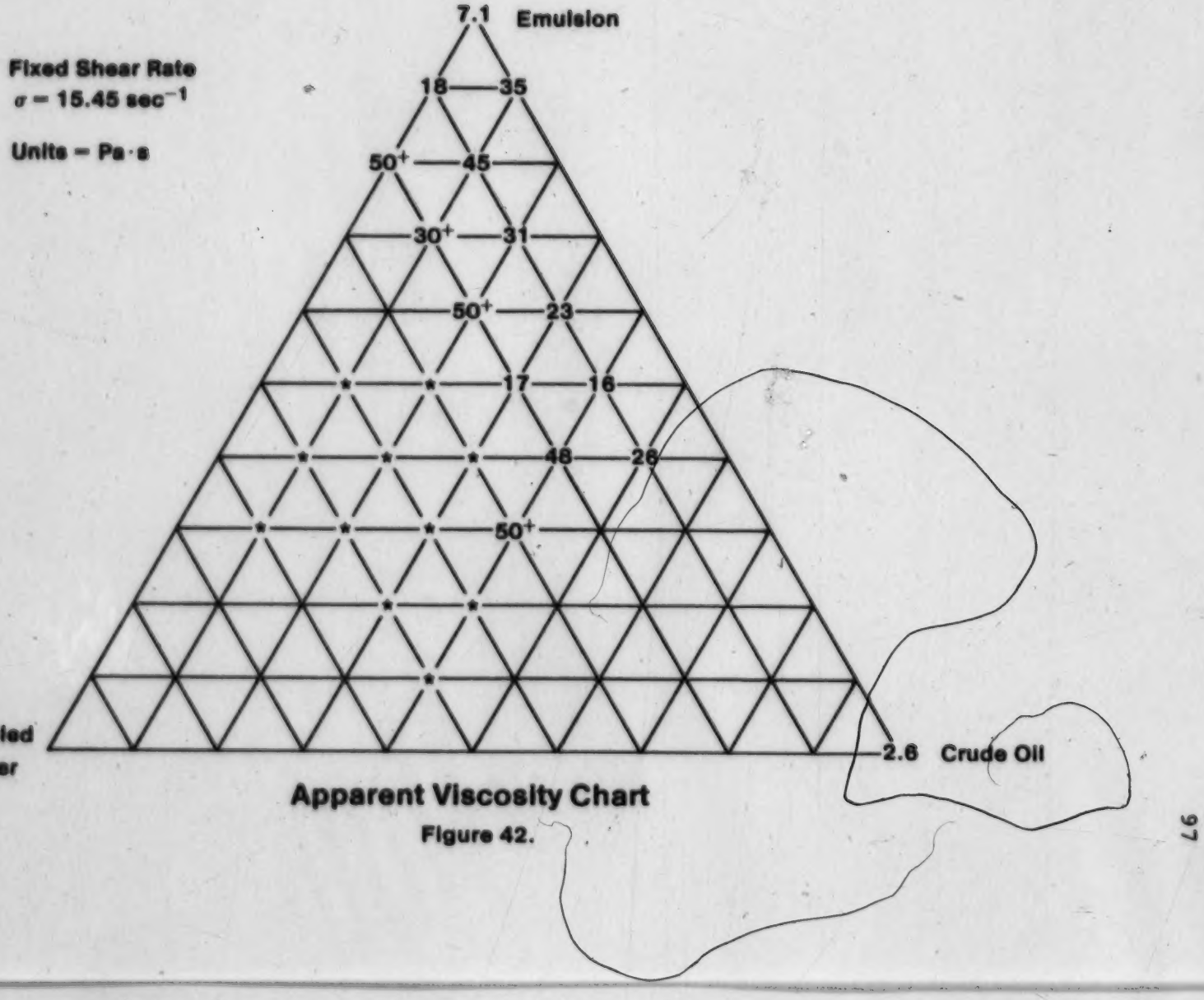

Apparent Viscosity Chart

Figure 42.

6.6 SOLVENT EFFECTIVENESS

The purpose of the solvent was to reduce effectively the viscosity of the chosen stable emulsion to a level at which injection would be feasible. Different solvents were used in different concentrations to assess both their effectiveness and their impact on stability. In the first series of trials, four solvents were considered: toluene, Varsol, benzene, and xylenes. Aromatics were chosen because they would not precipitate asphaltenes. Results are shown in Table E-3, Appendix E.

The first two solvents were soon discarded because even at low concentrations they destabilized the emulsion within forty eight hours. The remaining two were further tested.

It was observed that as the solvent concentration was increased, the rate of drop in apparent viscosity with increasing shear rate decreased. Figure 43 exemplifies this for the case of benzene. Data for Figure 43 is listed in Table E-4, Appendix E. The mixture became closer and closer to exhibiting Newtonian behaviour as the amount of solvent added increased. At the same time, the value of viscosity decreased sharply with increasing solvent content. Beyond 6 percent solvent, the gain in fluidity with increasing solvent concentration also decreased rapidly.

Both benzene and xylenes performed equally well as aromatics in the viscosity reduction process as shown in Figure 44. Data for Figure 44 is listed in Table E-7, Appendix E. Xylenes have a larger molecular weight than

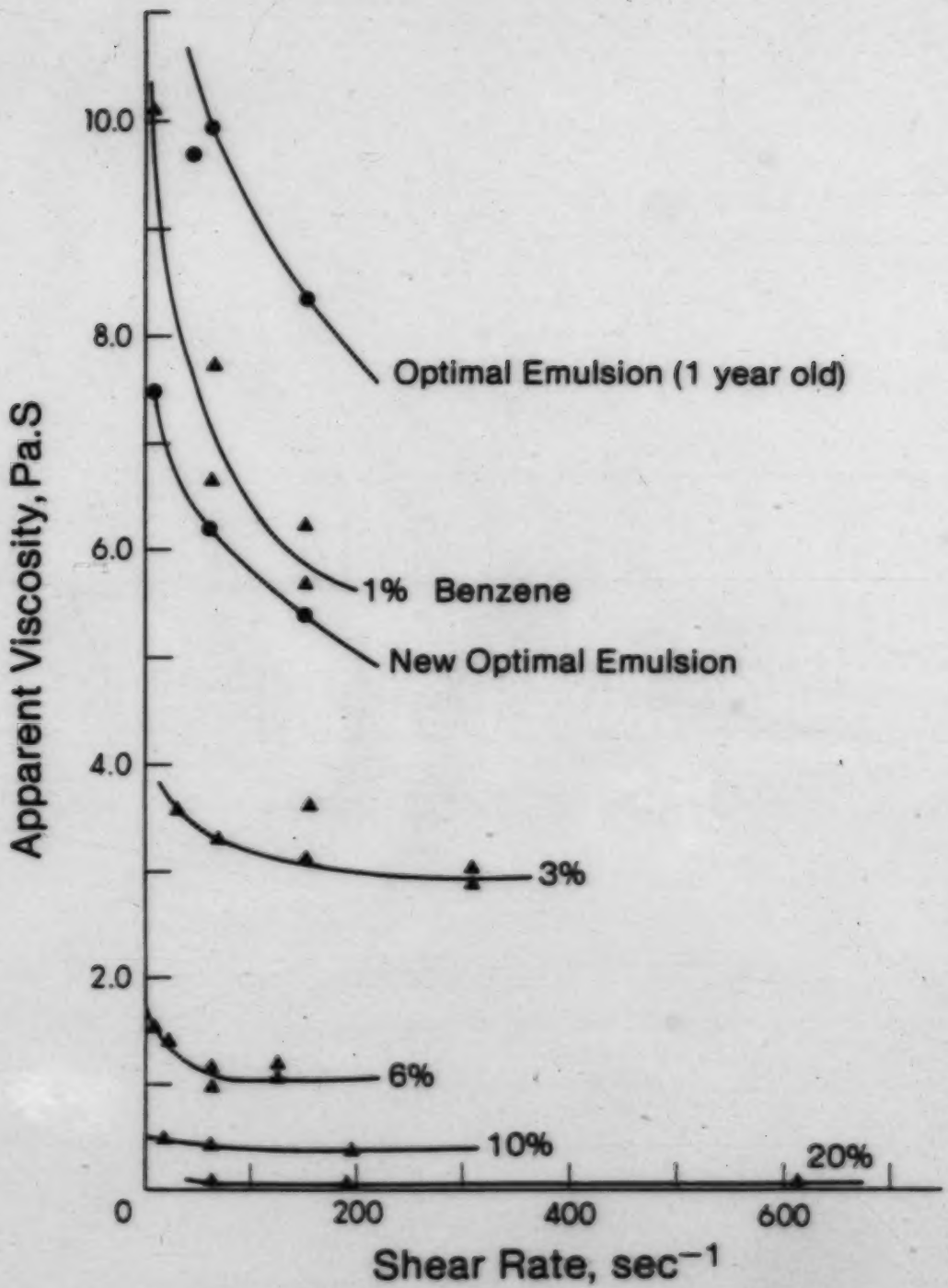

Figure 43. Effect of Benzene on Emulsion Viscosity.

benzene; both are equally toxic and highly flammable. Benzene costs twice as much as xylenes. Viscosity reduction data for xylenes is shown in Table E-5, Appendix E.

Emulsion stability was an important issue; at high solvent concentrations an aqueous phase was seen forming at the bottom of the samples while the top layer became oil-rich. At low concentrations, the water did not separate out but the reduction in viscosity was not sufficient. A further reduction in viscosity would be necessary which would mean larger fractions of solvent should be used. Such solvent cuts would be, however, expensive because of the high cost of benzene and xylenes. For this reason, the possible use of synthetic crude as a solvent was investigated.

Synthetic crude was not as effective a solvent as benzene or xylenes; it took about 10 percent synthetic crude to decrease the optimal emulsion viscosity to around 1 Pa·s or 1000 cp as can be seen in Figure 45 while 6 percent of benzene or xylenes achieved the same result. Data for Figure 45 is shown in Table E-6, Appendix E. However, since synthetic crude was so much cheaper, cuts of even 10 to 15 percent would be inexpensive.

6.7 HEAVY OIL RECOVERY EXPERIMENTS

These sand pack experiments were designed to simulate emulsion flooding in an oil reservoir. The major difference was that flow in a reservoir would occur in three dimensions

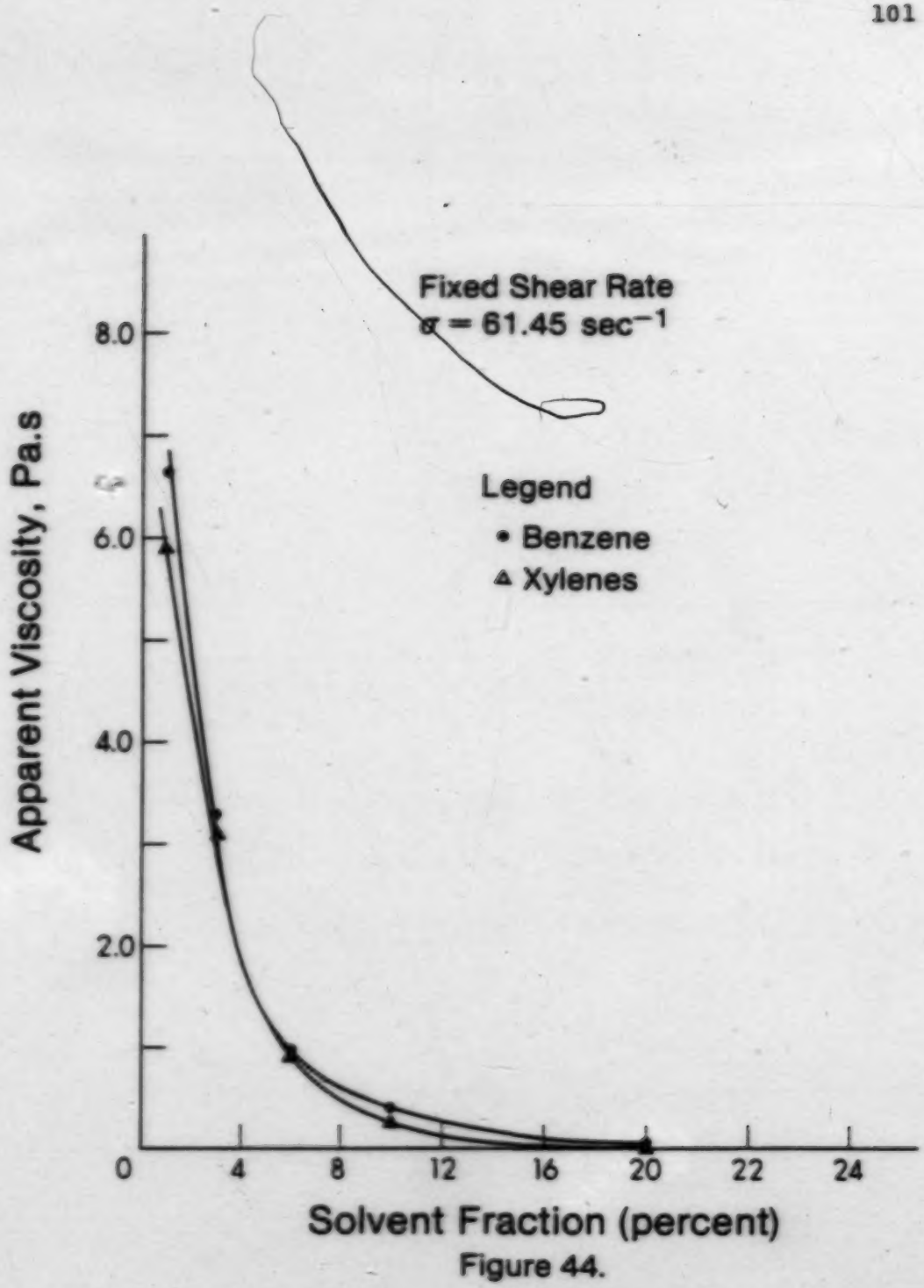

Figure 44.

Comparison of Solvents as Viscosity Reducing Agents.

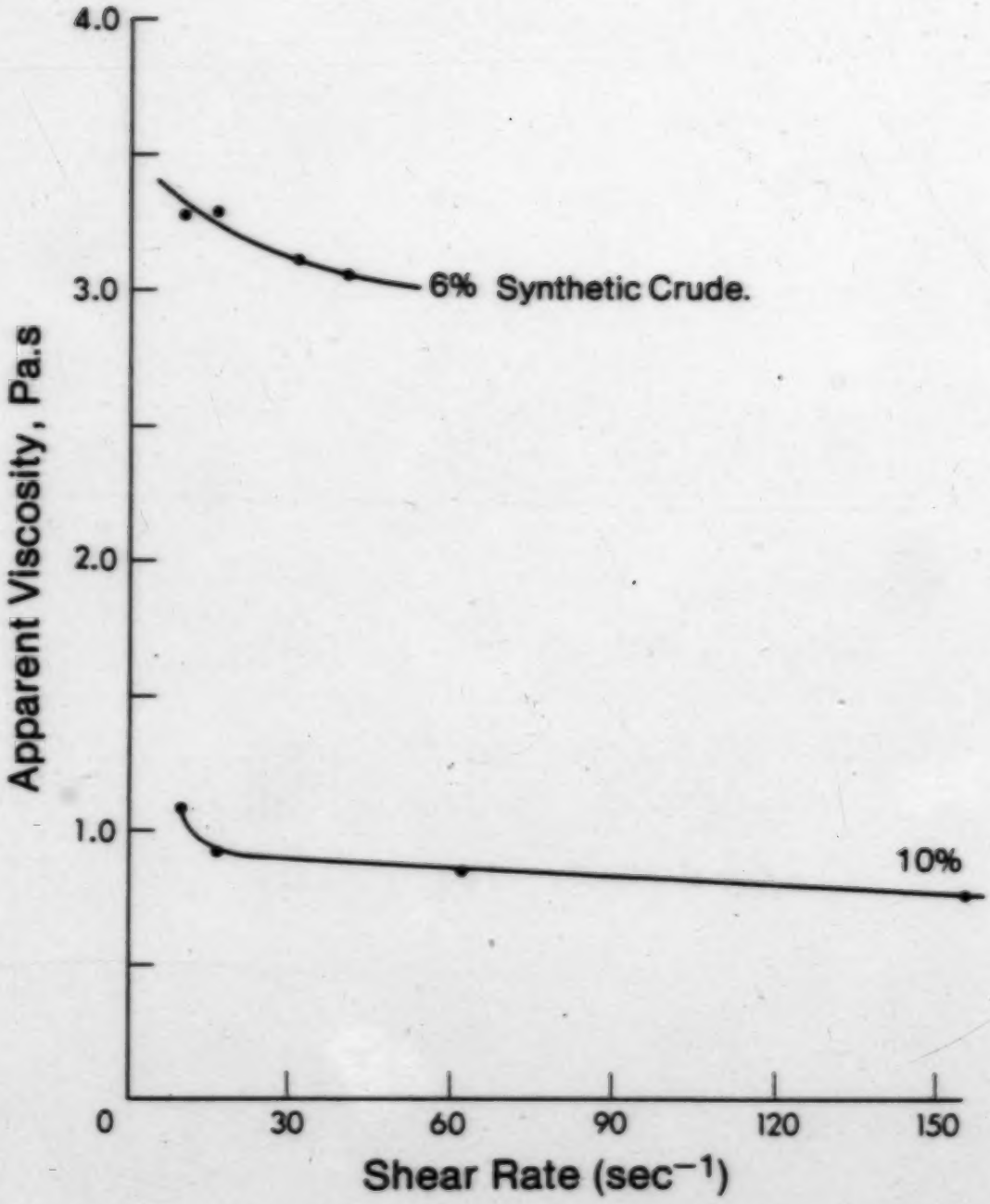

Figure 45. Effect of Synthetic Crude on Emulsion Viscosity.

while flow in the sand packs occurred in essentially one dimension. Therefore, sand pack displacements were to be at best indicative of what would happen in an idealized field situation. Moreover, the type of oil chosen to simulate reservoir oil was a refinery cut of medium viscosity (600 cp). Rheological properties of this oil and of the displacing emulsion can be seen in Figure 46. Calculated values of permeability for each sand pack are shown in Table G-1, Appendix G.

Within these constraints, six runs were conducted to evaluate the performance of the emulsion under various conditions. Table 2 shows the displacement parameters for each run. All runs were compared with the performance of a simple waterflood, used as a base reference. Pressure and oil cut histories for this waterflood can be seen in Figure 47. It can be observed that water breakthrough occurred early while oil production decreased stepwise. Inlet pressure first increased to 16 psi and then decreased monotonically as is usually the case for a waterflood. Initial increase in pressure can be due to presence of gas in the system or can simply mean that the lines account for limited compressibility. The run was stopped when the oil cut dropped below 5 percent. Recovery was 43.0 percent of the initial oil in place.

Figure 46: Rheology of Heavy Oil and Eyehill Emulsion

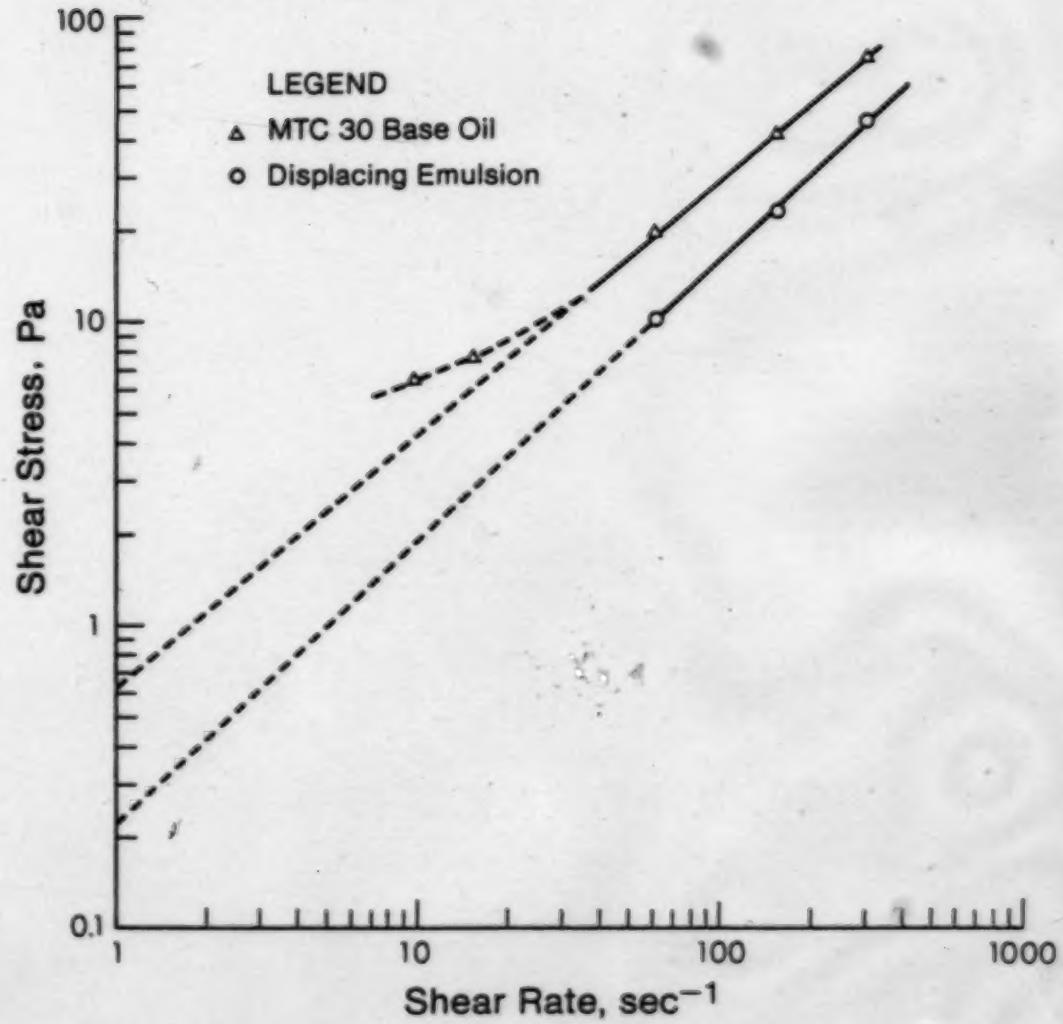

Porosity	: 41.5%	Core Length	: 0.609 m (2 ft)
Permeability	: 18.30 Darcys	Waterflood	: Complete
Pore Volume	: 765 ml	Oil Viscosity	: 620 cp
Initial Oil in Place	: 690 ml	Emulsion Viscosity	: 220 cp
Flow Rate	: 100 cc/hr	Emulsion Composition	: N/A
Slug Size	: 0% P.V.	Ultimate Recovery	: 43.0% IOIP

Figure 47: Pressure and Oil Cut Histories – Run 1

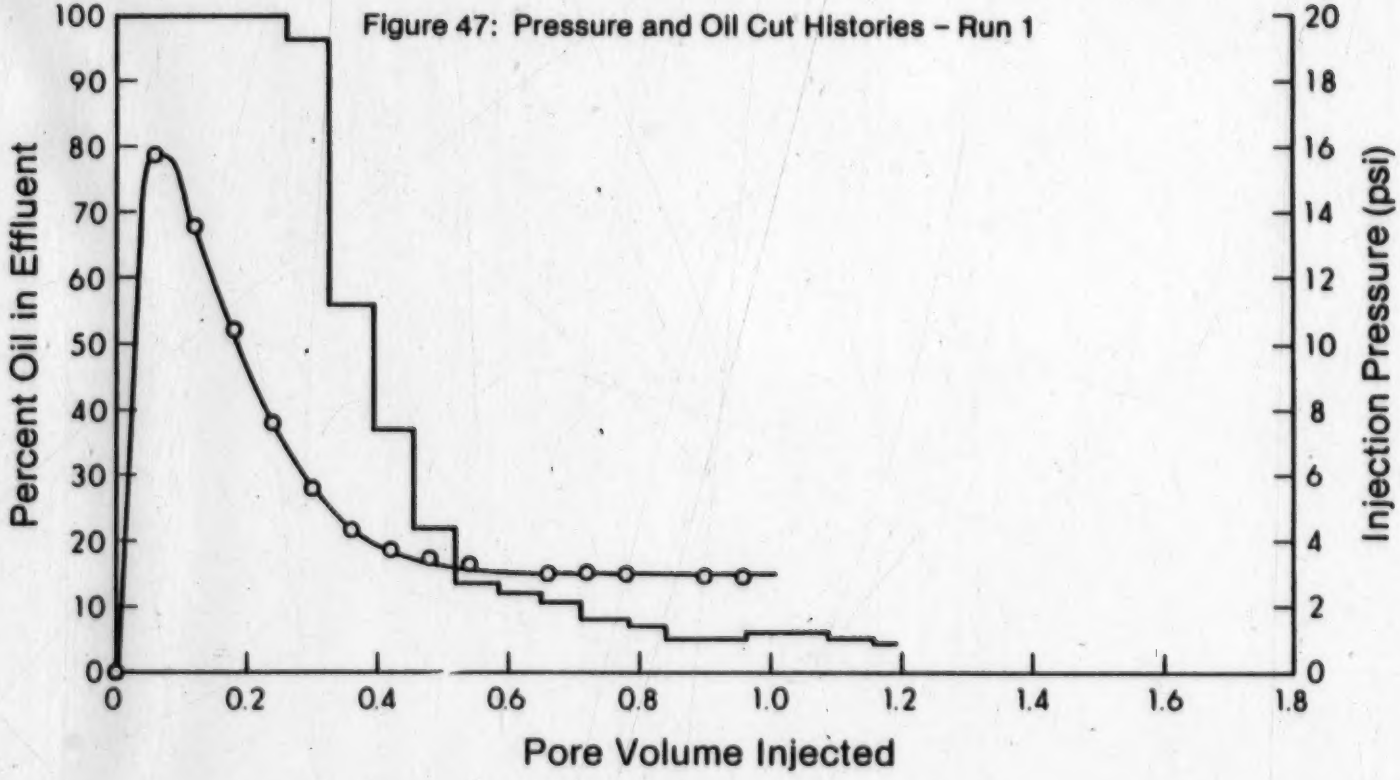

TABLE 2

Sand Pack Displacement Parameters

Run	Core #	Slug Size, Percent	Displacement Type	Core Length, m
1	3	0	Waterflood	0.609
2	4	10	Slug	0.609
3	2	20	Slug	0.609
4	1	30	Slug	0.609
5	5	30	Waterflood+Slug	0.609
6	6	30	Slug	1.218

Flow Rates in all Runs: 100 cc/hr

6.7.1 Effect of Slug Size

Three different slug sizes were tested: 10, 20, and 30 percent of the pore volume. In each case, no waterflood was conducted prior to emulsion slug injection.

As the size of the slug increased, the amount of oil produced prior to water breakthrough increased (see Figures 48 to 50). After breakthrough, the transition to large water production was sharp in the case of the 10 percent slug but became more and more progressive and step-like as the size of the emulsion slug increased to 20 and 30 percent.

Pressure histories for the three slug sizes were all different but showed a trend. In all three cases, as with the waterflood, pressure first increased to a local maximum. For the 10 percent slug size, injection of water to push the slug coincided with the maximum pressure (Figure 48). For the 20 percent slug size, inlet pressure started to decrease when water injection began (Figure 49). For the 30 percent slug size, inlet pressure dropped by 10 psi by the time water injection was initiated (Figure 50). In the case of the waterflood, maximum pressure formed a sharp peak. As the slug size increased from 10 to 30 percent this peak became less sharp and gradually decreased in size.

Two conclusions can be drawn from these observations. First, it seems that emulsion injection becomes easier with time because drop in inlet pressure is not linked with water injection. It will be seen later that water injection has a

Porosity	: 42.6%	Core Length	: 0.609 m (2 ft)
Permeability	: 13.85 Darcys	Waterflood	: None
Pore Volume	: 780 ml	Oil Viscosity	: 620 cp
Initial Oil in Place	: 675 ml	Emulsion Viscosity	: 220 cp
Flow Rate	: 100 cc/hr	Emulsion Composition	: 80% Crude, 7% Caustic, 13% Synthetic Crude
Slug Size	: 10% P.V.	Ultimate Recovery	: 54.8% IOIP

Figure 48: Pressure and Oil Cut Histories - Run 2

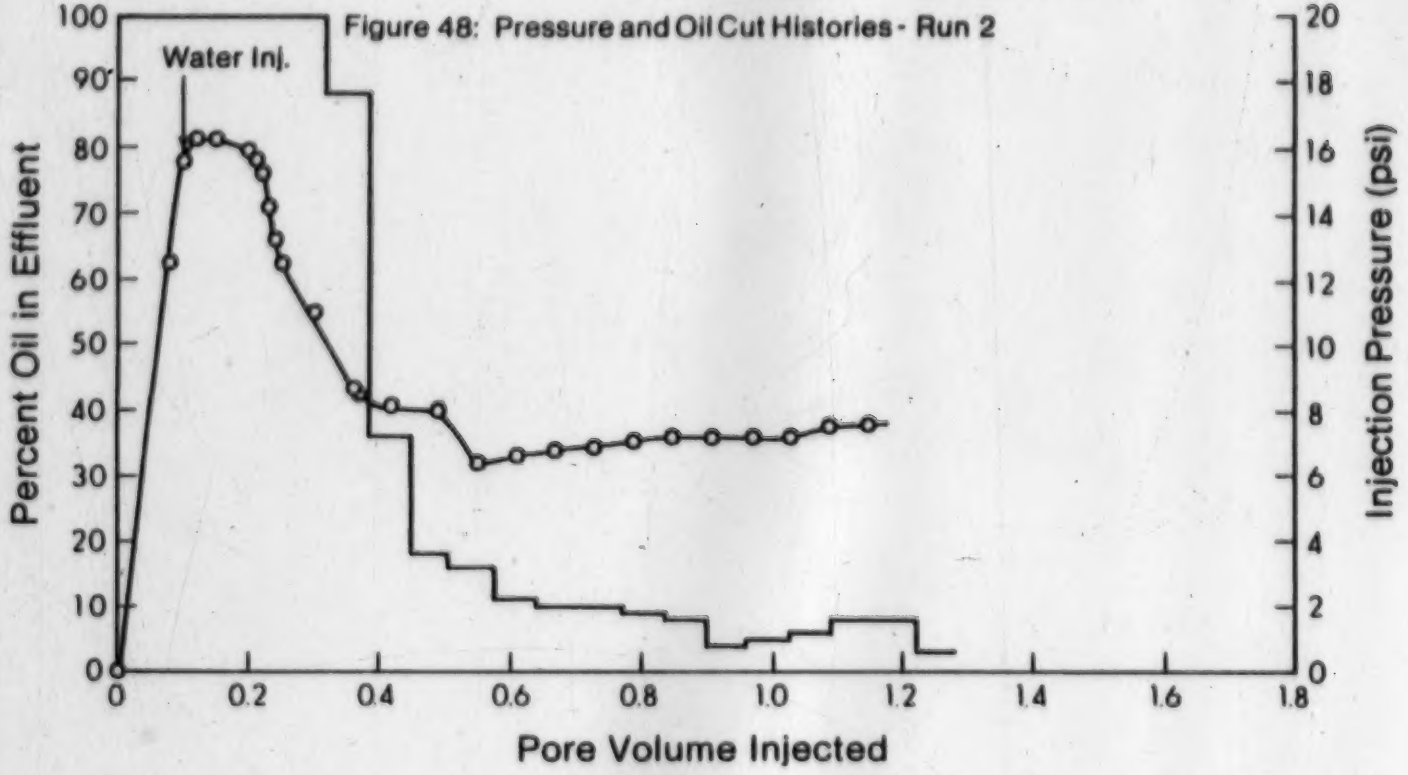

Porosity	: 41.9%	Core Length	: 0.609 m (2 ft)
Permeability	: 10.61 Darcys	Waterflood	: None
Pore Volume	: 767 ml	Oil Viscosity	: 620 cp
Initial Oil in Place	: 680 ml	Emulsion Viscosity	: 220 cp
Flow Rate	: 100 cc/hr	Emulsion Composition	: 80% Crude, 7% Caustic, 13% Synthetic Crude
Slug Size	: 20% P.V.	Ultimate Recovery	: 67.0% IOIP

Figure 49: Pressure and Oil Cut Histories - Run 3

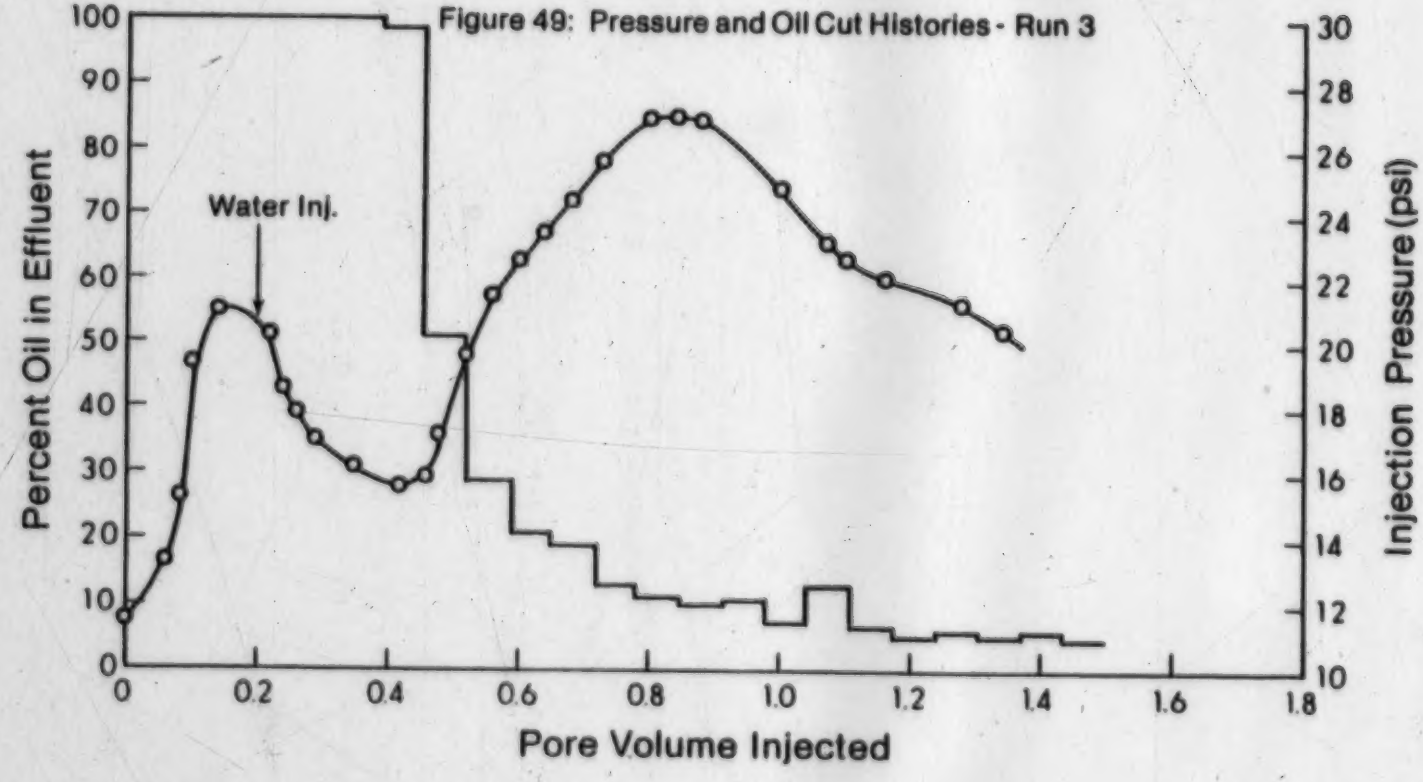

Porosity	: 42.7%	Core Length	: 0.609 m (2 ft)
Permeability	: 13.31 Darcys	Waterflood	: None
Pore Volume	: 782 ml	Oil Viscosity	: 620 cp
Initial Oil in Place	: 680 ml	Emulsion Viscosity	: 220 cp
Flow Rate	: 100 cc/hr	Emulsion Composition	: 80% Crude, 7% Caustic, 13% Synthetic Crude
Slug Size	: 30% P.V.	Ultimate Recovery	: 80.3% IOIP

Figure 50: Pressure and Oil Cut Histories - Run 4

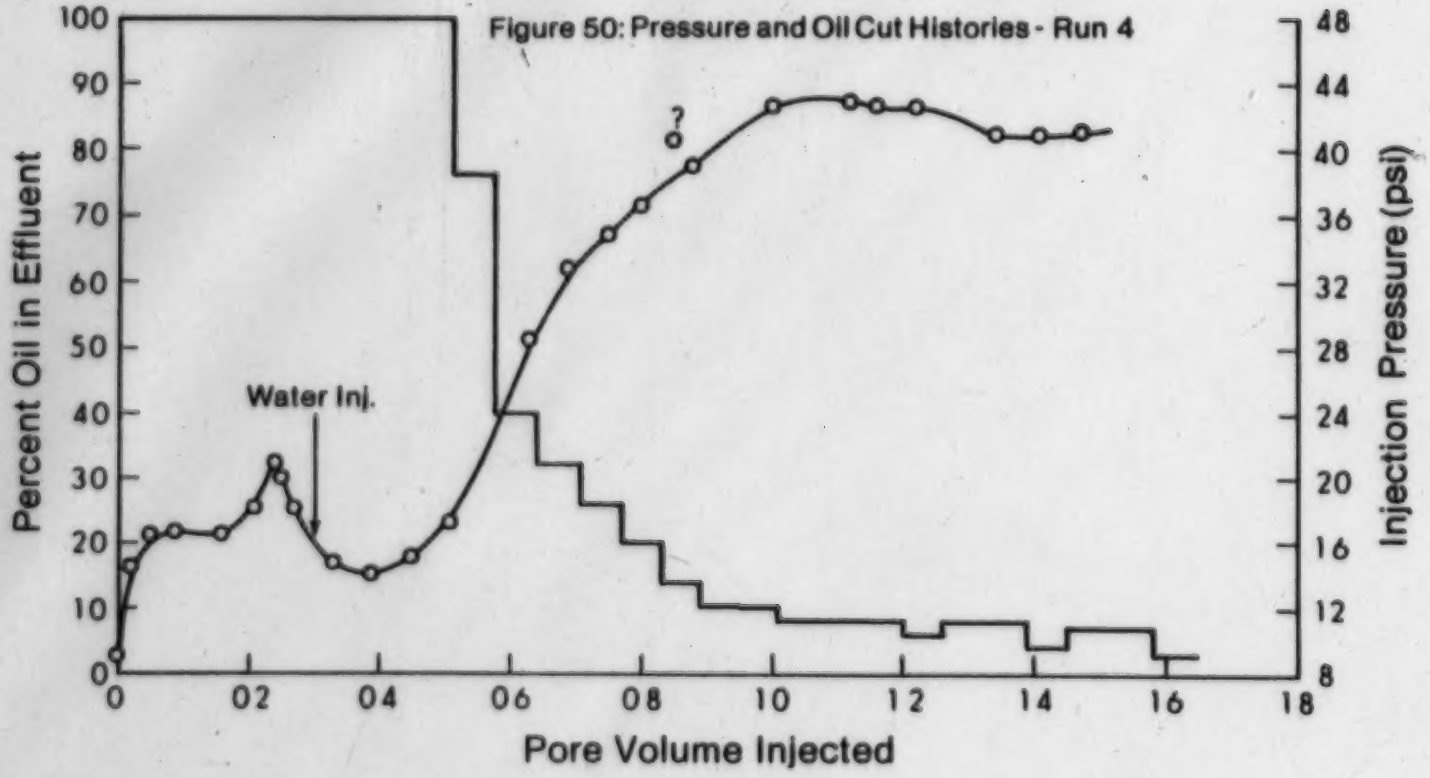

totally different effect. Second, even though the actual value of inlet pressure increases as the slug size increases, the maximum initial pressure required to inject the emulsion becomes less significant in terms of the overall pressure history.

In the case of a waterflood, pressure beyond the maximum decreased monotonically. But for every run where an emulsion slug was present, pressure first decreased then started to increase again. As slug size increased from 10 to 30 percent, the decrease in pressure became smaller and the subsequent increase steeper. The following interpretation of these observations is offered. It is based entirely on the observation of pressure behaviour because pressure was the only measurable variable in these experiments. Pressure was therefore used as an index to the mechanistic features of the emulsion slug processes.

Since water has a lower viscosity than both emulsion and oil, it is easier to push it through the porous medium. Since flow rate is kept constant, the inlet pressure drops. But as larger amounts of water come in contact with the emulsion, several phenomena may occur all of which would result in an increase in inlet pressure. Water and emulsion may mix giving a product of substantially higher viscosity as was reported in the chapter on rheological properties; such a fluid would necessitate a higher inlet pressure to flow through the sand pack. As a second possibility, water may try to bypass the emulsion. Because the water droplets

in the emulsion will plug the pore space, the area open to water flow will be greatly reduced; this would also necessitate a higher injection pressure to maintain a constant rate. Pressure increases were steady for the 10 and 30 percent slug sizes. In the case of the 20 percent slug, pressure increased steadily, then fell. This could be interpreted as a successful channeling of water through the slug and through the oil.

Recovery for the three slug sizes as a function of pore volume injected was reported in Figure 51. It was observed that the increase in recovery was almost proportional to the increase in slug size. The increase in oil recovered prior to breakthrough was also directly dependent on the increase in slug size (see Table 3). However the incremental recovery was not proportional to the slug size. For example, the use of a 30 percent slug which contained oil representing 9.8 percent of the pore volume allowed the recovery of an additional 37.3 percent of the initial oil in place, compared to a waterflood. The total recovery for that slug size was high: 80.3 percent of the initial oil in place against 43.0 percent for a waterflood.

Another observation of interest was the measurement of the salinity of the effluent for each run (Figure 52). Brine which was initially at irreducible saturation was the first water to be produced thereby indicating that the brine must have been banked ahead of the emulsion front.

Figure 51: Effect of Emulsion Slug Size on Recovery

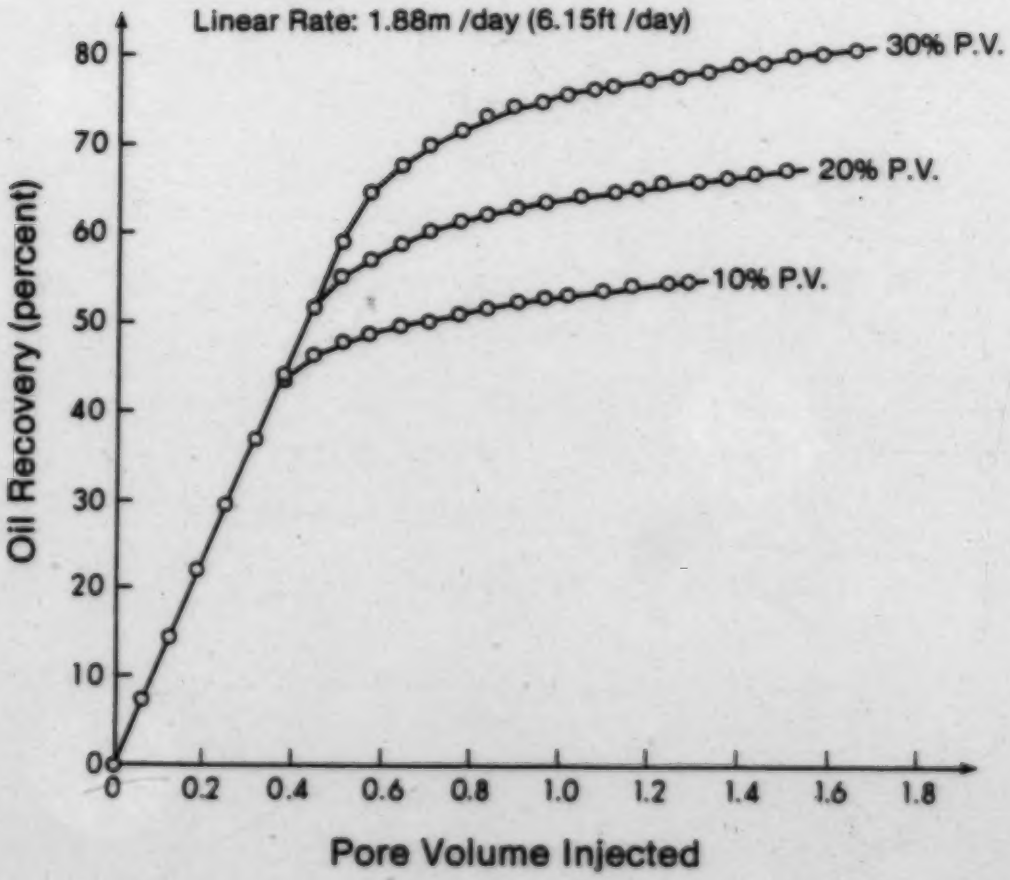

TABLE 3

Flood Results

Run #	Displacement type	Percent IOIP recovered
1	Waterflood	43.0
2	0.10 P.V. Slug	54.8
3	0.20 P.V. Slug	67.0
4	0.30 P.V. Slug	80.3
5	Waterflood+Slug	69.3
6	0.30 P.V. Slug	69.7

6.7.2 Effect of a Prior Waterflood on Emulsion Slug Process

This experiment was designed to investigate the applicability of an emulsion slug process in a situation where waterflooding was previously conducted. A waterflood was conducted on core #5 (Figure 53). When the effluent water cut approached 50 percent, an emulsion slug (30 percent of the pore volume) was injected followed by distilled water injection. A new oil bank was observed and oil recovery increased from 43.0 percent (simple waterflood) to 69.3 percent, after 1.6 volumes were injected. As shown in Figure 53, the second oil cut peak was almost as high as the initial one. Emulsion injection displaced a significant amount of oil which had been bypassed by the waterflood. Inlet pressure increased as soon as water was injected to push the emulsion slug. This observation seemed to confirm that the main effect of the emulsion was to effectively block the passage to water and restrict channeling. The remainder of the pressure history resembles that for run #4.

Therefore emulsion injection would still assist recovery even if a waterflood has already been started. The effect of the emulsion slug was also visible in the variation in effluent salinity (see Figure 54, run #5). A sudden increase in salinity was recorded, indicating that not all the brine had been driven out by the waterflood. No conclusion could therefore be drawn as to the existence of a brine bank formed in the sand pack ahead of the waterflood or of the emulsion slug.

Figure 52: Salinity of Aqueous Phase Recovered During Displacement

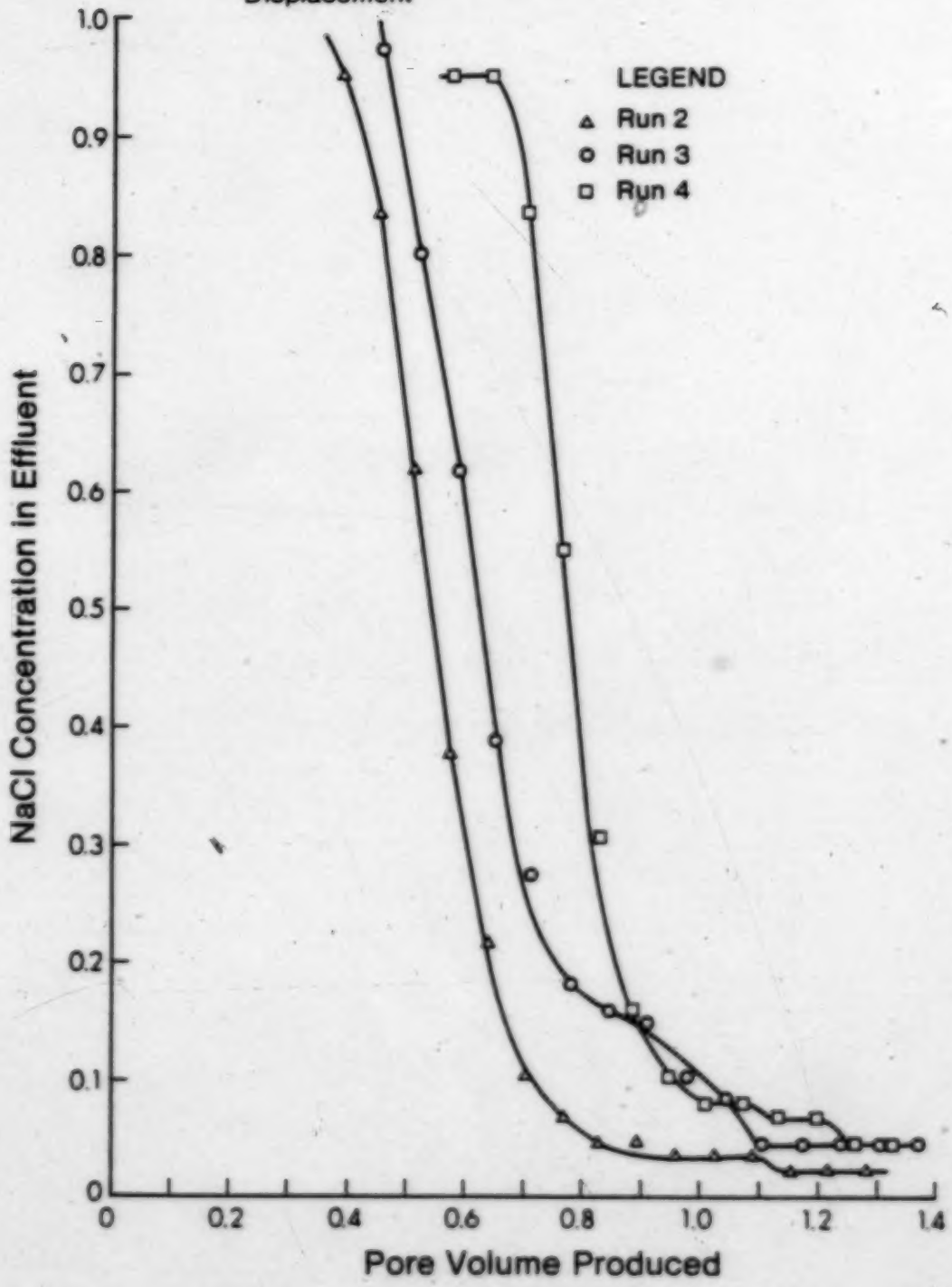

Porosity	: 39.9%	Core Length	: 0.609 m (2 ft)
Permeability	: 15.88 Darcys	Waterflood	: 43.7% Water Cut
Pore Volume	: 730 ml	Oil Viscosity	: 620 cp
Initial Oil in Place	: 695 ml	Emulsion Viscosity	: 220 cp
Flow Rate	: 100 cc/hr	Emulsion Composition	: 80% Crude, 7% Caustic, 13% Synthetic Crude
Slug Size	: 30% P.V.	Ultimate Recovery	: 69.3% IOIP

Figure 53: Pressure and Oil Cut Histories - Run 5

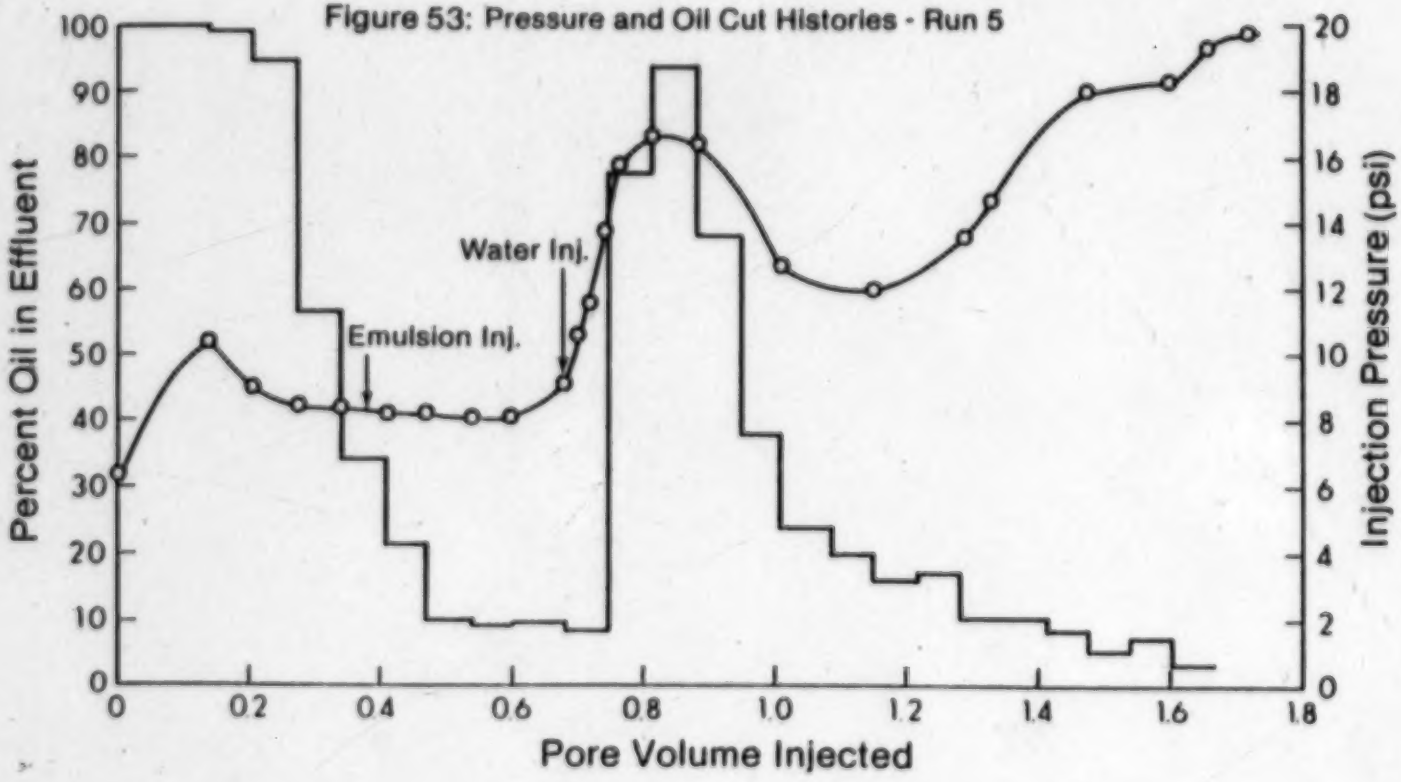

6.7.3 Effect of Core Length

Two emulsion slug displacements were performed in a 0.609 m (2 ft) and in a 1.22 m (4 ft) core. Similar oil cut profiles were observed (see Figures 50 and 55) except that water breakthrough occurred about 0.10 pore volume earlier in the longer core. Injection pressures followed the same trend in both cores and the inlet pressure in the long core was predictably higher than in the short core. However, the recovery for the longer core was only 69.7 percent of the oil in place while recovery in the short core was 80.3 percent for slug sizes representing the same fraction of the pore volume. It was anticipated that the recovery would be the same which would have meant that the oil recovery was independent of model size.

No definite explanation can be offered for the discrepancy between the two figures. It could be due to viscous fingering. Because the difference in viscosities between water (0.001 Pa·s or 1 cp) and emulsion (0.220 Pa·s or 220 cp) was so large at the back of the emulsion bank, the front between the two liquids would be unstable.

The discrepancy could also be caused by the difference between the amount of water injected in run #4 and in run #6. In the short core, fluid injection totalized 1.645 pore volumes. In the long core the fluids injected represented 1.256 pore volumes or 0.39 pore volume less than for the short core. It should be recalled that core flood experiments were stopped when the oil fraction in the

Figure 54: Salinity of Aqueous Phase Recovered During Displacement

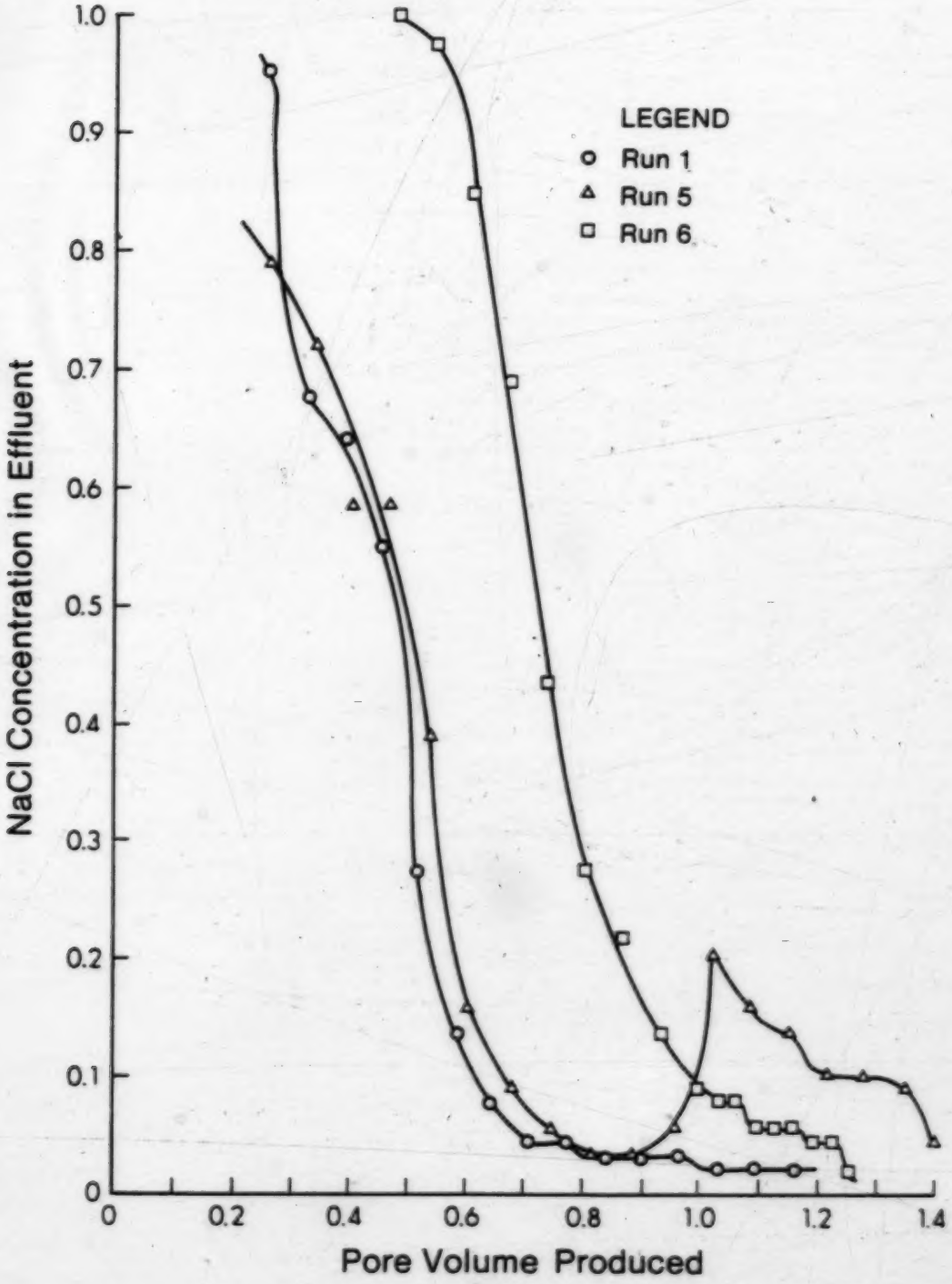

effluent dropped below 5 percent, in agreement with the procedure described in Paragraph 5.2.4.

In either case, the conclusion is that oil recovery was significantly lower in a long core (1.22 m or 4 ft) than in a short core (0.609 m or 2 ft). This is based upon only two runs, and could use future elaboration.

Oil recoveries for runs 1, 5, and 6, are compared in Figure 56. Waterflooding shows the lowest recovery. Slug injection after waterflood shows a net improvement in oil recovery. The sooner the slug injection begins, the larger the ultimate recovery will be. Finally oil recovery in a 1.22 m (4 ft) core is not as high as in a 0.609 m (2 ft) core.

Porosity	: 42.2%	Core Length	: 1.22 m (4 ft)
Permeability	: 15.51 Darcys	Waterflood	: None
Pore Volume	: 1552.5 ml	Oil Viscosity	: 620 cp
Initial Oil in Place	: 1370 ml	Emulsion Viscosity	: 220 cp
Flow Rate	: 100 cc/hr	Emulsion Composition	: 80% Crude, 7% Caustic, 13% Synthetic Crude
Slug Size	: 30% P.V.	Ultimate Recovery	: 69.7% IOIP

Figure 55: Pressure and Oil Cut Histories - Run 6

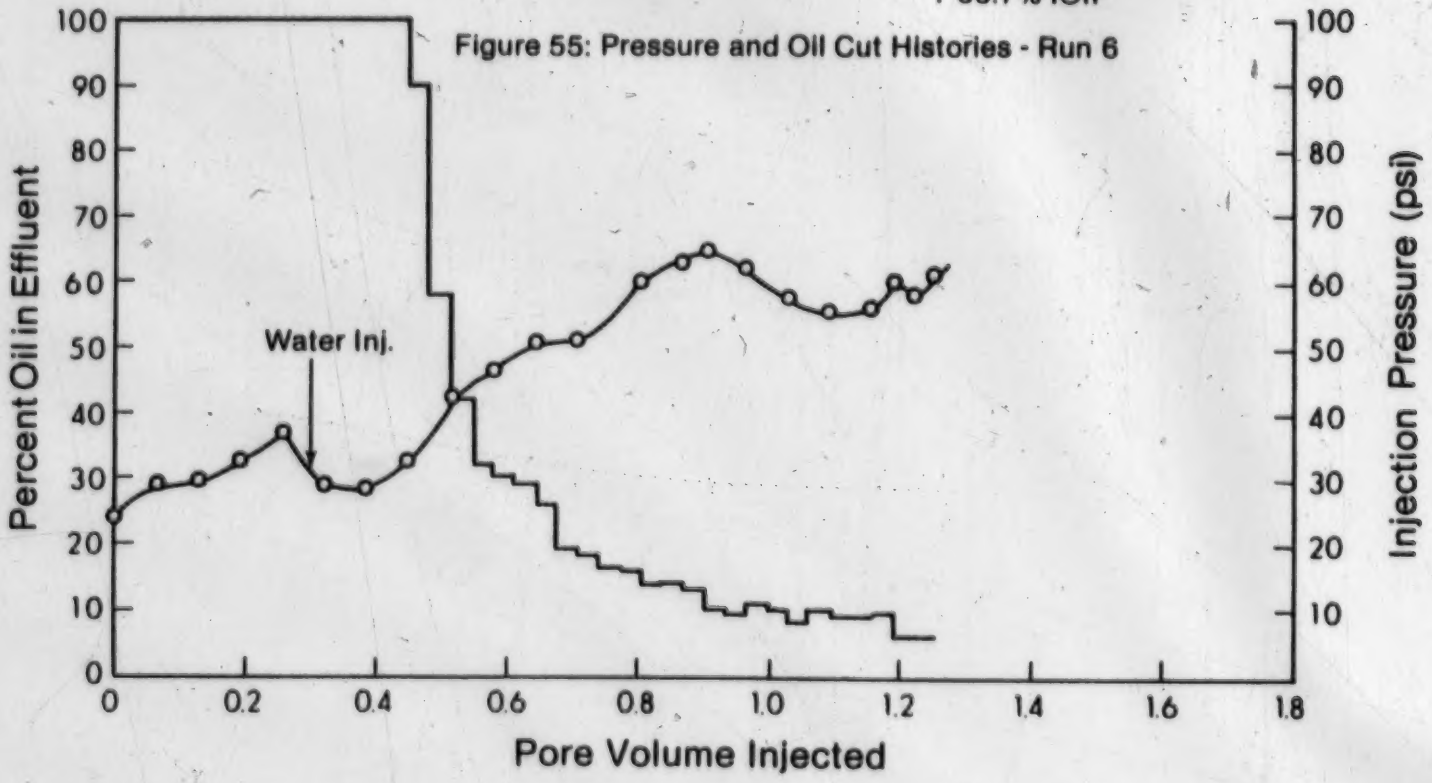

Figure 56: Effect of Emulsion on Waterflood Recovery

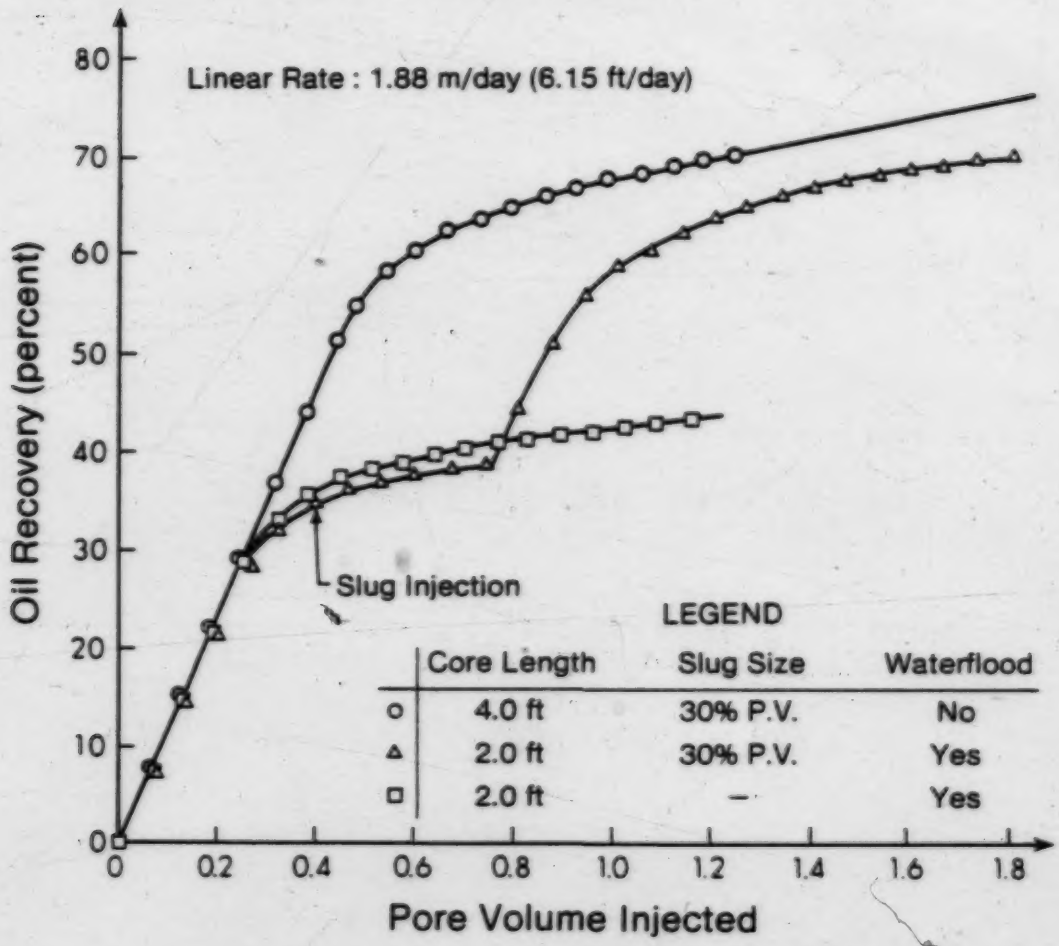

7. CONCLUSIONS

Study of Eyehill heavy oil emulsions and their oil displacement efficiency has led to the following guidelines and conclusions:

1. Heavy crude already containing connate water in the form of dispersed drops mixed only in limited amounts with aqueous caustic solutions. If larger amounts of caustic solution were added, two-phase mixtures resulted but the crude never reverted from a water-in-oil to an oil-in-water emulsion to accomodate the additional aqueous phase.

2. Certain combinations of emulsion, crude, and distilled water resulted in very viscous mixtures. Combinations containing more than 30 percent water resulted in a gel.

3. Emulsion viscosity can be effectively controlled by the addition of synthetic crude as a solvent. Benzene and toluene are more effective solvents, though more expensive.

4. Emulsion flooding in a partially waterflooded sand pack showed a jump in oil production and a total oil recovery of 69.3 percent of oil in place.

5. Based on only two runs, oil recovery with the same slug

size may be significantly affected by the length of the sand pack.

8. RECOMMENDATIONS

The following suggestions are offered for further study in the area of emulsion flooding.

1. The values of interfacial tension might not change if the volume of caustic solution is kept constant for measurements at different volume ratios. The effect of the size of the interfacial area on interfacial tension would also be useful to investigate.

2. All of the caustic solutions prepared contained no sodium chloride. It would be useful to know if addition of salt would promote better acceptance of the caustic solution by the crude upon mixing. Along the same lines, the ternary diagrams could be reproduced using different brine concentrations rather than distilled water; number of phases and mixture viscosities could be significantly altered by the presence of salt in the water.

3. Another study could be devoted to the effect of caustic on oil-in-water emulsions only. These emulsions would be easier to test and analyze because their viscosity would be so much lower than that of water-in-oil emulsions.

4. Hydrochloric acid could be used as an electrolyte for

both water-in-oil and oil-in-water emulsions.

5. Higher caustic concentrations may be able to promote larger acceptance of aqueous phase by the crude and/or phase inversion. This would provide more versatility to the emulsion flooding technique.

6. In the area of sand pack displacement experiments, different solvent concentrations could be used in the emulsion slug. The major problem in emulsion flooding occurs at the back of the slug where the discrepancy between emulsion and water viscosities gives rise to water fingering. A gradation of emulsion viscosity from that of oil to that of water would provide a better slug.

7. The problem of radial flow of emulsion around a well bore should be investigated. As the emulsion slug moves away from the wellbore its thickness will decrease rapidly and injection water may break through it rapidly. The efficiency of emulsion flooding would quickly be lost.

8. The question of brine banking ahead of the emulsion should be elucidated. Experiments with continuous emulsion injection are suggested in this regard.

9. References Cited

BERRIDGE, S.A. , THEW, M.T. , and LORISTON-CLARKE, A.G. , "The Formation and Stability of Emulsions of Water in Crude Petroleum and Similar Stocks." Journal of the Institute of Petroleum, 1968, v54, 333-357.

CHAN, P. , "The Emulsification of Oil by Sodium Hydroxide." M. Sc. Thesis, University of Alberta, Department of Mineral Engineering (1979).

COOKE, C.E. Jr, WILLIAMS, R.E. , and KOLODZIE, P.A. , "Oil Recovery by Alkaline waterflooding." JPT (Dec. 1974), 1365-1374.

CRATIN, P.D. , "A Quantitative Characterization of pH-dependent Systems." Industrial and Engineering Chemistry, 1969, v61, 35-45.

DERJAGUIN, B.V. , SHCHERBAKOV, L.M. , "Effect of Surface Forces on Phase Equilibria of Polymolecular Layers and on Contact Angle." Colloid Journal (USSR), 1961, v23, 33-43.

de WAELE, A. , Kolloidzietschrift, (1925), 36, 332.

DRANCHUK, P.M., SCOTT, J.D., and FLOCK, D.L. , "Effect of the Addition of Certain Chemicals on Oil Recovery during Waterflooding." JCPT (July-Sept. 1974), 27-36.

DUPEYRAT, M. ,MINSSIEUX, L. , and El Naggar, A. , "Investigation of the Physico-Chemical Mechanisms Involved in Oil-Water Interfacial Tension Lowering." presented at the European Symposium on Enhanced Oil Recovery (1978) Edinburg, Scotland, 5-7 July, 161-184.

FAROUQ ALI, S.M. , FIGUEROA, J.M. , AZUAJE, E.A. , and FARQUHARSON, R.G. , "Recovery of Lloydminster and Morichal Crudes by Caustic, Acid and Emulsion Floods." JCPT (Jan.-March, 1979) 53-59.

FLOCK, D.L. , STEINBORN, R. , "The Rheology of Heavy Crude Oils and their Emulsions." presented at the 33rd Annual Technical Meeting of the Petroleum Society of CIM, June 6-9, 1982, Calgary.

JAMESON, C.E. , "The Lloydminster Heavy Oil Area." JPT (July-Sept. ,1973), 17-19.

JENNINGS, H.Y. Jr, JOHNSON, C.E. Jr, and McAULIFFE, C.D. "A Caustic Waterflooding Process for Heavy Oils." JPT

(Dec. 1974), 1344-1352.

JONES, T.J. , NEUSTADTER, E.L. , and WITTINGHAM, K.P. , "Water in Crude Oil Emulsion Stability and Emulsion Destabilization by Chemical Demulsifiers." JCPT (April-June, 1978), 100-108.

KIMBLER, O.K. , REED, R.L. , SILBERBERG, I.H. , "Physical Characteristics of Natural Films formed at Crude Oil-Water interfaces." SPE June 1966, 153-165.

KIMMEL, T.B. , LAVIOLETTE, D.J. , "Heavy Oil Production in the Lloydminster Area." presented at the 6th Symposium on Engineering Applications of Mechanics, Calgary, June 6-9, 1982.

MACKAY, G.D.M. , MCLEAN, A.Y. , BETANCOURT, O.J. , and JOHNSON, B.D. , "The Formation of Water in Oil Emulsions subsequent to an Oil Spill." Journal of the Institute of Petroleum, v59, 1973.

MARTIN, A.N. , SWARBRICK, J. , and CAMMARATA, A. "Physical Chemical Principles in Pharmaceutical Science." 2nd ed. Philadelphia, Lea &Febiger, 1969, 545.

McAULIFFE, C.D. , "Crude Oil in Water Emulsion to Improve Fluid Flow in an Oil Reservoir." JPT (June 1973), 25 (6), 721-726.

McAULIFFE, C.D. , "Oil-in-Water Emulsions and their Flow Property in Porous Media." JPT (June 1973), 25 (6), 727-733.

McCAFFERY, F.G. , "Interfacial Tension and Aging Behaviour of some Crude Oils against Caustic Solutions." JPT (July-Sept. , 1976) 71-74.

OKANDAN, E. , "Improvement of Waterflooding of a Heavy Crude Oil by Addition of Chemicals to the Injection Water." (Middle East Tech. Univ.) int. SPE of AIME Oilfield and Geothermal Chem. Symp. (SAN DIEGO, CALIF. , 6127-29 /77) proc. p. 89-94, 1977. (SPE-6597).

PETROV, A.A. , PODNYSHEV, G.N. , NOVIKOVA, K.G. , and MANSUROV, R.I. , "Colloidal Stabilizers of Crude Oil Emulsions." NEFT. KHOZ. No. 1, pp 50-52, Jan. 1974.

RUBIN, E. , RADKE, C.J. , "Dynamic Interfacial Tension Minima in Finite Systems." Chem. Eng. Science, v35, 1129-1138, 1980.

SHERMAN, P. , "Emulsion Science." Academic Press, 1968, London.

SPEIGHT, J.G. , "A Structural Investigation of the Constituents of Athabasca Bitumen by Proton Magnetic Resonance Spectroscopy." Fuel (1970), 49, 76.

STRASSNER, J.E. , "Effect of pH on Interfacial Films and Stability of Crude Oil-Water Emulsions." SPEJ March 1968, 303-312.

SWEENEY, R.H. , and GECKLER, R.D. , "The Rheology of Suspensions." Journal of Applied Physics (1954), 25, 1135.

SYMONDS, R. , "Rate and Adsorption in Caustic Flooding." M. Sc. Thesis, University of Alberta, Department of Mineral Engineering, 1980.

TAKAMURA, K. "The Stability of Bitumen Emulsions." presented at the AOSTRA Conference on Advances in Petroleum Recovery and Upgrading Technology, (June 9-11, 1982) , Calgary.

10. Appendix A

INTERFACIAL TENSION DATA

PHASE 1

Equal Volumes of Oil and Water

In the first run, 60 ml of pure distilled water were tested against 60 ml of oil. For all subsequent runs a solution of 1.0 percent by weight sodium hydroxide was produced and varying amounts were used to reach a different sodium hydroxide concentration in each run.

Distilled water and solution were measured by pipette and placed first in a 150 ml beaker, then stirred. The ring was immersed well below the contact surface to avoid contamination by oil and attached to the tensiometer. Then the oil was poured slowly and uniformly over the water until it formed a layer equal in thickness to that of water. Equal volumes were obtained in this fashion.

Normal test would then proceed and the following interfacial tension readings were obtained:

TABLE A-1

ml of 1.0% NaOH Solution	Percent NaOH by Weight	Interfacial Tension Reading	Final Corrected Value
62.2	1.04	12.0	13.2
9.0	0.15	11.0	12.4
7.2	0.12	11.4	12.9
6.6	0.11	10.9	12.2
5.4	0.09	11.3	12.8
4.8	0.08	11.2	12.7
3.0	0.05	11.3	12.9
1.8	0.03	12.6	14.6
1.2	0.02	13.7	16.2
0.6	0.01	16.3	19.5
0.0	0.00	26.3	*

1*:Correction Factor not available.

PHASE 1

Densities

TABLE A-2

Percent NaOH by Weight	Densimeter Reading, T	Density g/cc	Correction Factor
1.04	0.752742	1.0084570	1.099
0.15	0.751257	1.0002154	1.125
0.12	0.751163	0.9996944	1.132
0.11	0.751255	1.0002043	1.122
0.09	0.751088	0.9992785	1.133
0.08	0.751120	0.9994563	1.131
0.05	0.750943	0.9984748	1.140
0.03	0.751024	0.9979257	1.161
0.02	0.750952	0.9975283	1.183
0.01	0.750969	0.9986191	1.199
0.00	0.750752	0.9974166	*

Oil T=0.745580 d=0.9688596 g/cc @t=23.1°C

Air T=0.542127 d=0.0010984 g/cc @t=22.9°C

Water T=0.750752 d=0.9974166 g/cc @t=23.5°C

PHASE 2

One Volume of Oil for Three Volumes of Water

In all runs, 60 ml of solution and 20 ml of oil were used. As in Phase 1 all solutions were obtained by combination in different amounts of distilled water and a 1.0 percent by weight (0.25 M) sodium hydroxide solution. Also, the same procedure was employed. The following interfacial tension values were measured:

TABLE A-3

ml of 1.0% NaOH Solution	Percent NaOH by Weight	Interfacial Tension Reading	Final Corrected Value
60.0	1.00	0.8	0.7
9.0	0.15	0.6	0.5
7.2	0.12	0.7	0.6
6.6	0.11	0.7	0.6
5.4	0.09	0.7	0.6
4.8	0.08	0.7	0.6
3.0	0.05	0.7	0.6
1.8	0.03	3.4	3.3
1.2	0.02	6.3	6.6
0.6	0.01	8.2	8.8
0.0	0.00	7.4	7.9

PHASE 2

Densities

TABLE A-4

Percent NaOH by Weight	Densimeter Reading, T	Density g/cc	Correction Factor
1.00	0.752866	1.010699	0.876
0.15	0.751268	1.001845	0.875
0.12	0.751254	1.001767	0.880
0.11	0.751241	1.001695	0.881
0.09	0.751180	1.001358	0.881
0.08	0.751128	1.001069	0.881
0.05	0.751081	1.000809	0.881
0.03	0.750953	1.000102	0.969
0.02	0.750980	1.000251	1.040
0.01	0.750948	1.000074	1.078
0.00	0.750502	0.997607	1.072

Air T=0.541071 d=0.0010996 g/cc @t=22.6°C

Water T=0.750502 d=0.997607 g/cc @t=22.7°C

PHASE 3

Three Volumes of Oil for One of Water

For all runs 15 ml of solution and 45 ml of oil were placed in a 100 ml beaker. The solutions were prepared from a 1.0 percent by weight (0.25 M) sodium hydroxide batch in volumes of 60 ml each time. Then 15 ml were taken from the 60 ml preparation and used for the interfacial tension test. It was felt that by preparing a larger volume of solution (60 ml) the propagation of errors would be minimized. The results are tabulated on the next page.

TABLE A-5

ml of 1.0% NaOH Solution	Percent NaOH by Weight	Interfacial Tension Reading	Final Corrected Value
60.0	1.00	11.5	11.6
9.0	0.15	11.3	12.8
7.2	0.12	11.4	13.0
6.6	0.11	11.5	13.1
5.4	0.09	11.2	12.8
4.8	0.08	11.3	12.9
3.0	0.05	11.8	13.6
1.8	0.03	14.5	17.3
1.2	0.02	14.9	17.9
0.6	0.01	20.1	*
0.0	0.00	15.6	18.7

*:Correction Factor not available.

PHASE 3

Densities

TABLE A-6

Percent NaOH by Weight	Densimeter Reading, T	Density g/cc	Correction Factor
1.00	0.752697	1.038295	1.012
0.15	0.751283	0.999187	1.131
0.12	0.751199	0.998723	1.139
0.11	0.751195	0.998701	1.140
0.09	0.751057	0.997940	1.140
0.08	0.751102	0.998189	1.140
0.05	0.751062	0.997968	1.150
0.03	0.750973	0.997477	1.191
0.02	0.750969	0.997455	1.200
0.01	0.750964	0.997428	*
0.00	0.750962	0.997417	1.201

Air T=0.540937 d=0.001097 g/cc @t=23.3°C

Water T=0.750962 d=0.997417 g/cc @t=23.5°C

*: Correction Factor not available.

ALBERTA Agriculture

Office of the Provincial Analyst

WATER ANALYSIS REPORT

Parts per million

Total Solids	55600	Conductivity	75000.0
Ignition Loss	2000	pH	7.36
Hardness	4813	Nature of	Bicarbonate
Sulphates	436	Alkalinity	of Ca & Mg
Chlorides	31905	Sodium	18860.0
Alkalinity	500	Potassium	508.0
Nitrite N_2	Nil	Salt	52643
Nitrate N	Nil		
iron	335.0		
Fluoride	1.05		
Calcium	856.0		
Magnesium	650.0		

11. Appendix B

EMULSION PREPARATION: PROCEDURE AND DATA

TABLE B-1

Percent Oil	Volume of Crude, ml	Weight of Crude, g	Beaker & Oil before, g	Beaker & Oil after, g
4.1	20	19.72	293.95	274.23
8.2	40	39.43	291.05	251.62
12.3	60	59.15	250.80	191.65
16.4	80	78.86	191.10	112.24
20.5	100	98.58	238.50	139.92
24.6	120	118.29	312.10	193.81
27.3	130	128.15	310.80	182.65
28.7	140	138.00	314.50	176.80
28.7	140	138.00	314.20	176.20
28.7	140	138.00	304.55	166.55
30.8	150	147.86	446.10	298.24
32.8	160	157.72	314.45	156.83
34.9	170	167.58	478.35	310.77
36.9	180	177.44	313.45	136.01
36.9	180	177.44	338.60	161.16
39.0	190	187.29	452.30	265.01

NOTE: The difference between crude and oil content stems from the fact that the crude contains 59 percent water.

TABLE B-2

Volume of crude, ml	Volume of solution, ml	Solution Temperature, C.	Emulsion Temperature, C.
20	180	23.1	32.0
40	160	22.9	32.4
60	140	23.0	36.5
80	120	23.0	33.0
100	100	23.0	41.0
120	80	24.5	32.0
130	70	23.0	28.5
140	60	23.0	29.0
140	60	21.5	30.0
140	60	23.5	30.5
150	50	23.5	29.0
160	40	22.9	29.5
170	30	23.5	31.0
180	20	23.0	31.0
180	20	21.5	34.0
190	10	23.5	31.0

TABLE B-3

Percent Oil	Phases Present	Volume Distilled, ml	Water Content, frac.
4.1	O in W W in O	10.0	0.41
8.2	O in W W in O	3.0	0.60
12.3	O in W W in O	7.0	0.57
16.4	O in W W in O	10.0	0.59
20.5	O in W W in O	10.0	0.63
24.6	O in W W in O	10.2	0.67

TABLE B-3 (cont'd)

Percent Oil	Phases Present	Volume Distilled, ml	Water Content, frac.
26.7	O in W W in O	25.0	0.62
28.7	W in O	25.0	0.66
28.7	O in W W in O	25.0	0.61
28.7	O in W W in O	25.0	0.61
30.8	O in W W in O	25.0	0.61
32.8	O in W W in O	10.0	0.66

TABLE B-3 (cont'd)

Percent Oil	Phases Present	Volume Distilled, ml	Water Content, frac.
	O in W		
34.9	W in O	25.0	0.58
36.9	W in O	11.0	0.65
36.9	W in O	25.0	0.62
39.0	W in O	25.0	0.60
41.0	W in O	25.0	0.59
41.0	W in O	25.0	0.59

TABLE B-4

Percent Oil	Phases Present	Relative Volumes, frac.	Percent NaOH Solution	pH
0.0			100.00	12.2
	O in W	0.93	100.00	10.8
4.1	W in O	0.07	0.00	*
	O in W	0.80	100.00	12.0
8.2	W in O	0.20	0.00	8.1
	O in W	0.70	100.00	12.3
12.3	W in O	0.30	0.00	8.0
	O in W	0.57	98.68	11.7
16.4	W in O	0.43	1.32	7.4
	O in W	0.36	98.52	10.4
20.5	W in O	0.64	1.48	6.7

*: not enough substance available for a correct measurement.

TABLE B-4 (cont'd)

Percent Oil	Phases Present	Relative Volumes, frac.	Percent NaOH Solution	pH
	O in W	0.17	93.36	10.2
24.6	W in O	0.83	6.64	7.0
	O in W	0.43	94.00	9.5
26.7	W in O	0.57	6.00	7.9
28.7	W in O	1.00	8.84	7.0
	O in W	0.32	95.30	9.0
28.7	W in O	0.68	4.70	8.0
	O in W	0.30	95.30	8.8
28.7	W in O	0.70	4.70	7.4
	O in W	0.29	94.00	8.6
30.8	W in O	0.71	6.00	6.9

TABLE B-4 (cont'd)

Percent Oil	Phases Present	Relative Volumes, frac.	Percent NaOH Solution	pH
	O in W	0.05	83.20	8.0
32.8	W in O	0.95	16.80	6.5
	O in W	0.18	48.00	8.1
34.9	W in O	0.82	52.00	6.1
36.9	W in O	1.00	100.00	6.2
36.9	W in O	1.00	100.00	7.0
39.0	W in O	1.00	100.00	6.2
41.0	W in O	1.00	0.00	6.5
41.0	W in O	1.00	0.00	5.4

NOTE: %NaOH Solution=(%distilled water-59%)/(total %NaOH Solution).

Mixture Composition

TABLE B-5

Run #	Crude, frac.	Emulsion, frac.	Distilled Water, frac.
1	0.00	0.90	0.10
2	0.10	0.90	0.00
3	0.10	0.80	0.10
4	0.00	0.80	0.20
5	0.10	0.70	0.10
6	0.20	0.70	0.10
7	0.20	0.60	0.20
8	0.10	0.60	0.30
9	0.30	0.60	0.10
10	0.20	0.50	0.30
11	0.30	0.50	0.20
12	0.30	0.40	0.30
13	0.10	0.50	0.40
14	0.20	0.40	0.40
15	0.30	0.30	0.40

TABLE B-5 (cont'd)

Run #	Crude, frac.	Emulsion, frac.	Distilled Water, frac.
16	0.40	0.50	0.10
17	0.40	0.40	0.20
18	0.40	0.30	0.30
19	0.40	0.20	0.40
20	0.10	0.40	0.50
21	0.20	0.30	0.50
22	0.30	0.20	0.50
23	0.40	0.10	0.50
24	0.10	0.30	0.60
25	0.50	0.40	0.10

TABLE B-6

Conversion from Crude content to Oil content

Percent Oil Present	Percent Crude Utilised
4.1	10.0
8.2	20.0
12.3	30.0
16.4	40.0
20.5	50.0
24.6	60.0
26.7	65.0
28.7	70.0
30.8	75.0
32.8	80.0
34.9	85.0
36.9	90.0
39.0	95.0
41.0	100.0

12. Appendix C

MICROSCOPE OBSERVATIONS

Table C-1

Eyehill Crude Aging

Particle Size Distribution

Eyehill-1981

average drop size:	7.77668	microns
standard deviation:	12.25895	microns
relative deviation:	1.57637	microns
sample size:	285	

Eyehill-1982 (Top Phase)

average drop size:	1.69601	microns
standard deviation:	3.23464	microns
relative deviation:	1.90721	microns
sample size:	231	

Eyehill-1982 (Bottom Phase)

average drop size:	9.83889	microns
standard deviation:	25.84911	microns
relative deviation:	2.62724	microns
sample size:	131	

Error range

average drop size:	31.05652	microns
standard deviation:	1.59766	microns
relative deviation:	0.05144	microns
sample size:	10	

13. Appendix D

EMULSION STABILITY

Water Content Estimation

TABLE D-1

Percent Oil only	Percent Crude	Phase	Water Content, frac	Variation in rdg., frac.
		Top	0.540	
36.9	90.0	Bottom	0.600	0.100
		Top	0.560	
36.9	90.0	Bottom	0.560	0.000
		Top	0.576	
36.9	90.0	Bottom	0.572	0.007
		Top	0.600	
38.9	95.0	Bottom	0.640	0.066
		Top	0.600	
38.9	95.0	Bottom	0.620	0.033
		Top	0.612	
38.9	95.0	Bottom	0.616	0.006

Confirmation of Optimality of 92% Emulsion

TABLE D-2

Percent Crude	Emulsion Temperature,C	Number of Phases
92.0	35.0	1
92.0	29.5	1
92.0	34.5	1
92.0	34.5	1
92.0	34.0	1
92.0	33.5	1
92.0	30.5	1
92.0	31.0	1
92.0	32.5	1
92.0	34.5	1
92.0	34.0	1
92.0	35.2	1
92.0	35.0	1
92.0	28.0	1
92.0	35.0	1
92.0	30.0	1

W/O Phase Data

TABLE D-3

Run #	Density, g /cc	Relative Volume, frac.	Water Content, frac.
1	0.9736757	0.946	0.536
2	0.9954134	1.000	0.624
3	0.9932367	1.000	0.652
4	*	0.970	0.650
5	0.9961058	0.857	0.684
6	0.9785137	0.990	0.630
7	*	0.966	0.705
8	0.9936092	0.683	0.670
9	0.9960505	0.929	0.604
10	0.9962706	0.857	0.750
11	0.9998106	0.923	0.648
12	0.9895882	0.622	0.640
13	0.9943256	0.660	0.615
14	0.9945741	0.667	0.690
15	0.8673017	0.636	0.715

W/O Phase Data

TABLE D-3 (cont'd)

Run #	Density, g /cc	Relative Volume, frac.	Water Content, frac.
16	0.9952793	1.000	0.680
17	0.9943090	0.884	0.650
18	0.9865301	0.773	0.640
19	0.9930074	0.800	0.635
20	0.9962958	0.561	0.620
21	*	*	0.700
22	0.9040698	*	0.630
23	0.9933589	*	0.640
24	*	*	0.720
25	*	*	0.652

Note: (*) indicates that the measurement was not technically feasible.

Phase Diagram Data

TABLE D-4

Run #	Mixture Temperature,C	Number of Phases
1	28.0	2 E-W
2	37.0	1
3	27.0	1
4	28.5	2 E-W
5	30.5	3
6	31.0	2 E-O
7	31.5	2 E-W
8	30.0	2 E-W
9	28.8	3
10	32.0	2 E-W
11	29.5	3
12	30.0	2 E-W
13	30.0	2 E-W
14	35.0	2 E-W
15	30.5	2 E-W

TABLE D-4 (cont'd)

Run #	Mixture Temperature,C	Number of Phases
16	29.0	2 E-O
17	29.5	2 E-W
18	30.0	2 E-W
19	32.5	2 E-W
20	30.0	2 E-W
21	32.0	2 E-W
22	30.0	2 E-W
23	32.5	2 E-W
24	30.0	2 E-W
25	38.0	2 E-W

N. B.: E-emulsion

O-oil

W-aqueous solution

14. Appendix E

APPARENT VISCOSITY

VISCOSITY CHARTS

RHEOLOGICAL DATA

Eyehill Crude

TABLE E-1

Shear Rate 1/sec	Shear Stress dynes/sq cm	Apparent Viscosity cp	Flow Index
0.12714	407.1	3202.1	
0.20123	651.4	3237.0	1.04
0.31784	1058.6	3330.6	1.09
0.50586	1791.3	3541.1	1.04
0.80133	2768.4	3454.8	0.94
1.27140	4274.7	3362.2	0.93
2.01230	6513.9	3237.0	0.95
3.17840	10178.0	3202.2	0.93
5.05860	15389.0	3042.1	0.92
8.01330	23895.0	2981.9	0.87
12.71400	34395.0	2705.3	0.82
16.00400	42422.0	2650.7	0.88
20.12300	51411.0	2554.8	0.85
31.78400	76031.0	2392.1	0.85
50.58600	112236.0	2218.7	0.83
80.13300	163647.0	2042.2	0.80
127.14000	235333.0	1851.0	0.78
201.23000	336708.0	1673.2	0.77
252.92999	397532.0	1571.7	

TABLE E-2

Sample	Shear Rate, 1/sec	Apparent Viscosity, Pa·s
1	9.706	21.35
	15.448	18.33
	61.453	10.99
2	9.706	39.62
	15.448	34.59
	30.760	25.88
3	9.706	56.66-70.16
	15.448	45.27
4	1.545	308.52
	3.883	187.50-304.19
5	1.545	59.33
	3.883	55.98
	9.706	38.59-43.17
	30.760	14.99-17.88

TABLE E-2 (cont'd)

Sample	Shear Rate, s^{-1}	Apparent Viscosity, Pa·s
	1.545	62.72
6	3.883	58.68
	9.760	38.43-46.95
	15.448	31.06-37.30
7	1.545	339.03
	3.883	184.13-242.81
8	1.545	406.84
	3.883	190.20-323.75
	1.545	57.64
	3.883	50.59
9	9.706	28.71
	15.448	22.88-26.24
	30.760	18.56
	61.453	15.24-16.19

TABLE E-2 (cont'd)

Sample	Shear Rate, s^{-1}	Apparent Viscosity, Pa·s
10	0.049	10,626.23
	0.309	3,644.56
	1.545	45.09
11	3.883	36.54
	9.706	22.60-28.06
	15.448	17.55-19.84
12	0.049	8,211.07
	0.309	2,017.22
13	0.049	17,173.77
15	0.049	18,676.43
	1.545	116.42
16	3.883	70.98-81.56
	9.706	43.61-49.65
	15.448	16.95-75.72

TABLE E-2 (cont'd)

Sample	Shear Rate, s^{-1}	Apparent Viscosity, Pa·s
	1.545	168.07
17	3.883	95.26-113.52
	9.706	66.92-120.51
	15.448	48.32
18	0.309	864.53
	1.545	389.88-559.40
	1.545	57.39
25	3.883	45.02
	9.706	30.76
	15.448	26.28
	9.706	7.509
Optimal	15.448	7.092
Emulsion	61.453	6.184
	154.480	5.432

TABLE E-3

Solvent Effectiveness

Run #	Shear rate	Voltage	Shear stress	Apparent viscosity
	s^{-1}	volt	pa	Pa·s
1%	Toluene			
	9.706	0.48	143.30	14.764
1	15.448	0.62	185.10	11.982
	61.453	1.60-1.85	477.68-552.31	8.988-7.77
	154.480	3.25-3.60	970.28-1074.78	6.957-6.281
1%	Varsol			
	9.706	0.55	164.20	16.918
2	15.448	0.72	214.96	13.915
	61.453	2.15-1.85	641.88-552.31	10.445-8.988
	154.480	4.10-3.65	1224.0-1089.71	7.924-7.054

TABLE E-3 (cont'd)

Solvent Effectiveness

1%	Benzene			
	9.706	0.33	98.52	10.15
3	15.448	0.50	149.27	9.66
	61.453	1.60-1.37	477.68-409.01	7.773-6.656
	154.480	3.22-2.95	961.33-880.72	6.223-5.701
1%	Xylenes			
	9.706	0.27	80.61	8.305
4	15.448	0.44	131.36	8.503
	61.453	1.37-1.22	409.01-364.23	6.656-5.927
	154.480	2.77-2.65	826.98-791.16	5.353-5.121
	Emulsion			
	9.706	0.45	134.35	13.8417
	15.448	0.65	194.06	12.5619
	61.452	1.95-2.05	612.03-582.173	9.9594-9.4736
	154.480	4.05-4.32	1289.7-1209.1	8.3485-7.8268

TABLE E-4

Solvent Effectiveness

Benzene

Run #	Shear rate	Voltage	Shear stress	Apparent viscosity
	s^{-1}	volt	pa	Pa·s
3%	Benzene			
	30.760	0.37	110.46	3.5909
5	61.453	0.68	203.01	3.3036
	154.486	1.62-1.87	558.29-483.65	3.614-3.131
	307.604	2.95-3.10	925.51-880.72	3.009-2.863
6%	Benzene			
	9.706	0.41	15.02	1.548
6	15.448	0.66	22.69	1.468
	61.453	2.25-1.92	71.433-61.316	1.162-0.9978
	123.042	4.67-4.30	145.63-134.28	1.184-1.0914

TABLE E-4 (cont'd)

Solvent Effectiveness

Benzene

10%	Benzene			
	15.448	0.18	7.969	0.5158
7	61.453	0.77	26.058	0.4240
	128.042	1.50	48.439	0.3937
	194.133	2.38	75.419	0.3885
20%	Benzene			
	61.453	0.07	4.596	0.07479
8	194.133	0.24	9.808	0.05052
	614.526	0.75	25.440	0.04140
	1941.330	2.44	77.260	0.03979

TABLE E-5

Solvent Effectiveness

Xylenes

Run #	Shear rate s^{-1}	Voltage volt	Shear stress pa	Apparent viscosity Pa·s
3%	Xylenes			
	9.706	1.20	39.241	4.043
9	15.448	1.87	59.783	3.870
	30.760	3.42	107.304	3.488
	38.827	4.15	129.685	3.340
6%	Xylenes			
	15.448	0.42	15.327	0.992
10	61.452	1.70	54.571	0.888
	123.042	3.27	102.705	0.835

TABLE E-5 (cont'd)

Solvent Effectiveness

Xylenes

10%	Xylenes			
	15.448	0.13	6.4357	0.4166
	61.453	0.55	19.3120	0.3143
11	154.486	1.35	43.8400	0.2838
	307.604	2.55	80.6310	0.2621
	488.749	4.00	125.0870	0.2559
20%	Xylenes			
	194.133	0.15	7.0488	0.0363
12	614.526	0.45	16.2460	0.0264
	970.664	0.67	22.9920	0.0237
	1941.327	1.37	44.4530	0.0229

TABLE E-6

Solvent Effectiveness

Synthetic Crude

Run #	Shear rate	Voltage	Shear stress	Apparent viscosity
	s^{-1}	volt	pa	Pa·s
	Synth.	crude		
	970.66	0.05	3.9829	0.004103
	3076.05	0.28	11.0345	0.003587
6%	Synth.	crude		
	9.706	0.96	31.883	3.285
13	15.448	1.58	50.891	3.294
	30.760	3.06	96.267	3.129
	38.827	3.80	118.955	3.064
10%	Synth.	crude		
	9.706	0.25	10.115	1.042
14	15.448	0.39	14.407	0.933
	61.453	1.65	53.038	0.863
	154.480	3.80	118.955	0.770

TABLE E-7

Apparent Viscosities at a fixed shear rate: 61.45 s^{-1}

Concentration	Benzene	Xylenes
	cp	cp
1%	6,656	5,927
3%	3,304	3,157
6%	998	888
10%	424	314
20%	74	44

15. Appendix F

RHEOLOGICAL DATA

Figure F-1. Calibration Fluid

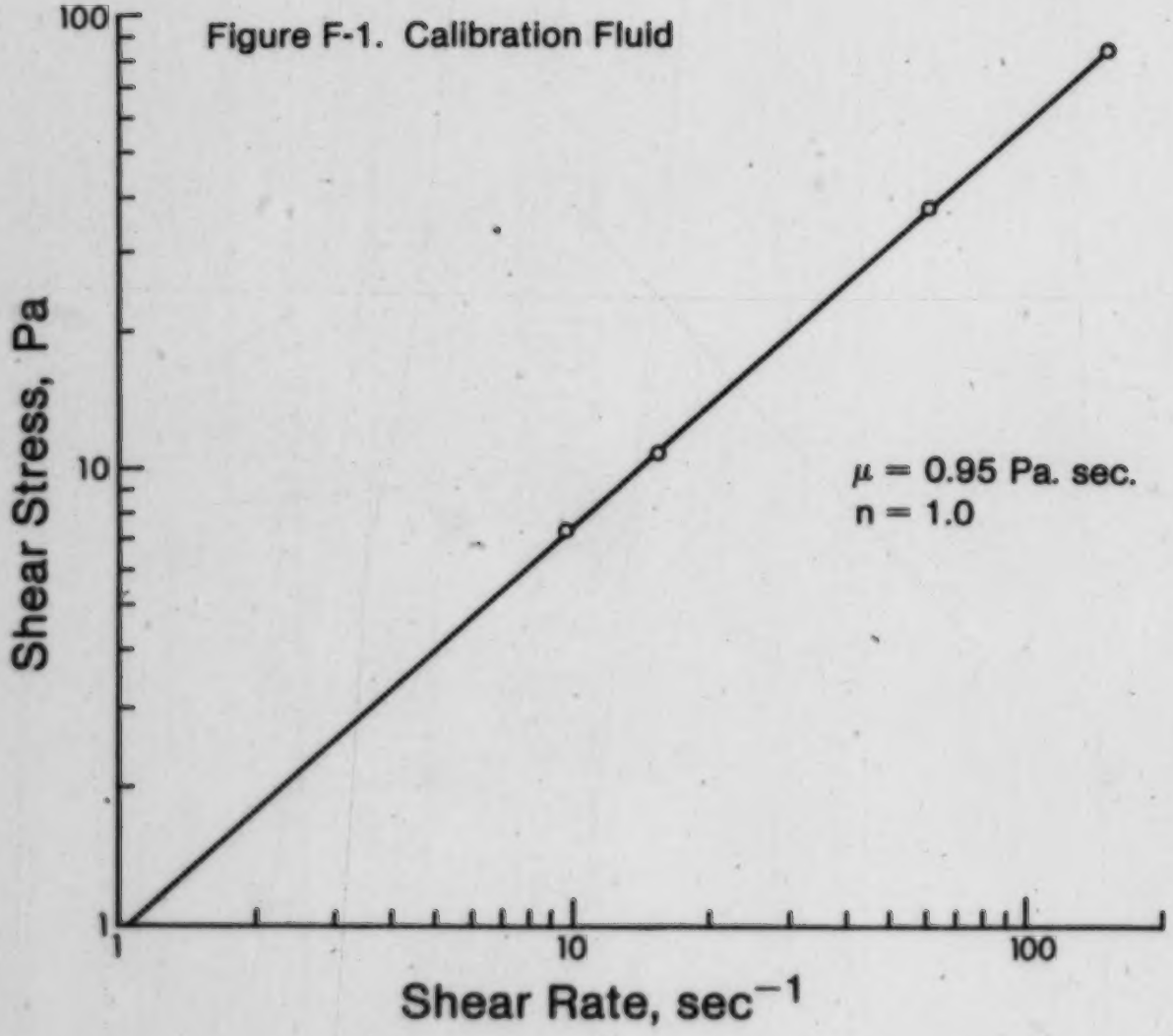

Figure F-2. Rheogoniometer Shear Stress Transducer Calibration.

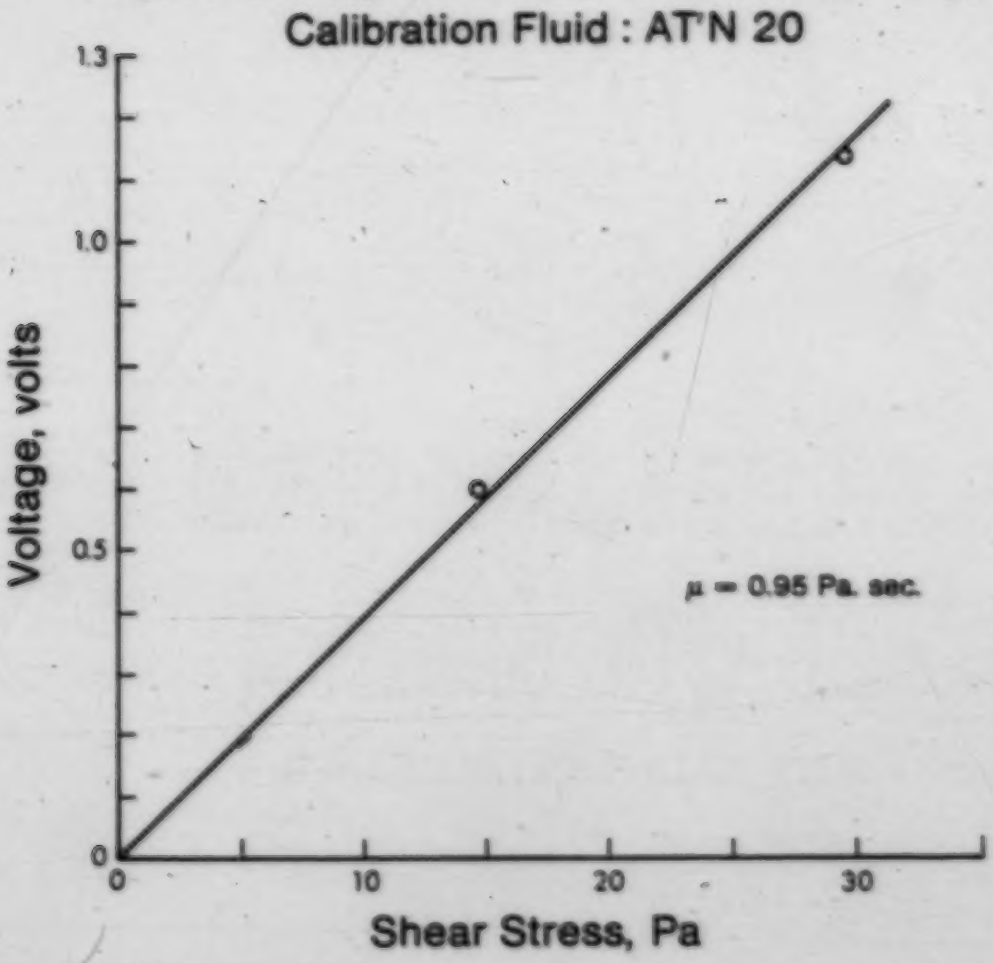

Figure F-3. Rheogoniometer Shear Stress Transducer Calibration.

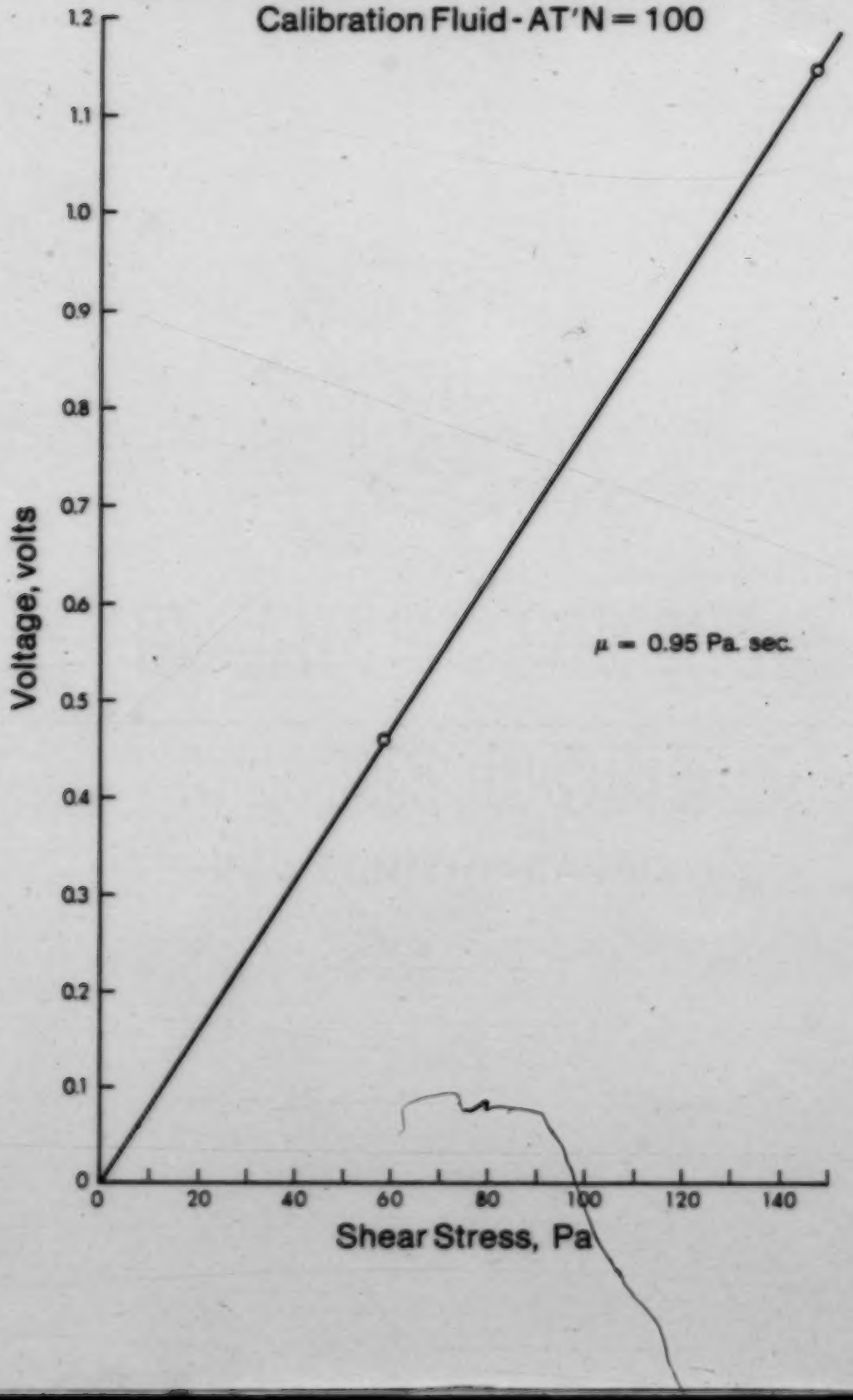

Figure F-4. Rheogoniometer Shear Stress Transducer Calibration.

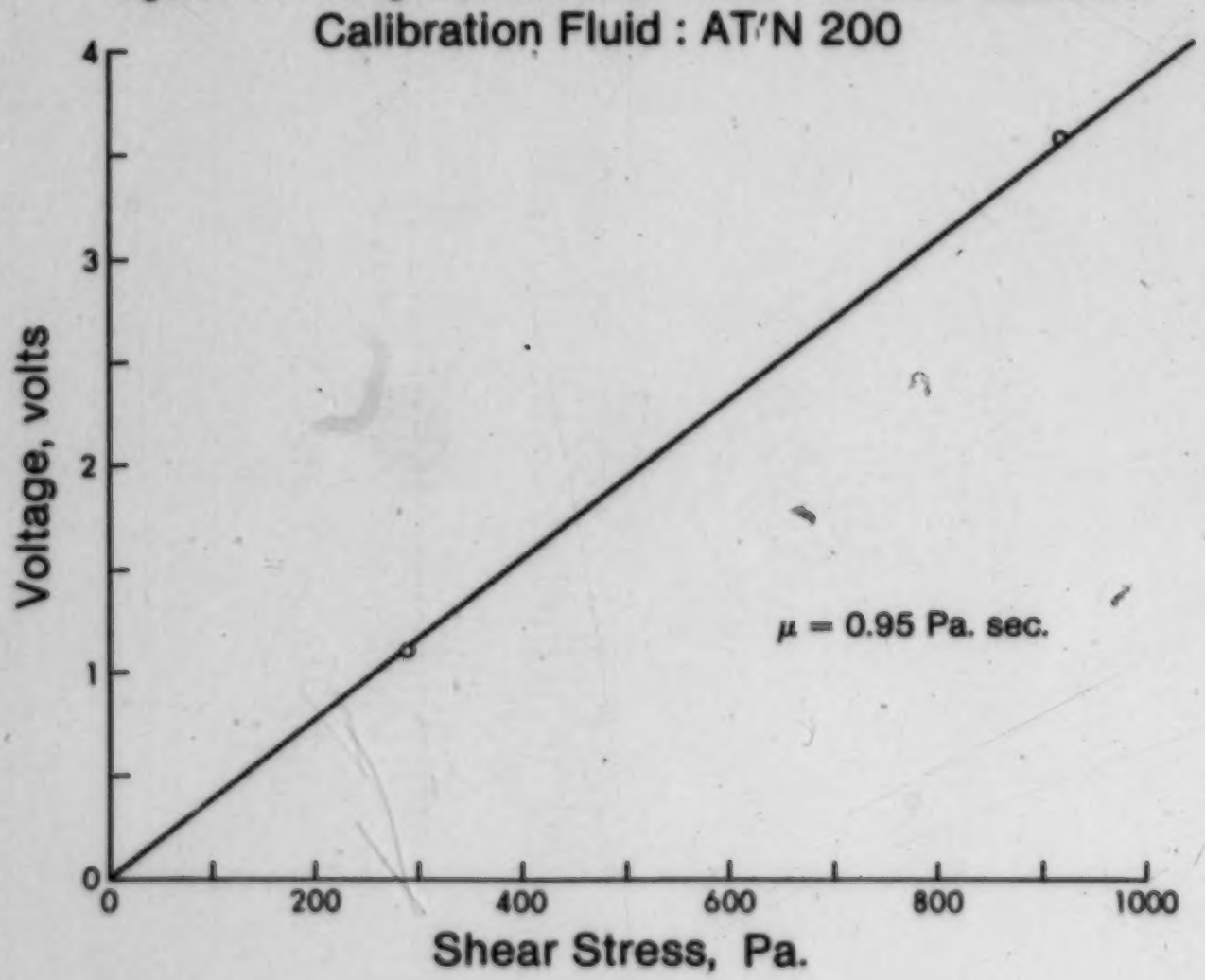

TABLE F-1

At'n	r. p. m.	Shear rate, s^{-1}	Voltage, volt	Shear stress, pa
		Calibration		
20	0.452	15.448	0.60	14.6756
	0.900	30.760	1.24	29.2220
100	1.798	61.453	0.46	58.3804
	4.520	154.480	1.14	146.7560
200	9.000	307.600	1.10	291.6500
	28.400	970.660	3.56	922.1270
	Optimal	Emulsion (92% crude)		
20	0.284	9.706	3.24	72.89
	0.452	15.448	4.88	109.56
100	1.798	61.453	3.00	380.01
200	4.520	154.480	3.20	839.13
		Sample 1		
100	0.284	9.706	1.636	207.23
	0.452	15.448	2.236	283.23
200	1.798	61.453	2.580	675.70

TABLE F-1 (cont'd)

At'n	r. p. m.	Shear rate, s^{-1}	Voltage, volt	Shear stress, pa
		Sample 2		
100	0.284	9.706	3.036	384.57
200	0.452	15.448	2.040	534.28
	0.900	30.760	3.040	796.18
		Sample 3		
200	0.284	9.706	2.10-2.60	549.99-680.94
	0.452	15.448	2.670	699.27
		Sample 4		
200	0.1136	3.883	2.78-4.51	728.08-1181.17
	0.0452	1.545	1.82	476.66
		Sample 5		
	0.0452	1.545	0.35	91.66
200	0.1136	3.883	0.83	217.38
	0.2840	9.706	1.43-1.60	374.52-419.04
	0.9000	30.760	1.76-2.10	460.94-549.99

TABLE F-1 (cont'd)

At'n	r. p. m.	Shear rate, s^{-1}	Voltage, volt	Shear stress, pa
		Sample 6		
	0.0452	1.545	0.37	96.90
200	0.1136	3.883	0.87	227.85
	0.2840	9.706	1.42-1.74	372.95-455.71
	0.4520	15.448	1.83-2.20	479.80-576.18
		Sample 7		
200	0.0452	1.545	2.00	523.80
	0.1136	3.883	2.73-3.60	714.99-942.84
		Sample 8		
200	0.0452	1.545	2.40	628.56
	0.1136	3.883	2.82-4.80	738.56-1257.12

TABLE F-1 (cont'd)

At'n	r. p. m.	Shear rate, s^{-1}	Voltage, volt	Shear stress, pa
		Sample 9		
200	0.0452	1.545	0.34	89.05
	0.1136	3.883	0.75	196.43
100	0.2840	9.706	2.20	278.67
	0.4520	15.448	2.79-3.20	353.41-405.34
200	0.9000	30.760	2.18	570.94
	1.7980	61.453	3.58-3.80	936.30-995.22
		Sample 10		
200	0.001428	0.04880	1.98	518.56
	0.004520	0.30900	4.30	1126.17
		Sample 11		
	0.0452	1.545	0.55	69.67
100	0.1136	3.883	1.12	141.87
	0.2840	9.706	1.73-2.15	219.39-272.34
	0.4520	15.448	2.14-2.42	271.07-306.54

TABLE F-1 (cont'd)

At'n	r. p. m.	Shear rate, s^{-1}	Voltage, volt	Shear stress, pa
		Sample 12		
200	0.001428	0.04880	1.53	400.70
	0.004520	0.30900	2.38	623.32
		Sample 13		
200	0.001428	0.04880	3.20	838.08
		Sample 15		
200	0.001428	0.04880	3.48	911.41
		Sample 16		
100	0.0452	1.545	1.42	179.87
	0.1136	3.883	2.18-2.50	275.63-316.68
200	0.2840	9.706	1.62-1.84	423.23-481.90
	0.4520	15.448	2.03-2.20	531.66-576.18

TABLE F-1 (cont'd)

At'n	r. p. m.	Shear rate, s^{-1}	Voltage, volt	Shear stress, pa
		Sample 17		
100	0.0452	1.545	2.05	259.67
	0.1136	3.883	2.92-3.48	369.88-440.81
200	0.2840	9.706	2.20-2.48	576.18-649.51
	0.4520	15.448	2.85	746.42
		Sample 18		
200	0.00452	0.3090	1.02	267.14
	0.04520	1.5450	2.30-3.30	602.37-864.27
		Sample 25		
100	0.0452	1.545	0.70	88.67
	0.1136	3.883	1.38	174.80
200	0.2840	9.706	1.14	298.57
	0.4520	15.448	1.55	405.94

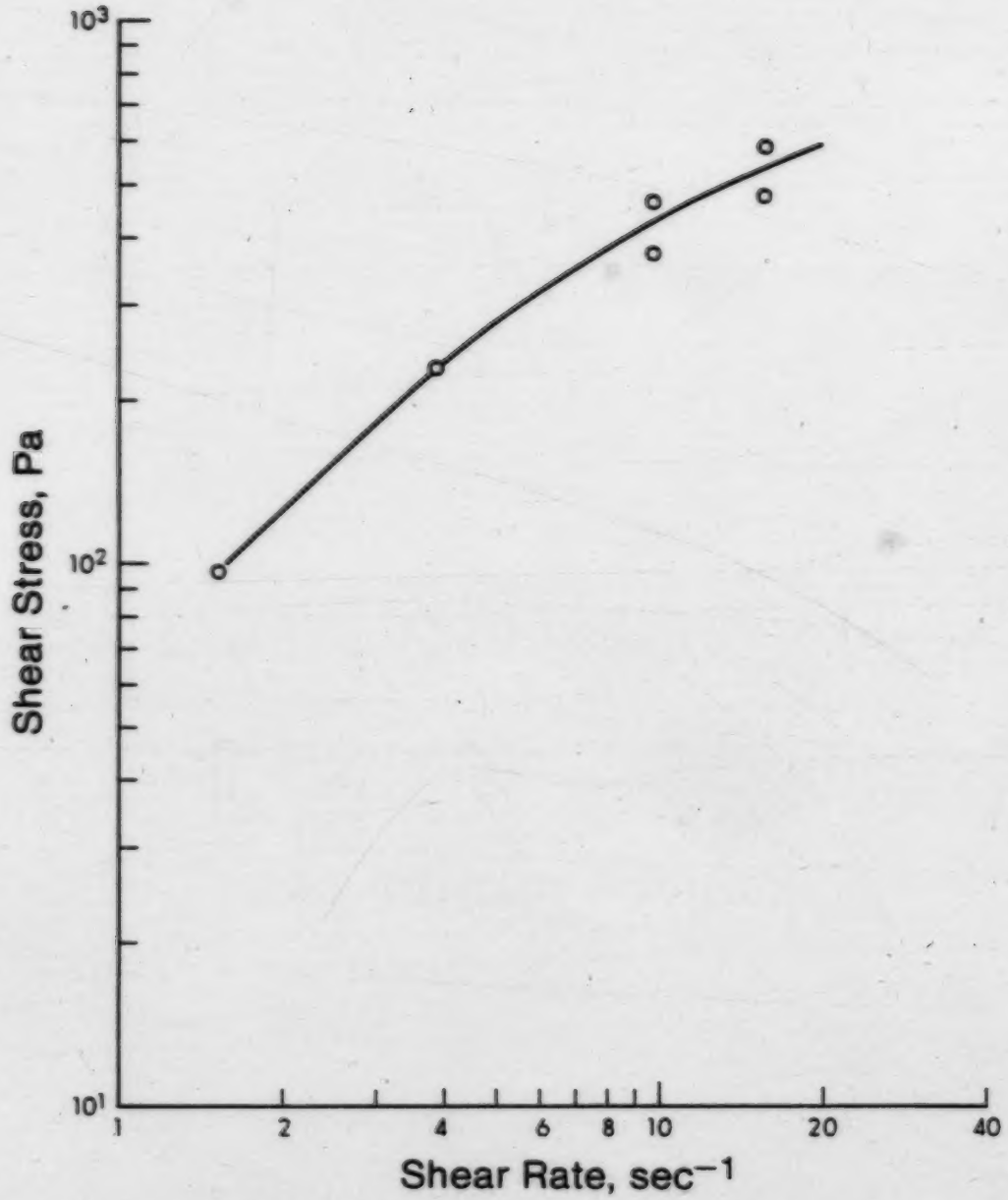

Figure F-5. Sample 6 Rheology; Log-Log Scales.

Figure F- 6. Rheological Behavior; Arithmetic Scales.

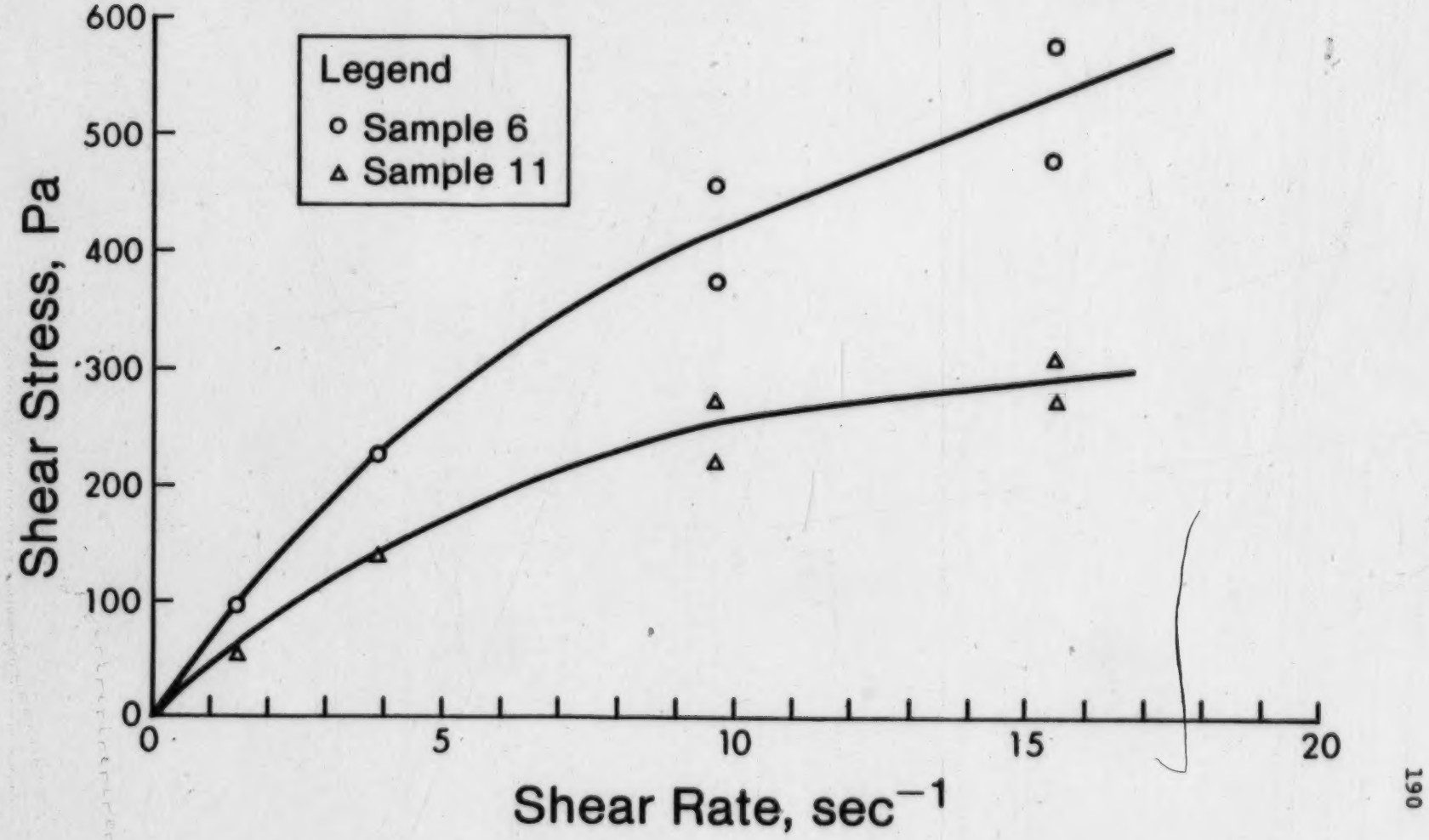

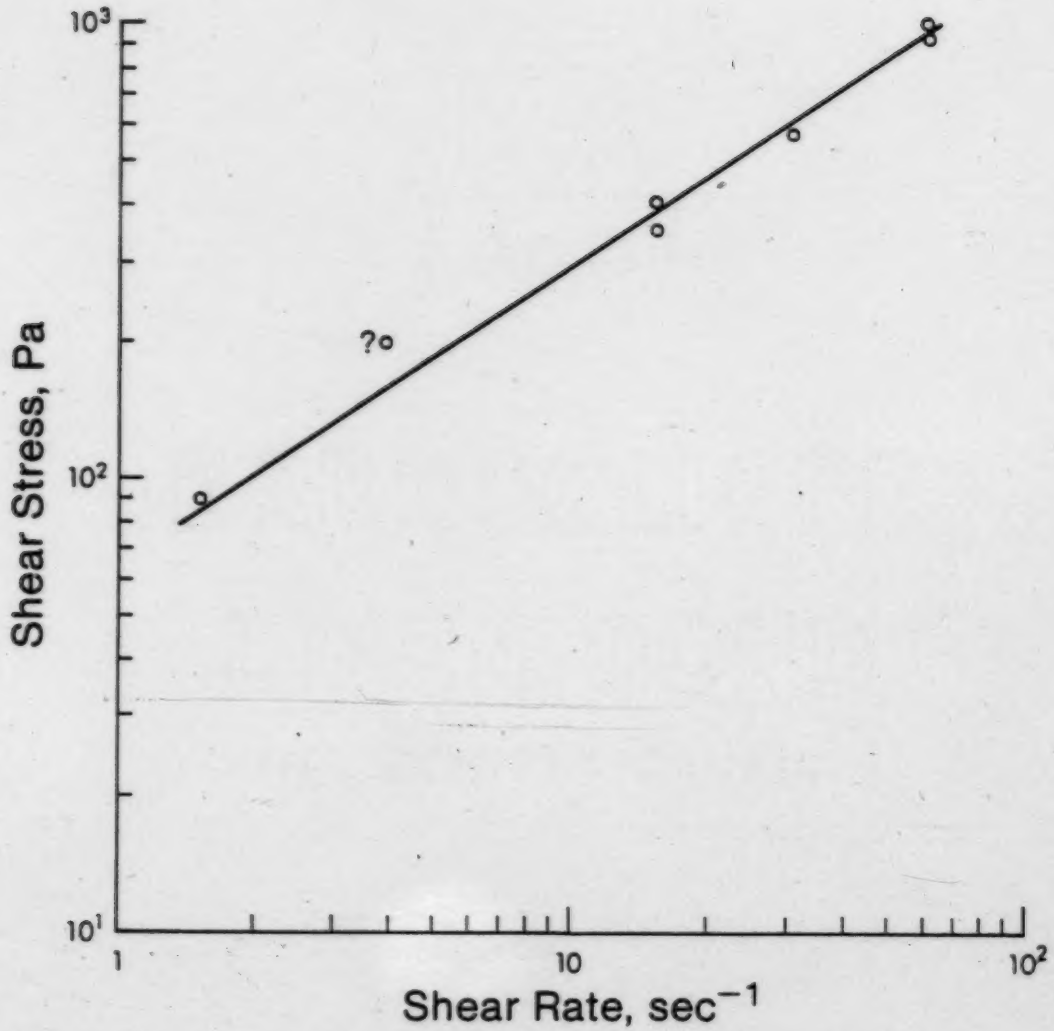

Figure F-7. Sample 9 Rheology

Linear Regression Analysis

TABLE F-2

Sample	Flow Index n	Consistency Index, K
9	0.615	72,865
16	0.487	148,219
17	0.459	214,282
25	0.653	68,582
Optimal Emulsion	0.886	9,739

TABLE F-3

Optimal Emulsion and Heavy Oil

Rheology

Shear Rate	Voltage	Shear Stress	Apparent Viscosity
s^{-1}	volt	pa	Pa·s
Eyehill Emulsion			
61.45	0.25	10.11	0.164
154.48	0.68	23.30	0.151
307.60	1.42	45.99	0.150
MTC 30	Base		
9.71	0.13	6.44	0.664
15.45	0.17	7.66	0.496
61.45	0.55	19.31	0.314
154.48	1.25	40.77	0.263
307.60	2.35	74.50	0.242

16. Appendix G

SAND PACK DISPLACEMENTS

TABLE G-1

Permeability Calculations

Core	Flow Rate, cc/sec	Pressure Drop, psi	Permeability, darcy
1	1.509	3.00	13.31
2	1.323	3.30	10.61
3	2.016	2.90	18.30
4	1.698	3.25	13.85
5	1.947	3.25	15.88
6	0.626	2.10	15.71

TABLE G-2

Pore Volume Determination
from Effluent Water Salinity Analysis

Core #	Cum. Vol. Inj., ml	Refractive Index	NaCl Concentration
	720	1.3326	0.0009
	740	1.3330	0.045
	760	1.3344	0.206
	780	1.3378	0.596
1	800	1.3400	0.849
	820	1.3407	0.929
	840	1.3410	0.964
	860	1.3410	0.964
	883	1.3412	0.987
	903	1.3414	1.000

TABLE G-2 (cont'd)

Pore Volume Determination
from Effluent Water Salinity Analysis

Core #	Cum. Vol. Inj., ml	Refractive Index	NaCl Concentration
	700	1.3326	0.0009
	720	1.3329	0.0336
	740	1.3335	0.103
2	760	1.3359	0.378
	780	1.3390	0.734
	800	1.3409	0.952
	820	1.3414	1.000
	840	1.3414	1.000

TABLE G-2 (cont'd)

Pore Volume Determination

from Effluent Water Salinity Analysis

Core #	Cum. Vol. Inj., ml	Refractive Index	NaCl Concentration
	670	1.3326	0.0009
	690	1.3328	0.022
	710	1.3329	0.034
	730	1.3330	0.045
3	750	1.3350	0.275
	770	1.3389	0.722
	790	1.3405	0.906
	810	1.3409	0.952
	830	1.3410	0.964
	850	1.3414	1.000

TABLE G-2 (cont'd)

Pore Volume Determination
from Effluent Water Salinity Analysis

Core #	Cum. Vol. Inj., ml	Refractive Index	NaCl Concentration
	720	1.3326	0.0009
	740	1.3333	0.079
	761	1.3344	0.206
	781	1.3369	0.493
	801	1.3395	0.791
4	820	1.3406	0.918
	840	1.3410	0.964
	859	1.3414	1.000
	880	1.3414	1.000
	900	1.3414	1.000
	920	1.3414	1.000

TABLE G-2 (cont'd)

Pore Volume Determination
from Effluent Water Salinity Analysis

Core #	Cum. Vol. Inj., ml	Refractive Index	NaCl Concentration
	688	1.3326	0.0009
	708	1.3330	0.045
	728	1.3384	0.665
	748	1.3404	0.895
5	768	1.3409	0.952
	788	1.3410	0.964
	808	1.3412	0.987
	828	1.3413	0.998
	848	1.3414	1.000
	868	1.3414	1.000

TABLE G-2 (cont'd)

Pore Volume Determination
from Effluent Water Salinity Analysis

Core #	Cum. Vol. Inj., ml	Refractive Index	NaCl Concentration
	1320	1.3325	0.0000
	1400	1.3326	0.0009
	1421	1.3326	0.0009
	1460	1.3326	0.0009
	1480	1.3328	0.022
	1500	1.3330	0.045
	1520	1.3338	0.137
	1540	1.3360	0.390
6	1560	1.3390	0.734
	1580	1.3404	0.895
	1600	1.3407	0.929
	1620	1.3408	0.941
	1640	1.3409	0.952
	1660	1.3411	0.975
	1680	1.3414	1.000
	1700	1.3414	1.000

Fig G-1 : Pore Volume Determination

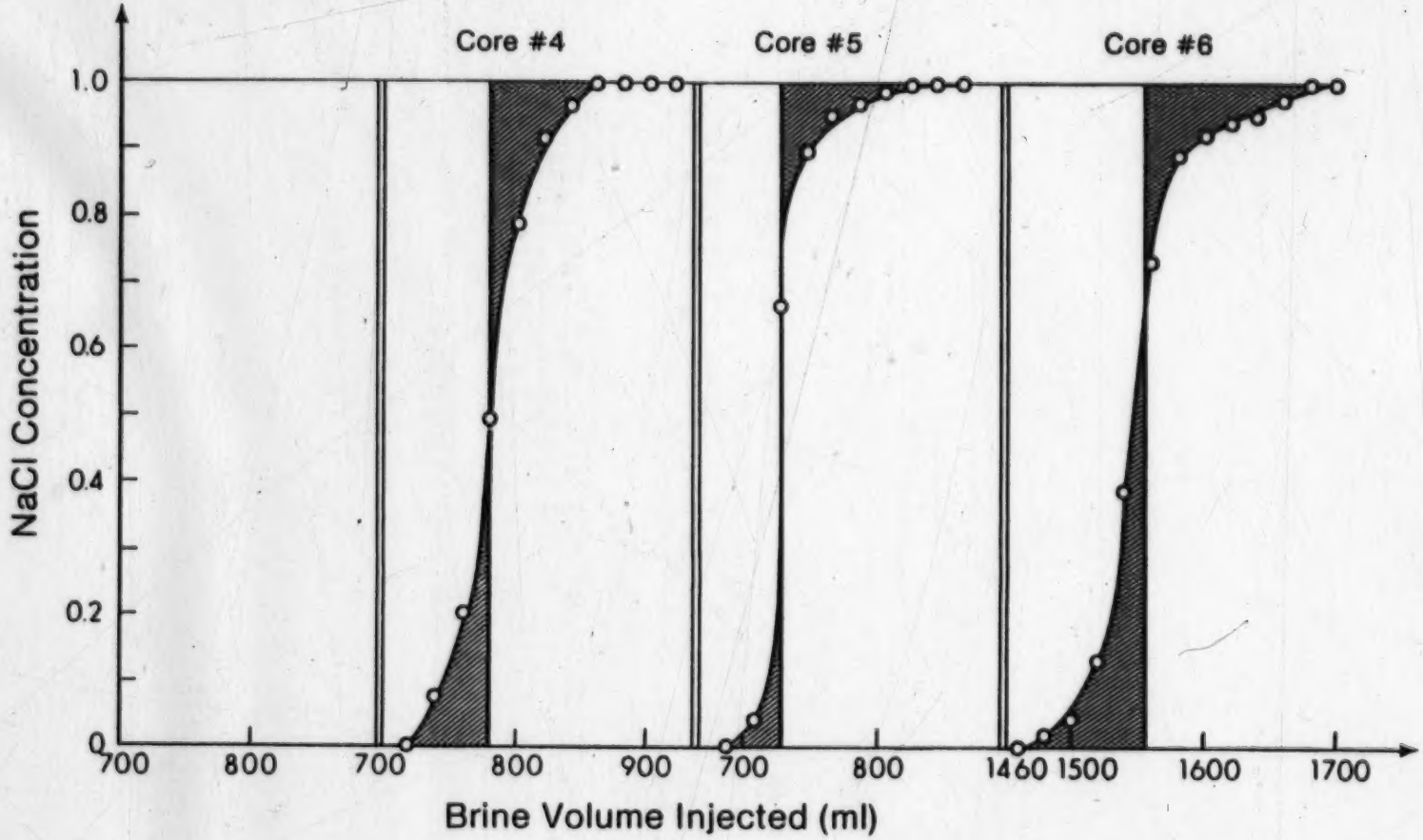

TABLE G-3

Initial Sand Pack Conditions

Core #	Pore Volume, ml	Porosity, percent	Oil Sat., frac.	Water Sat., frac.
1	782	42.7	0.870	0.130
2	767	41.9	0.887	0.113
3	765	41.5	0.902	0.098
4	780	42.6	0.865	0.135
5	730	39.9	0.952	0.048
6	1552.5	42.2	0.882	0.118

TABLE G-4

Effluent Analysis-Run 1

Cum. Vol. Inj., ml	Oil Produced frac.	Water Produced frac.
150	1.000	0.000
200	0.964	0.036
250	0.560	0.440
300	0.370	0.630
350	0.220	0.780
398	0.135	0.865
448	0.120	0.880
495	0.106	0.894
544	0.082	0.918
592	0.073	0.927
640	0.052	0.948
689	0.051	0.949
738	0.061	0.939
787	0.061	0.939
836	0.051	0.949
889	0.047	0.953

TABLE G-5

Pressure History-Run 1

Cumulative Time min	Inlet Pressure psi
0	0.0
30	15.8
60	13.5
90	10.4
120	7.6
150	5.6
180	4.3
210	3.7
240	3.5
270	3.3
345	3.0
385	3.0
445	3.0
475	3.0

TABLE G-6

Oil Production History-Run 1

Pore Vol. Inj., frac.	Cum. Oil Prod., ml	% IOIP Prod.
0.065	50	7.2
0.131	100	14.5
0.196	150	21.7
0.261	198.2	28.7
0.327	226.2	32.8
0.392	244.7	35.5
0.458	255.7	37.1
0.520	262.2	38.0
0.586	268.2	38.9
0.647	273.2	39.6
0.711	277.2	40.2
0.774	280.7	40.7
0.837	283.2	41.0
0.900	285.7	41.4
0.965	288.7	41.8
1.029	291.7	42.3
1.093	294.2	42.6
1.162	296.7	43.0

TABLE G-7

Effluent Water Salinity Analysis-Run 1

Run #	P. V. Prod. frac.	Refractive Index	NaCl Concentration
	0.261	1.3409	0.952
	0.327	1.3385	0.677
	0.392	1.3382	0.642
	0.458	1.3374	0.550
	0.520	1.3350	0.275
	0.586	1.3338	0.137
	0.647	1.3333	0.079
4	0.711	1.3330	0.045
	0.774	1.3330	0.045
	0.837	1.3329	0.034
	0.900	1.3329	0.034
	0.965	1.3329	0.034
	1.029	1.3328	0.022
	1.093	1.3328	0.022
	1.162	1.3328	0.022

TABLE G-8

Effluent Analysis-Run 2

Cum. Vol. Inj., ml	Oil Produced frac.	Water Produced frac.
100	1.00	0.00
200	1.00	0.00
300	0.88	0.12
350	0.36	0.64
400	0.18	0.82
450	0.16	0.84
500	0.11	0.89
550	0.10	0.90
600	0.10	0.90
650	0.09	0.91
700	0.08	0.92
750	0.04	0.96
800	0.05	0.95
850	0.06	0.94
900	0.08	0.92
950	0.08	0.92
1000	0.03	0.97

TABLE G-9

Pressure History-Run 2

Cumulative Time min	Inlet Pressure psi
0	0.0
40	12.5
50	15.5
60	16.2
75	16.2
92	15.9
96	15.6
100	15.2
110	14.2
120	13.2
140	12.5
160	11.0
191	8.6
200	8.5

TABLE G-9 (cont'd)

Pressure History-Run 2

Cumulative Time min	Inlet Pressure psi
226	8.1
260	8.0
290	6.4
320	6.6
350	6.8
380	6.9
410	7.1
440	7.2
470	7.2
500	7.2
530	7.2
560	7.6
590	7.6

TABLE G-10

Oil Production History-Run 2

Pore Vol. Inj., frac.	Cum. Oil Prod. ml	% IOIP Prod.,
0.0641	50	7.5
0.128	100	14.8
0.192	150	22.2
0.256	200	29.6
0.321	250	37.0
0.385	294	43.6
0.449	312	46.2
0.513	321	47.6
0.576	329	48.7

TABLE G-10 (cont'd)

Oil Production History-Run 2

Pore Vol. Inj., frac.	Cum. Oil Prod. ml	% IOIP Prod.,
0.641	334.5	49.6
0.705	339.5	50.3
0.769	344.5	51.0
0.833	349.0	51.7
0.897	353.0	52.3
0.962	355.0	52.6
1.026	357.5	53.0
1.089	360.5	53.4
1.153	364.5	54.0
1.218	368.5	54.6
1.282	370.0	54.8

TABLE G-11

Effluent Water Salinity Analysis-Run 2

Run #	P. V. Prod. frac.	Refractive Index	NaCl Concentration
	0.385	1.3409	0.952
	0.449	1.3399	0.837
	0.513	1.3380	0.619
	0.576	1.3359	0.378
	0.641	1.3345	0.217
	0.705	1.3335	0.103
	0.769	1.3332	0.068
1	0.833	1.3330	0.045
	0.897	1.3330	0.045
	0.962	1.3329	0.034
	1.026	1.3329	0.034
	1.089	1.3329	0.034
	1.153	1.3328	0.022
	1.218	1.3328	0.022
	1.282	1.3328	0.022

TABLE G-12

Effluent Analysis-Run 3

Cum. Vol. Inj., ml	Oil Produced frac.	Water Produced frac.
300	1.00	0.00
350	0.98	0.02
400	0.51	0.49
450	0.29	0.71
500	0.21	0.79
553	0.19	0.81
603	0.13	0.87
653	0.11	0.89
703	0.10	0.90
756	0.10	0.90
807	0.07	0.93
852	0.13	0.87
900	0.06	0.94
950	0.05	0.95
1000	0.06	0.94
1100	0.06	0.94

TABLE G-13

Pressure History-Run 3

Cumulative Time min	Inlet Pressure psi
0	11.6
33	13.3
40	15.3
60	19.4
82	21.0
125	20.2
137	18.6
150	17.8
165	17.0
198	16.2
245	15.6
260	15.9
273	17.2
288	19.6

TABLE G-13 (cont'd)

Pressure History-Run 3

Cumulative Time min	Inlet Pressure psi
303	21.5
323	22.6
337	23.4
360	24.4
390	25.6
433	27.0
455	27.0
473	26.9
533	24.8
570	23.1
585	22.6
615	22.0
675	21.2

TABLE G-14

Oil Production History-Run 3

Pore Vol. Inj., frac.	Cum. Oil Prod. ml	% IOIP Prod.,
0.0652	50	7.4
0.130	100	14.7
0.196	150	22.1
0.261	200	29.4
0.326	250	36.8
0.391	300	44.1
0.456	349.25	51.4
0.522	374.75	55.1
0.587	389.25	57.2
0.652	399.75	58.8
0.717	409.75	60.3

TABLE G-14 (cont'd)

Oil Production History-Run 3

Pore Vol. Inj., frac.	Cum. Oil Prod. ml	% IOIP Prod.,
0.782	416.25	61.2
0.847	421.75	62.0
0.913	426.75	62.8
0.978	432.25	63.6
1.043	435.75	64.1
1.108	439.25	64.6
1.173	442.25	65.0
1.239	444.75	65.4
1.303	447.75	65.8
1.369	450.25	66.2
1.434	453.25	66.7
1.499	455.50	67.0

TABLE G-15

Effluent Water Salinity Analysis-Run 3

Run #	P. V. Prod. frac.	Refractive Index	NaCl Concentration
	0.456	1.3411	0.975
	0.522	1.3396	0.803
	0.587	1.3380	0.619
	0.652	1.3360	0.390
	0.717	1.3350	0.275
	0.782	1.3342	0.183
	0.847	1.3340	0.160
2	0.913	1.3339	0.148
	0.978	1.3335	0.103
	1.043	1.3333	0.079
	1.108	1.3330	0.045
	1.173	1.3330	0.045
	1.239	1.3330	0.045
	1.369	1.3330	0.045
	1.499	1.3330	0.045

TABLE G-16

Effluent Analysis-Run 4

Cum. Vol. Inj., ml	Oil Produced frac.	Water Produced frac.
400	1.00	0.00
450	0.76	0.24
500	0.40	0.60
550	0.32	0.68
600	0.26	0.74
650	0.20	0.80
693	0.14	0.86
741	0.10	0.90
790	0.10	0.90
839	0.08	0.92
936	0.08	0.92
986	0.06	0.94
1036	0.08	0.92
1086	0.08	0.92
1136	0.04	0.96
1286	0.03	0.97

TABLE G-17

Pressure History-Run 4

Cumulative Time min	Inlet Pressure psi
0	9.2
10	14.6
25	16.4
50	16.6
85	16.4
110	18.2
125	21.1
128	20.0
140	18.2
170	14.8
200	14.2
230	15.2
260	17.4
320	28.4

TABLE G-17 (cont'd)

Pressure History-Run 4

Cumulative Time min	Inlet Pressure psi
350	32.8
380	34.9
406	36.4
425	40.4
450	39.0
510	42.4
570	43.0
600	42.4
630	42.4
690	41.0
720	41.0
750	41.0

TABLE G-18

Oil Production History-Run 4

Pore Vol. Inj., frac.	Cum. Oil Prod. ml	% IOIP Prod.,
0.064	50	7.4
0.128	100	14.7
0.192	150	22.1
0.256	200	29.4
0.320	250	36.8
0.384	300	44.1
0.448	350	51.5
0.512	400	58.8
0.575	438	64.4
0.639	458	67.4
0.703	474	69.7
0.767	487	71.6
0.831	497	73.1

TABLE G-18 (cont'd)

Oil Production History-Run 4

Pore Vol. Inj., frac.	Cum. Oil Prod. ml	% IOIP Prod.,
0.886	503	74.0
0.948	508	75.4
1.073	516.5	76.0
1.134	520.5	76.5
1.197	524.5	77.1
1.261	527.5	77.6
1.325	531.5	78.2
1.389	535.5	78.8
1.453	537.5	79.0
1.517	541	79.6
1.581	544.5	80.0
1.645	546	80.3

TABLE G-19

Effluent Water Salinity Analysis-Run 4

Run #	P. V. Prod. frac.	Refractive Index	NaCl Concentration
	0.575	1.3409	0.952
	0.639	1.3409	0.952
	0.703	1.3399	0.837
	0.767	1.3374	0.550
	0.831	1.3353	0.309
3	0.886	1.3340	0.160
	0.948	1.3335	0.103
	1.010	1.3333	0.079
	1.073	1.3333	0.079
	1.134	1.3332	0.068
	1.197	1.3332	0.068
	1.261	1.3330	0.045
	1.325	1.3330	0.045

TABLE G-20

Effluent Analysis-Run 5

Cum. Vol. Inj., ml	Oil Produced frac.	Water Produced frac.
150	0.998	0.002
200	0.945	0.055
248	0.563	0.437
298	0.340	0.660
344	0.215	0.785
394	0.100	0.900
444	0.090	0.910
498	0.093	0.907
547	0.082	0.918
596	0.776	0.224
645	0.934	0.066
695	0.680	0.320

TABLE G-20 (cont'd)

Effluent Analysis-Run 5

Cum. Vol. Inj., ml	Oil Produced frac.	Water Produced frac.
744	0.378	0.622
792	0.274	0.726
840	0.240	0.760
887	0.200	0.800
934	0.160	0.840
984	0.170	0.830
1031	0.106	0.894
1079	0.104	0.896
1126	0.085	0.915
1172	0.076	0.924
1220	0.053	0.947
1268	0.073	0.927
1320	0.039	0.961

TABLE G-21

Pressure History-Run 5

Cumulative Time min	Inlet Pressure psi
0	6.4
30	15.8
80	11.0
85	10.4
115	9.0
145	8.5
148	8.4
170	8.2
190	8.2
210	8.1
230	8.1
250	9.1
260	10.6
270	11.6
280	13.8

TABLE G-21 (cont'd)

Pressure History-Run 5

Cumulative Time min	Inlet Pressure psi
293	15.7
310	16.6
340	16.4
410	12.7
470	12.0
540	13.6
557	14.7
576	16.0
640	18.0
700	18.3
725	19.3
759	19.8
782	20.4

TABLE G-22

Oil Production History-Run 5

Pore Vol. Inj., frac.	Cum. Oil Prod. ml	% IOIP Prod.,
0.069	50	7.2
0.137	100	14.4
0.205	149.9	21.6
0.274	197.15	28.4
0.339	224.15	32.3
0.408	241.15	34.7
0.471	251.15	36.1
0.540	256.15	36.9
0.608	260.65	37.5
0.682	265.65	38.2
0.749	269.65	38.8
0.816	307.65	44.3
0.884	353.40	50.8
0.952	387.4	55.7

TABLE G-22 (cont'd)

Oil Production History-Run 5

Pore Vol. Inj., frac.	Cum. Oil Prod. ml	% IOIP Prod.,
1.019	405.9	58.4
1.085	418.9	60.3
1.151	430.4	61.9
1.215	439.9	63.3
1.279	447.4	64.4
1.350	455.9	65.6
1.412	460.9	66.3
1.478	465.9	67.0
1.542	469.9	67.6
1.605	473.4	68.1
1.671	475.9	68.5
1.737	479.4	69.0
1.808	481.4	69.3

TABLE G-23

Effluent Water Salinity Analysis-Run 5

Run #	P. V. Prod. frac.	Refractive Index	NaCl Concentration
	0.274	1.3395	0.791
	0.339	1.3389	0.722
	0.408	1.3377	0.585
	0.471	1.3377	0.585
	0.540	1.3360	0.390
	0.608	1.3340	0.160
	0.682	1.3334	0.091
5	0.749	1.3331	0.057
	0.816	1.3329	0.034
	0.884	1.3331	0.057
	0.952	1.3343	0.205
	1.019	1.3340	0.160
	1.085	1.3338	0.137
	1.151	1.3335	0.103
	1.279	1.3334	0.091
	1.350	1.3330	0.045
	1.808	1.3330	0.045

TABLE G-24

Effluent Analysis-Run 6

Cum. Vol. Inj., ml	Oil Produced frac.	Water Produced frac.
700	1.000	0.000
750	0.898	0.102
800	0.580	0.420
850	0.420	0.580
900	0.320	0.680
950	0.306	0.694
1000	0.292	0.708
1050	0.260	0.740
1100	0.190	0.810
1150	0.184	0.816
1200	0.163	0.837
1250	0.160	0.840
1300	0.135	0.865

TABLE G-24 (cont'd)

Effluent Analysis-Run 6

Cum. Vol. Inj., ml	Oil Produced frac.	Water Produced frac.
1350	0.140	0.860
1400	0.130	0.870
1450	0.100	0.900
1500	0.093	0.907
1550	0.111	0.889
1600	0.100	0.900
1650	0.080	0.920
1700	0.100	0.900
1750	0.090	0.910
1800	0.090	0.910
1850	0.096	0.904
1900	0.061	0.939
1950	0.061	0.939

TABLE G-25

Pressure History-Run 6

Cumulative Time min	Inlet Pressure psi
0	24.5
30	29.2
60	29.6
90	29.7
127	30.7
157	32.5
187	34.6
216	36.8
252	32.5
281	29.0
311	28.2
341	28.6
371	30.2
401	32.6
459	42.2
488	43.8
518	46.4

TABLE G-25 (cont'd)

Pressure History-Run 6

Cumulative Time min	Inlet Pressure psi
582	50.8
643	51.0
670	52.8
729	60.2
760	63.0
793	64.7
823	61.8
851	61.9
880	60.4
910	57.7
940	56.0
970	55.6
1000	56.0
1030	56.2
1063	60.2
1093	58.0
1123	61.2

TABLE G-26

Oil Production History-Run 6

Pore Vol. Inj., frac.	Cum. Oil Prod. ml	% IOIP Prod.
0.064	100	7.3
0.129	200	14.6
0.193	300	21.9
0.258	400	29.2
0.322	500	36.5
0.386	600	43.8
0.451	700	51.1
0.483	744	54.3
0.515	773	56.4
0.548	794	58.0
0.580	812	59.3
0.612	825	60.2
0.644	839	61.2
0.676	852	62.2
0.709	861.5	62.9

TABLE G-26 (cont'd)

Oil Production History-Run 6

Pore Vol. Inj., frac.	Cum. Oil Prod. ml	% IOIP Prod.,
0.741	870.5	63.5
0.773	878.5	64.1
0.805	886.5	64.7
0.837	893.0	65.2
0.869	900.0	65.7
0.902	906.0	66.1
0.934	911.0	66.5
0.966	915.5	66.8
0.998	921.0	67.2
1.030	926.0	67.6
1.062	930.0	67.9
1.095	935.0	68.2
1.127	939.5	68.6
1.159	944.0	68.9
1.192	948.5	69.2
1.224	951.5	69.5
1.256	954.5	69.7

TABLE G-27

Effluent Water Salinity Analysis-Run 6

Run #	P. V. Prod. frac.	Refractive Index	NaCl Concentration
	0.483	1.3414	1.000
	0.515	1.3413	0.998
	0.548	1.3411	0.975
	0.580	1.3408	0.941
	0.612	1.3400	0.849
6	0.644	1.3393	0.768
	0.676	1.3386	0.688
	0.709	1.3374	0.650
	0.741	1.3364	0.435
	0.773	1.3356	0.343
	0.805	1.3350	0.275
	0.837	1.3345	0.217

TABLE G-27 (cont'd)

Effluent Water Salinity Analysis-Run 6

Run #	P. V. Prod. frac.	Refractive Index	NaCl Concentration
	0.869	1.3345	0.217
	0.902	1.3349	0.263
	0.934	1.3338	0.137
	0.966	1.3336	0.114
	0.998	1.3334	0.091
6	1.030	1.3333	0.079
	1.062	1.3333	0.079
	1.095	1.3331	0.057
	1.127	1.3331	0.057
	1.159	1.3331	0.057
	1.192	1.3330	0.045
	1.224	1.3330	0.045
	1.256	1.3328	0.022